

Impact of FM Broadcast Signals on Aeronautical Radionavigation

Rodrigo Berquó de Aguiar Viveiros Santos

Thesis to obtain the Master of Science Degree in
Electrical and Computer Engineering

Examination Committee

Chairperson: Prof. José Sanguino

Supervisor: Prof. Luis M. Correia

Member of Committee: Prof. António Moreira

Member of Committee: Eng. Carlos Silva

February 2015

To everyone in my life

Acknowledgements

First and foremost, I want to give my profound thanks to Prof. Luis M. Correia, who was responsible not only for supervising this Thesis but also for helping my professional development throughout this last year. He helped me gain various skills by presenting discipline, professionalism, and providing technical support through our weekly meetings. I want to thank him as well for giving me the opportunity for doing this Thesis under his supervision, and additionally in collaboration with NAV Portugal, which presented two valuable experiences for my personal development.

I want to express my gratitude to NAV Portugal and their engineers, namely Eng. Carlos Alves, Eng. Carlos Silva and Eng. Luís Pissarro, for presenting exceptional availability and for being supportive through the development of this work. I also want to thank them for providing essential technical guidelines and information that were critical in the realisation of the study.

I am thankful to Eng. Fernanda Girão from ANACOM for providing detailed information regarding the FM audio broadcasting stations located in Portugal, which made possible the development of the regional scenarios that were in the core of this Thesis.

My next dedication goes to all the GROW members, for integrating the M.Sc. Students in their group and for helping the development of my presentation skills in the GROWing meetings.

To all my M.Sc. colleagues, which, through feelings of camaraderie and support, were able to lighten the work load and accumulated stress along this journey. I want to thank Bruno P., David D., Gonçalo F., Marco C., Pedro F., Pedro G., Pedro V. and Vasco S.

Lastly, but not least, I want to thank my family for their unwavering support through this last year, not only for providing me a good education, but also for being there whenever I needed them. In my short visits to Azores, my godmother, grandmother, father, and brother supported me when I felt I hit a dead end, and they were critical to my emotional perseverance. I also express my deepest gratitude to Raquel, for all her sacrifices that she made for my greater good, whether spell checking my work, as providing emotional support throughout this long year.

Abstract

The main focus of this work was to study the impact of FM audio broadcasting signals on the aeronautical radionavigation systems. This Thesis was done with the cooperation of NAV Portugal. One assessed the transmissions in the VHF band, and thus, the systems that presented to be relevant for the study included the VHF Omnidirectional Range and the Instrument Landing System Localiser. The study was accomplished through the establishment and implementation of models regarding the characterisation of the transmitters and their signals, as well the definition of the aircraft path throughout flight routes and approaches. The assessment of interference was performed by using two criteria: one consisted on the raw analysis of the ratio between the wanted and interfering signals, and the other was based on an ITU-R Recommendation. One focused on the interference generated due the intermodulation of multiple FM broadcasting signals. Simulations were done taking into account possible scenarios occurring in the Portuguese airspace. One verified the non-existence of any harmful interference generated by any of the commercial FM broadcasting networks. The most noticeable impact is verified in the approach on runway 03 of the Lisbon airport, where the high power FM transmitters located in Monsanto generate a decrease of the carrier to interference ratio down to a minimum of 43.5 dB.

Keywords

Radionavigation, FM broadcasting, ILS, VOR, Interference, Intermodulation.

Resumo

O foco principal deste estudo foi averiguar o impacto que os sinais de radiodifusão em FM têm nos sistemas de radionavegação aeronáutica. Esta tese foi realizada em cooperação com a NAV Portugal. Foram estudados os sistemas aeronáuticos que transmitem na banda VHF, e os que se apresentaram ser relevantes para o estudo foram o sistema de navegação omnidireccional em VHF, VOR, e o ILS pertencente ao sistema de aterragem por instrumentos. O estudo foi realizado através do estabelecimento e implementação de modelos para a caracterização dos transmissores e de seus sinais, tal como para a definição do caminho percorrido pela aeronave, quer em rota quer em aterragem. A averiguação da existência de interferência foi baseada em dois critérios: um baseia-se na análise da razão entre o sinal aeronáutico e os sinais interferentes, e o outro numa recomendação ITU-R. A avaliação foi centralizada na interferência gerada pelos produtos obtidos da intermodulação de vários sinais de radiodifusão. Realizaram-se simulações para averiguar possíveis cenários no espaço aéreo português. De acordo com os resultados obtidos, verificou-se a inexistência de qualquer interferência perigosa causada pela rede de radiodifusão FM. O impacto mais significativo foi obtido na aproximação à pista 03 do aeroporto de Lisbon, em que os transmissores de alta potência no Centro Emissor de Monsanto geraram uma queda da razão de sinal para interferência até um mínimo de 43.5 dB.

Palavras-chave

Radionavegação, Radiodifusão FM, ILS, VOR, Interferência, Intermodulação.

Table of Contents

Acknowledgements	v
Abstract.....	vii
Resumo	viii
Table of Contents.....	ix
List of Figures	xii
List of Tables.....	xiv
List of Acronyms	xv
List of Symbols.....	xvii
List of Software	xx
1 Introduction	1
1.1 Overview.....	2
1.2 Motivation and Contents	4
2 Basic Concepts	7
2.1 VOR.....	8
2.1.1 System Overview	8
2.1.2 Operation Mode	9
2.1.3 Radio Interface	10
2.2 ILS	11
2.2.1 System Overview	11
2.2.2 LOC System	13
2.3 FM Broadcasting	15
2.3.1 System Overview	15
2.3.2 Radio Interface	16
2.4 Interference	18
2.4.1 Problem Assessment.....	18
2.4.2 Interference Mechanisms	18

2.5	State of the Art.....	20
3	Model Development	23
3.1	Propagation Models.....	24
3.2	Radiation Patterns	28
3.2.1	Navigation Systems.....	29
3.2.2	FM Broadcasting.....	33
3.3	Flight Routes	35
3.4	Radio Characterisation	37
3.4.1	Radionavigation Systems	37
3.4.2	FM Broadcasting.....	38
3.5	Interference Assessment.....	40
3.5.1	FM Broadcasting Selection.....	40
3.5.2	Power Level	41
3.5.3	ITU-R Recommendation	43
3.6	Simulator Development	47
3.6.1	Methodology and Input Data	47
3.6.2	Transmitters and Receiver	49
3.6.3	Link Characterisation and Analysis	50
3.7	Model Assessment	52
4	Data Analysis	59
4.1	Transmitters.....	60
4.2	Scenarios Definition.....	64
4.2.1	Flight Routes.....	64
4.2.2	Approaches.....	64
4.3	Results and Data Assessment.....	66
4.3.1	VOR Results	66
4.3.2	ILS LOC Results	68
5	Conclusions.....	75
Annex A.	Aeronautical Channel Frequencies	81
A.1	ILS LOC.....	82
A.2	VOR.....	82
Annex B.	FM Broadcasting Stations	85
Annex C.	Flight Route Charts	105
Annex D.	VOR Results	109

Annex E. FM Broadcasting Stations in Evaluation.....	111
References.....	113

List of Figures

Figure 1.1 - Flight flow evolution from 1985 to expected in 2015 (extracted from [EUCO14]).	2
Figure 1.2 - Portuguese delegated airspace (extracted from [EMFA14]).	3
Figure 2.1 - VOR operation illustration (extracted from [NAV12a]).	10
Figure 2.2 - Frequency spectrum of a DVOR (CVOR) (extracted from [NAV12a]).	11
Figure 2.3 - ILS LOC lobes diagram (extracted from [ILSy14]).	12
Figure 2.4 - Coverage of an ILS LOC system (extracted from [ITUR10]).	14
Figure 2.5 - CSB and SBO field strength using a two-frequency 16-element LPDA (extracted from [Indr13]).	15
Figure 2.6 - FM stereo pilot tone system baseband (extracted from [AxTe14]).	17
Figure 2.7 - IMD products of two signals and their frequency relations with the carriers (extracted from [RFGN14]).	19
Figure 3.1 - Diagram of the links of the system in study.	24
Figure 3.2 - Diagram of the Flat Earth Model.	26
Figure 3.3 - Diagram of the Spherical Earth Model and the Flat Earth equivalent parameters.	27
Figure 3.4 - VOR normalised vertical radiation pattern.	29
Figure 3.5 - Horizontal radiation pattern of an LPDA.	30
Figure 3.6 - 16-element LPDA antenna system course CSB radiation pattern.	32
Figure 3.7 - Vertical radiation pattern of the ILS LOC in Lisbon RWY03.	32
Figure 3.8 - VDA vertical radiation pattern (12 elements).	34
Figure 3.9 - VDA vertical radiation pattern (2 elements).	34
Figure 3.10 - VDA vertical radiation pattern (tilted 12 elements).	35
Figure 3.11 - Frequency spectrum of an ILS LOC carrier with frequency f_0 .	38
Figure 3.12 - Frequency spectrum of an VOR carrier with frequency f_0 and the total bandwidth.	38
Figure 3.13 - Out-of-band transmission mask for FM broadcasting transmitters (extracted from [ITUR14]).	39
Figure 3.14 - General methodology of the simulator.	48
Figure 3.15 - Discretisation of the Ponta Delgada approach path into 10 points.	49
Figure 3.16 - Algorithm for the selection of FM broadcasting stations.	50
Figure 3.17 - Simulator result assessment flowchart.	52
Figure 3.18 - Flight route RN870a and relevant transmitters.	53
Figure 3.19 - FM station antenna models assessment (FL45).	53
Figure 3.20 - FM station antenna models assessment (FL300).	54
Figure 3.21 - VOR antenna models assessment (FL45 and FL300).	54
Figure 3.22 - VOR and FM stations signal propagation models assessment.	55
Figure 3.23 - ILS LOC models assessment.	56
Figure 3.24 - Assessment of the power assessment of an IMD product.	57
Figure 4.1 - Location of the VOR located in Portugal mainland.	61
Figure 4.2 - Location of the ILS LOC maintained by NAV Portugal.	63
Figure 4.3 - Plot of the received power in flight route Y207b.	67
Figure 4.4 - Plot of the received power during the approach to Lisbon runway 03 for the various FM broadcasting antenna models.	69

Figure 4.5 - Plot of the CIR of the approach to Lisbon runway 03 for the various FM broadcasting antenna models.....	69
Figure 4.6 - Plot of the received power during the approach to Lisbon runway 21 for the various FM broadcasting antenna models.	70
Figure 4.7 - Plot of the CIR of the approach to Lisbon runway 21 for the various FM broadcasting antenna models.....	70
Figure 4.8 - Plot of the obtained results for Lisbon runway 03 scenario for the various FM broadcasting antenna models considering the terrain profiles.	71
Figure 4.9 - Geographical representation of the FM stations in consideration for the obstacle implementation and simulation in Lisbon runway 03.	72
Figure 4.10 - Representation of the terrain profile and Fresnel ellipsoid of the transmission link between FM station 261 and the aircraft at 7 km from the touchdown zone.....	73
Figure C.1 - Navigational chart presenting both the assessed segments of flight route Y207 (extracted from [NAV14c]).	106
Figure C.2 - Navigational chart presenting both the assessed segments of flight route UN872 (extracted from [NAV14c]).	107
Figure D.1 - Results obtained from the simulation of the Y207a scenario.	110
Figure D.2 - Results obtained from the simulation of the Y207b scenario.	110
Figure D.3 - Results obtained from the simulation of the UN872a scenario.	110

List of Tables

Table 2.1 - VOR/DME classes and ranges (adapted from [FAAG14]).....	9
Table 3.1 - 16-element LPDA antenna system course CSB characteristics (adapted from [Indr13]).....	31
Table 3.2 - Break points of spectrum limit mask for FM broadcasting (extracted from [ITUR14]).	39
Table 3.3 - FM broadcasting stations classes' characteristics (adapted from [FCC14a]).	41
Table 3.4 - Type A1 interference protection ratios for aeronautical receivers (extracted from [ITUR10]).	45
Table 3.5 - Type A2 interference protection ratios for aeronautical receivers (extracted from [ITUR10]).	45
Table 3.6 - C_t depending on the frequency difference between the wanted signal and IMD products (extracted from [ITUR10]).	46
Table 4.1 - VOR positions and transmitting characteristics (provided by [NAV14b]).	60
Table 4.2 - Height of the terrain on VOR locations.	61
Table 4.3 - ILS LOC transmitting characteristics and positions (provided by [NAV14b]).	62
Table 4.4 - Approach runways elevation (extracted from [NAV14c]).	62
Table 4.5 - Maximum gains of the ILS LOC arrays (provided by [NAV14b]).	63
Table 4.6 - Flight routes considered for evaluation of the VOR located in Santa Maria FIR.	64
Table 4.7 - Flight routes considered for evaluation of the VOR located in Lisboa FIR.	65
Table 4.8 - Approach routes considered for evaluation.	66
Table 4.9 - Results from the scenario assessment at FL45.....	67
Table 4.10 - Results obtained from the simulator regarding the approach scenarios considering no obstacles in the propagation of FM broadcasting signal.	68
Table A.1 - ILS LOC channel frequencies.....	82
Table A.2 - VOR channel frequencies.....	83
Table B.1 - Characteristics of the FM sound broadcasting stations in Portugal (adapted from [ANAC14]).....	86
Table E.1 - List of the FM broadcasting stations considered in Lisbon runway 03 scenario.	112
Table E.2 - List of the FM broadcasting stations considered in Lisbon runway 21 scenario.	112

List of Acronyms

AIP	Aeronautical Information Package
AM	Amplitude Modulated
ANACOM	Autoridade Nacional de Comunicações
ANSP	Air Navigation Service Provider
CIR	Carrier to Interference Ratio
CSB	Carrier-plus-sideband
CVOR	Conventional VOR
DDM	Difference in Depth Modulation
DH	Decision Height
DME	Distance Measuring Equipment
DSB-SC	Double Sideband Suppressed Carrier
DVOR	Doppler VOR
ERP	Effective Radiated Power
FCC	Federal Communication Commission
FIR	Flight Information Region
FL	Flight Level
FM	Frequency Modulated
GS	Glide Slope
HAAT	Height Above Average Terrain
ICAO	International Civil Aviation Organisation
ILS	Instrument Landing System
IM	Inner Marker
IMD	Intermodulation Distortion
INAC	Instituto Nacional de Aviação Civil
IP3	Third order Intercept Point
ITU	International Telecommunication Union
ITU-R	ITU Radiocommunication Sector
LF	Low Frequency
LOC	Localiser
LPDA	Log-Periodic Dipole Array
MB	Marker Beacon
MM	Middle Marker
MSL	Mean Sea Level
NDB	Non Directional Beacon

OM	Outer Marker
RDS	Radio Data System
RF	Radiofrequency
RPS	Rotations Per Second
RVR	Runway Visibility Range
SBO	Sideband Only
SCA	Subsidiary Communications Authority
SSV	Standard Service Volume
UHF	Ultra High Frequency
VDA	Vertical Dipole Array
VHF	Very High Frequency
VOR	VHF Omnidirectional Range

List of Symbols

α_{desc}	Descent angle
α_{mag}	Magnetic route angle
α_{real}	Real route angle
α_{var}	Variation angle given in relation to the magnetic West
γ	Phase delay
δ	Electric phase difference between the N^{th} antenna and the reference one
$\Delta\phi$	Phase difference between using the Flat and Spherical Earth Models
θ	Angle between the beam and the receiver in the vertical plane.
θ_{t-air}	Earth circumference angle between the station and the aircraft
λ	Wavelength of the signal
λ_{air}	Longitude of the aircraft
λ_t	Longitude of the receiver
ν	Obstacle impediment coefficient
$\Sigma\phi_i$	Vertical spacing of the parallel i
φ	Angle between the beam and the receiver in the horizontal plane
ϕ_{air}	Latitude of the aircraft
ϕ_t	Latitude of the transmitter
a_q	Electrical current ratio between the N^{th} antenna and the reference one
A_t	Decrease of the power level relative to the maximum output power
B	Signal bandwidth
(C/I)	Carrier to interference ratio
d	Ground distance between the terminal and the aircraft
d_1	Ground distance between the terminal and the reflection point
d_2	Ground distance between the aircraft and the reflection point
d_{dip}	Distance between dipoles
d_{dr}	Length of the direct ray
d_i	Relative distance in a point i to the end of the approach
$d_{interval}$	Distance between fixed intervals
d_{path}	Length of the path between two points
d_{RH}	Distance to the radio horizon
d_r	Distance from the obstacle to the receiver

d_t	Distance from the obstacle to the transmitter
f	Frequency of the signal
f_Δ	Frequency deviation relative to f_c
F_a	Array factor
f_B	Frequency of the FM broadcasting signal
f_c	Frequency of the carrier
F_N	Noise figure of the receiver
f_n	Frequency of the n^{th} FM signal
f_{IMD}	Frequency of the IMD product
F_{IP3}	Figure of merit regarding the IMD
$G_{antenna}$	Gain of the array antenna element
G_{array}	Gain of the array
G_h	Normalised horizontal gain
G_{max}	Maximum gain of the antenna
G_r	Gain of the receiver
G_t	Gain of the transmitter
G_v	Normalised vertical gain
h_{air}	Height of the aircraft
$h_{ef,r}$	Equivalent effective height of the receiver in the Flat Earth Model
$h_{ef,t}$	Equivalent effective height of the transmitter in the Flat Earth Model
h_{final}	Aerodrome runway height above mean sea level
h_i	Height in a point i of the approach
$h_{initial}$	Initial approach height above mean sea level
h_{ofe}	Height from the tip of the obstacle to the centre of the Fresnel Ellipsoid
h_r	Height of the receiver
h_t	Height of the transmitter
$h_{terrain}$	Height of the terrain
$h_{t,MSL}$	Height above mean seal level of the transmitter
i	Current test position
k	Wave number
k_n	Random integer value for the n^{th} FM signal
L_{C1}	Correction factor to account for changes in the wanted signal level (Type B1)
L_{C2}	Correction factor to account for changes in the wanted signal level (Type B2)
$L_{Deygout}$	Losses due to obstacles using Deygout model
l_{dip}	Length of the dipole
L_{KE}	Losses due to obstacles using Knife Edge model
L_o	Path loss

L_{ob}	Losses due to obstacles
n	Order of the Fresnel Ellipsoid
N	Order of the generated IMD product
N_{ant}	Number of elements on the array
n_i	Number of interfering signals
N_{points}	Number of points to be tested in the path
P_{IMD3}	Power of the generated 3 rd order IMD product
P_N	Average noise power of the receiver
P_r	Power of the signal at the receiver
$P_{r,A}$	Wanted aeronautical wanted signal level at the input of the receiver
$P_{r,C}$	Power of the carrier signal
$P_{r,cor}$	Corrected received signal level
$P_{r,max}$	Maximum FM broadcasting signal level allowed at the input of the aeronautical receiver
$P_{r,I}$	Sum of the powers of the interfering signals
$P_{r,I,k}$	Power of a interfering signal
$P_{r,IMD3}$	Power of the IMD product in the aeronautical frequency
$P_{r,ref}$	Reference level of the wanted aeronautical signal
P_t	Power of the transmitter signal
$P_{t,FM}$	Power of the signal transmitter by FM broadcasting stations
$P_{t,max}$	Maximum transmitted power of the FM broadcasting station
R	Earth radius
R_e	Effective Earth radius
$R_{fe,n}$	Radius of the Fresnel Ellipsoid of order n
z	Distance from Fresnel Ellipsoid point to the terminal

List of Software

Google Earth

Google Maps Javascript API v3

Mathworks Matlab r2013a

Microsoft Excel 2010

Microsoft PowerPoint 2010

Microsoft Word 2010

Paint

Geographical and terrain information system

Terrain profile extractor software

High technical computing software

Calculation and chart tool software

Presentation software

Text editor software

Image editing software

Chapter 1

Introduction

This chapter gives the context of the study in nowadays' systems. In order to better understand the relevance of the work, a brief overview of it is given as well its impact in the area of study. It is finalised with a brief presentation of the structure of this study.

1.1 Overview

With the constant progression of technology, mankind was able to connect the whole world. Nowadays, it is possible to communicate with another being on the opposing side of the planet in a matter of milliseconds, and even fly across the world within hours. These travels across the globe were made viable due to a progressive evolution of their efficiency, costs and safety.

It all started in the beginning of the XX century, when flights were limited due to the lack of visibility, whether due to the darkness of the night or to weather conditions. Thus, mankind started using bonfires to provide visual guidance to pilots through defined paths. This indicated the beginning of the use of ground beacons to assist pilots in the navigation throughout the airspace. And, as telecommunication technologies evolved, pilots started navigating through the assistance of various radio beacons spread throughout the land, which lead to the radionavigation practiced today.

Since 1989, air traffic flows increased 33%, and in 20 years, they are expected to nearly double [EUCO14]. In Figure 1.1, one can observe a representation of the aforementioned statistics, and denote the increase of the density in flights throughout Europe.

In 2013, the number of airplane flights worldwide reached 33 million [ICAO14]. The number of yearly flights has been increasing around 5% the last few years, with 5.2% expected in 2014. The constant increase of flights implies the need to have precise systems that can supply an uninterrupted flow of accurate information to aircrafts regarding their position and path.

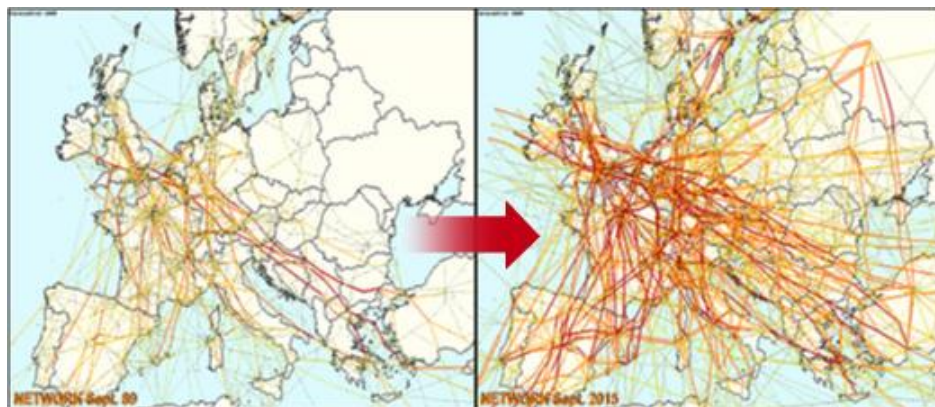


Figure 1.1 - Flight flow evolution from 1985 to expected in 2015 (extracted from [EUCO14]).

For that end, every flight, whether national or international, is supervised by an entity that manages the air traffic. Figure 1.2 presents the airspace internationally delegated to Portugal, being divided into various Flight Information Regions (FIRs). These FIRs are controlled by an Air Navigation Service Provider (ANSP), which is in charge of controlling and assisting the departure and arrival of aircrafts, and also maintaining a secure traffic throughout the airspace.

Each of the ANSPs must comply with numerous quality standards, whether national or international.

At a worldwide scale, the International Civil Aviation Organisation (ICAO) is responsible for assessing and supervising the required standards for the provision of air traffic control or information services. These requirements comprise every area that is involved in this process, and radio equipment and telecommunication regulations are not excluded.

NAV Portugal is the Portuguese ANSP, being responsible for both the Santa Maria and Lisboa FIRs [NAV14a], Santa Maria is one of the largest FIRs located in the Atlantic Ocean, and it oversees a big part of the traffic between Europe and America. This requires NAV Portugal to present quality service and ground assistance to every aircraft that flies through Portuguese airspace. In Portugal, ICAO is represented by the Instituto Nacional de Aviação Civil (INAC), which is the major regulating entity supervising the services provided by NAV Portugal.

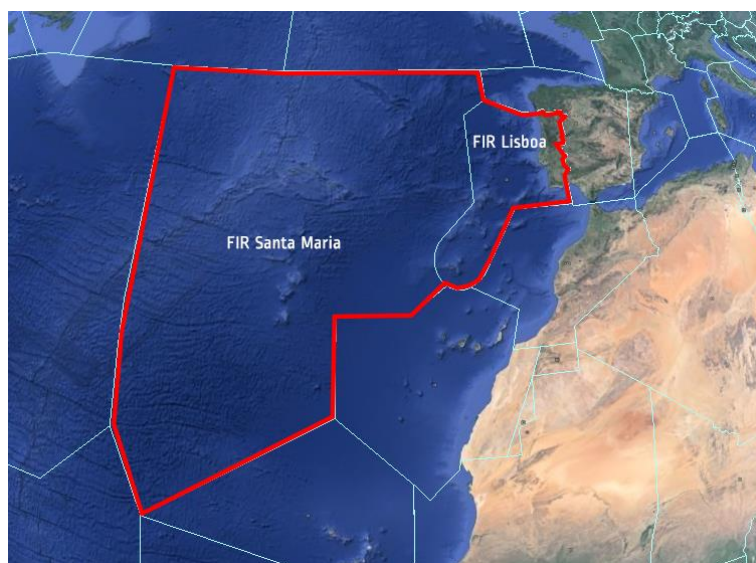


Figure 1.2 - Portuguese delegated airspace (extracted from [EMFA14]).

There are numerous systems that allow the pilot to check and control various parameters regarding the navigation of the aircraft. Amongst them, there are some that rely on the support of ground antennas. NAV Portugal is responsible for maintaining these ground radio aids, which assist the aircraft positioning throughout its defined route.

Two of the most important guidance systems that pilots rely on are the VHF Omnidirectional Range (VOR) and the Instrument Landing System (ILS). The VOR allows the aircraft to receive guidance relative to fixed ground locations during its flight, playing a significant part on the en-route radionavigation. The ILS assists during the approach and landing procedures, and for operations with low visibility, the utilisation of this radio aid is crucial. Both of these systems transmit signals in the VHF band, being comprised within [108, 137] MHz [ICAO96].

Frequency Modulated (FM) audio broadcasting stations transmit in the lower adjacent frequency band. There are over 700 FM audio transmitters in Portugal, which provide coverage throughout the territory. These are usually positioned on the top of hills, in order to strategically provide coverage to the surrounding regions with the minimum obstacles obstructing the view. The chosen locations without surrounding terrain or buildings obstructing the propagation of the signal also make the signal

propagation into the airspace unobstructed, and this may cause interference in the signals used by aeronautical radionavigation systems.

Autoridade Nacional de Comunicações (ANACOM) is the entity responsible for the distribution of the frequency spectrum throughout the various telecommunication services. The frequency band reserved for FM audio broadcast in Portugal is within [87.5, 108] MHz [ANAC13], implying that FM broadcasting systems may interfere with radionavigation systems.

The main goal of this work is to assess the impact that these FM audio broadcasting stations have on aeronautical radio aids, namely VOR and ILS. It also intended to evaluate various scenarios, to quantify the interference in each one of them and to verify if there is any relevant perturbation in the aeronautical radionavigation system. To that end, a simulator was developed to analyse the signals present at the aircraft, whether from radionavigation systems or from FM broadcasting stations, and to verify the effect of interfering signals.

At the end of the XX century, there were a high number of papers regarding this topic, coinciding with the emergence of the high dependence on radionavigation systems; since FM broadcasting was also in a constant evolution, studies on their interaction were inevitable. Nowadays, there are documents providing recommendations to both aeronautical radionavigation and FM broadcasting systems, to allow their co-existence with the least amount of interaction. This Thesis presents a focalised study and evaluation of real case scenarios through interference assessment criteria.

1.2 Motivation and Contents

The focus of this work consists of assessing whether FM audio broadcasting systems have any impact in the quality of the radionavigation ground aids maintained by NAV Portugal. To that end, the assessment of the received power of both the wanted and interfering signals is done. Afterwards, two theoretical models were be used to assess if there is any interference caused to the radionavigation signal, the first one being an evaluation of the ratio between the wanted and interfering signals, and the second one being based on a recommendation from the International Telecommunication Union (ITU).

This Thesis was done in collaboration with NAV Portugal. Crucial assistance was provided throughout the development of this work, both supplying essential information regarding aeronautical radionavigation systems, and discussing results.

This Thesis is divided into a total of 5 chapters, including the present introductory one, and it is complemented with 5 annexes.

In Chapter 2, one begins by presenting the basic concepts concerning the radionavigation aids under study. Following the theoretical introduction of VOR and ILS, FM broadcasting systems are presented, and, afterwards, the assessment of the interference that these may cause on radionavigation systems

is done. In the end, the state of the art regarding the focus of this Thesis is briefly presented.

Chapter 3 consists of the chosen theoretical models used to fulfil the purpose of this study. It includes the modelling of wave propagation, antenna and radio systems, and the path taken by the aircraft. In this chapter, one also presents the models developed for the assessment of interference. A simulator was implemented to assist the study, and a thorough description of the implementation of the models into the program is done. In order to verify the implementation of the simulator, this chapter concludes with the assessment of the models and the simulator.

In Chapter 4, the scenarios that were chosen for evaluation are presented. This includes all the radio equipment included in the study, as well as aircraft paths. Afterwards, one presents the results obtained from the developed simulator regarding each one of the scenarios, accompanied by various observations and remarks that were derived from the output of the aforementioned simulator.

Chapter 5 is the closing chapter, containing a brief summary of the work done in this Thesis, as well as the conclusions that were obtained from it. It also includes some recommendations for future work to be done in this area of study.

This Thesis is complemented with a set of annexes with complementary information to the study. In Annex A, the frequencies of all radio channels that may be used in the radionavigation systems under study are presented. Annex B contains a list of all FM audio broadcasting systems installed in Portugal. It also includes the relevant individual characteristics of each one of the FM stations, as well as their locations. In Annex C, the navigational charts of the flight routes relevant for the study are presented. In Annex D, the results extracted from the simulator are presented. Only VOR results are presented in an appendix since they are extensive. Annex E contains a listing of the FM broadcasting stations considered in the evaluation of obstacles in the ILS related scenarios.

Chapter 2

Basic Concepts

This chapter presents the two radionavigation systems that are going to be studied (ILS and VOR) and also FM audio broadcasting systems. One will also present how the interference between these systems is originated, followed by the state of the art in this area.

2.1 VOR

This section presents a brief explanation of a VOR and its components, being based on [Fern13].

2.1.1 System Overview

A VOR is a radionavigation system operating in the VHF band that supplies aircrafts with positioning relative to ground stations/beacons (bearing). The VOR provides azimuth guidance to the aircraft by displaying in the receiver end the bearing relative to the ground station radial and if the airplane is going “to/from” the ground station [NAV12a]. The VOR ground station provides guidance by transmitting 360 radials separated by 1° , which provides the orientation of the aircraft relative to the beacon’s position. The radial corresponding to 360° is used as a reference, being pointed to the magnetic North.

The beacons are constantly transmitting two different types of signals: a reference one and various radials with bearing information. Each of these radials carry the guidance information through an RF phase-shift relative to the 360° radial measured in a clockwise rotation, e.g., the 90° radial corresponding to the magnetic east has a 90° phase-shift relative to the reference one.

Considering that the information is carried through the phase-shift of the signals, there are repeated signals in 180° angles that render the aircraft unable to distinguish between the two directions. As a countermeasure, the VOR is complemented with a Distance Measuring Equipment (DME) that supplies the user with the distance between the aircraft and the ground station. This pairing of equipment is given the name of VOR/DME.

The airplane’s DME transmits a pair of pulses separated with a defined time interval. The ground system receives them, and transmits back with the same format but in a different frequency. The DME then calculates the traveling distance depending on the elapsed time between sending and receiving the signal. This system uses frequencies in between 960 and 1 215 MHz [FAAG14].

There are various kinds of VORs with different purposes besides the Conventional VOR (CVOR), but nowadays, only one more type is used in radionavigation, the Doppler VOR (DVOR) that takes advantage of the Doppler Effect on the transmitted signals to generate the required phase-shift for the variable signal. The one that is most commonly used as a navigation aid is the DVOR due to being less affected than the CVOR by the surrounding terrain, and since the receiver does not differentiate between DVOR and CVOR ground stations, the latter has been gradually replaced by DVORs [NAV12b].

The transmitting power of a DVOR station is typically around 50 W, being adjustable between 25 and 100 W, depending on the desired range. The effective range of the VOR is also determined by the flight altitude of the aircraft due to RF propagation characteristics. The range of a VOR can go up to

130 NM for higher altitudes. The receiver thresholds are defined by Standard Service Volume (SSV) designations. Table 2.1 presents the different SSV classes and the ranges for the different flight altitudes and designations.

Table 2.1 - VOR/DME classes and ranges (adapted from [FAAG14]).

SSV Class designator	Altitude [ft]	Range [NM]
T (Terminal)	1 000 – 12 000	25
L (Low Altitude)	1 000 – 18 000	40
H (High Altitude)	1 000 – 14 500	40
	14 500 – 60 000	100
	18 000 – 45 000	130

Besides the horizontal range, the ground system also has a blind spot in its propagation region. The antennas propagate signals up to 60° above the horizon, which leaves a zone above the beacon unattended with any viable VOR information. For the region covered by the VOR signal, it must be guaranteed a minimum signal level of –79 dBm to provide an effective radio aid [ICAO96].

2.1.2 Operation Mode

As stated in Subsection 2.1.1, the VOR works through the comparison of the phase difference between a reference signal and a variable one, providing the aircraft with azimuth guidance to the VOR beacon. To that end, the ground station is composed of a non-directional transmitter along with an array of antennas that loop at 30 Rotations per Second (RPS). The former transmits the reference signal and the latter the radials with bearing information.

Due to the electronic or mechanical loop done in the antennas, it is possible to generate a signal transmission corresponding to 30 Hz Amplitude Modulated (AM) waves. This rotation implies that the difference between the phase of each of the radials and the reference signal with a phase-shift equals the deviation of its propagation direction and the magnetic North. By calculating the phase-shift between both received signals, the aircraft VOR receiver is able to obtain the magnetic bearing leading to the position of the ground beacon. Figure 2.1 depicts the VOR operation and signals transmitted.

The receiver in the aircraft interprets the signals originated from both the CVOR and DVOR alike, not being able to differ in between them. Even though there is no difference in the receiver end, the generation of the signals differs in the two systems, the main difference being in the modulation of both reference and variable signals. One of the differences between the CVOR and DVOR is the fact that the CVOR does the loop through mechanical means, while the DVOR does it electronically. However, nowadays, the CVOR also depends on electronic loops to generate its signals, although its operation differs from a DVOR ground beacon.

In a DVOR, the modulation of the signals is reversed compared to the CVOR, that is, the reference signal is an AM one and the variable is FM. The frequency shift for the FM signal is generated through

a Doppler shift, which corresponds to an apparent FM signal, since its modulation is done through an equivalent Doppler Effect. The generation of the signal of the VOR is complex, being explained further in the following subsection.

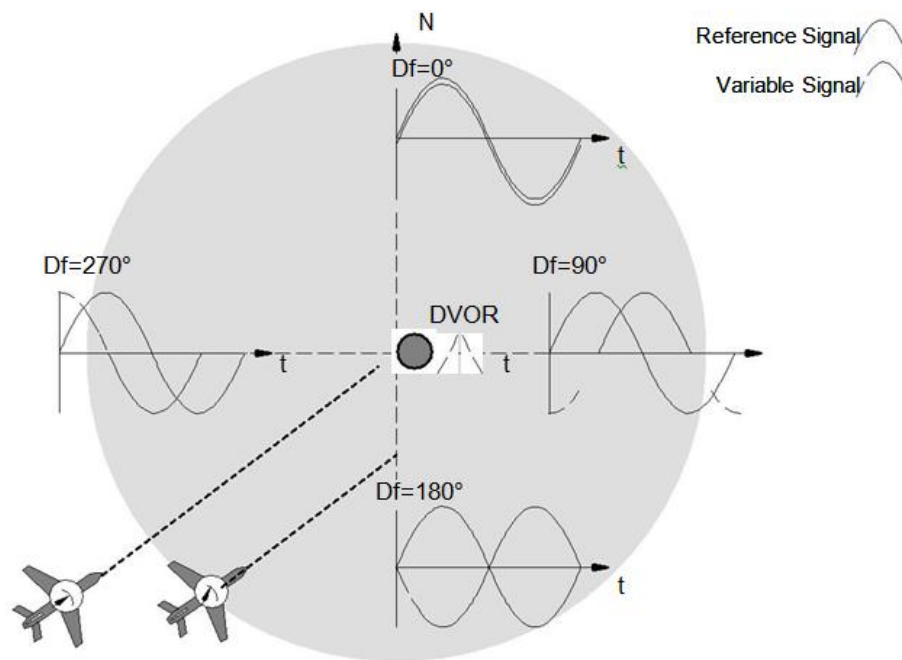


Figure 2.1 - VOR operation illustration (extracted from [NAV12a]).

2.1.3 Radio Interface

The VOR ground station transmitter is composed of horizontally polarised antennas with omnidirectional characteristics transmitting on RF carriers within [108.00, 117.95] MHz, with a 50 kHz channel spacing. It only uses the ones with the first decimal place even for frequencies lower than 112.00 MHz, due to sharing the band with the ILS. Regarding transmission, one must characterise the signals, since they are critical for its understanding. The reference phase signal modulates a subcarrier with an offset of the carrier frequency of $\pm 9\,960$ Hz with a frequency shift of ± 480 Hz [NAV12a].

Two crossed omnidirectional dipoles radiate the variable signal. The dipoles receive a sideband signal, i.e., with a suppressed carrier, from the sideband transmitters with a 90° phase difference in the envelope. An omnidirectional antenna transmits the carrier, hence, there is a superposition of the carrier and the 30 Hz sidebands in the field, with the resulting 30 Hz signal depending on the azimuth and related to the reference signal. This antenna also transmits identity codes along with the carrier. These identity codes are transmitted in Morse code and they correspond to a 3 letter identification. A VOR may also transmit a broadcasting signal within $\pm[300, 3\,000]$ kHz.

As stated before, the variable phase and the reference phase signals in a DVOR are transmitted in FM and AM respectively, opposite to the CVOR ground beacon. One of the major benefits of using a DVOR is its wide-base antenna system, which can only be done by the utilisation of the Doppler

Effect, reducing significantly the interference due to obstacles.

Figure 2.2 presents the frequency allocation of the signals transmitted by the DVOR and the CVOR. The modulation depth of the each frequency can be adjusted within a certain range, the acceptable range being as follows [NAV12a]:

- 30 Hz navigation signal: 30%.
- 9 960 Hz auxiliary carrier: 30%.
- Voice: 30%.
- Identity code: 10%.

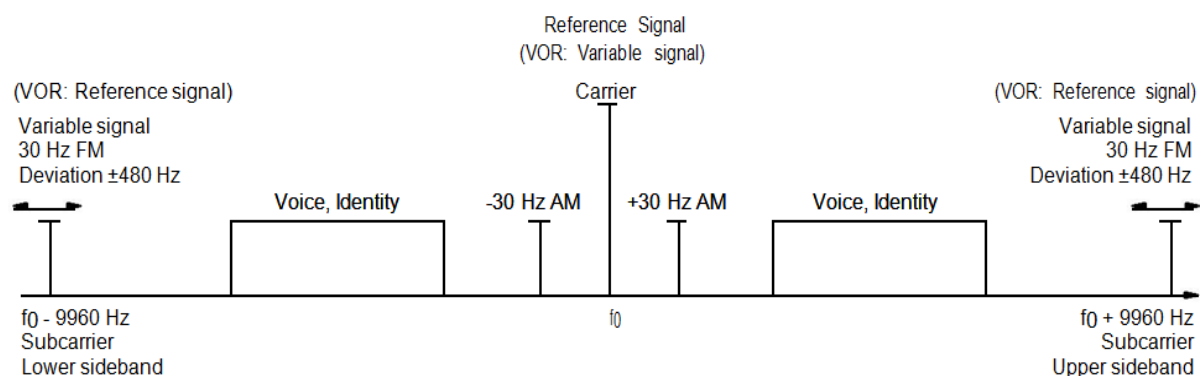


Figure 2.2 - Frequency spectrum of a DVOR (CVOR) (extracted from [NAV12a]).

2.2 ILS

This section addresses the ILS, focusing firstly on its overall constitution and then on the specifications of its Localiser component.

2.2.1 System Overview

The ILS is a radionavigation system operating in VHF and Ultra High Frequency (UHF) bands that is installed at the threshold of a landing runway in an aerodrome, assisting the airplane aligning for landing. The system is divided in three components that supply the pilot with a 3 dimensional guidance into the landing zone.

The Localiser (LOC) works in the VHF band, being used to position the aircraft correctly in the horizontal axis of the runway, i.e., azimuth guidance [THAL05a]. The horizontal orientation is done through the reading of the Difference in the Depth of Modulation (DDM) of two signals transmitted by the LOC ground system, which will be explained in further detail in Subsection 2.2.2 [THAL04]. Both of the transmitted signals are equally AM on 90 Hz (left lobe) and 150 Hz (right lobe) transmitted in a Radiofrequency (RF) carrier within [108.10, 111.95] MHz. There are 40 LOC channels with a 50 kHz spacing, corresponding to the frequencies within the band with odd tenths, e.g., 108.10, 108.15, and 108.30.

The ILS LOC is composed of an antenna array spread horizontally, being located at the threshold of the runway. Figure 2.3 shows the orientation of both lobes of the transmitted signals. The sector centred at the runway has a null value of DDM, and as the aircraft deviates from the centreline, the receiver captures a higher value of DDM, enabling the orientation relative to the track. Additionally, the ILS LOC also transmits a 1020 Hz audio Morse code with the identification of the ILS.

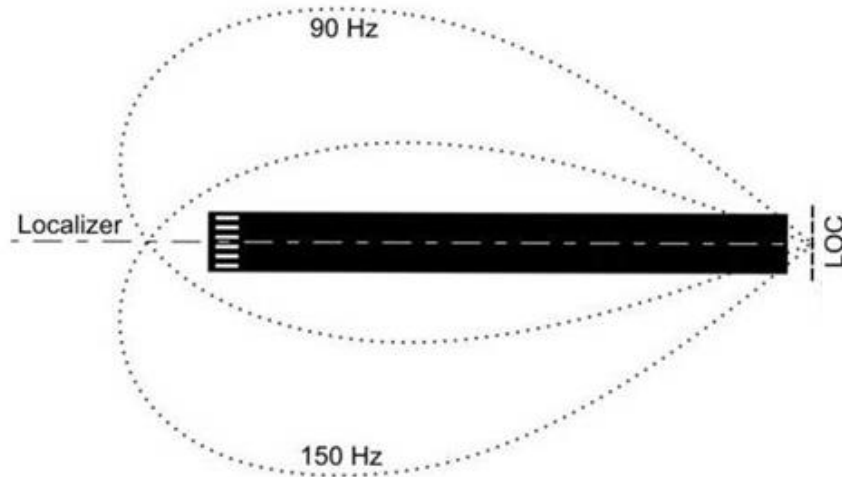


Figure 2.3 - ILS LOC lobes diagram (extracted from [ILSy14]).

The Glide Slope (GS) is a system similar to the LOC, but instead of providing guidance to the runway centreline, it informs about the vertical alignment of the plane relative to a reference glide path. This glide path is normally tilted around 3° relative to the ground [FAAG14]. The antenna array is positioned outside the runway approximately 230 to 380 m from the threshold, spaced 80 to 200 m from its centreline. The two lobes are AM signals of 90 Hz (upper lobe) and 150 Hz (lower lobe) sine waves, transmitted on a carrier within [329.15, 335.00] MHz. As stated before, there are 40 ILS channels, and the GS frequencies have a channel spacing of 150 kHz. Each of the 40 ILS channels corresponds to a pairing of a LOC and a GS frequency.

The last variable that the ILS indicates corresponds to the remaining distance until the touchdown zone. The Marker Beacons (MB) correspond to a maximum of three beacons spread along the extended runway front-course. All of these beacons are composed of directional antennas sending the signal vertically, making the form of an inverted cone. The Outer Marker (OM) is placed 6.5 to 11 km from the threshold and the Middle Marker (MM) located around 1 km. Some aerodromes have an Inner Marker (IM) that is placed around 60 m from the runway. The markers send signals in the 75 MHz band, and as the plane enters in the inverted cone defining the beacons' line of sight, the receiver differentiates between the different beacons and displays in which region the airplane is located.

Some aerodromes have a DME associated with the ILS, located near the landing runway, being used instead of the marker beacons to provide the distance information. The DME is typically calibrated to give the distance relative to either the touchdown or the threshold of the runway, instead to the location of the DME equipment.

There are three ILS categories that depend on the ground and airborne equipment. Each of these

categories have minimum Decision Heights (DH), at which the pilot decides if the landing manoeuvre is possible or needs to be repeated, and the Runway Visibility Range (RVR). The heights are typically given in imperial units and horizontal visibility ranges in metric ones. The categories are defined as follows [ICAO13]:

- Category I (CAT I) is the most basic one, and it requires minimum DH of 200 ft and either an RVR not less than 550 m or a visibility equal or higher than 800m.
- Category II (CAT II) is more calibrated than a CAT I operation. Its DH is within 100 and 200 ft and the minimum RVR of 300 m.
- Category III (CAT III) presents the most precise equipment, requiring special airborne equipment to fully grasp the functionality of the system. The CAT III approach is divided in three subcategories:
 - CAT IIIa is intended for operations with a DH higher lower than 100 ft or no DH at all, and a minimum RVR of 175 m.
 - CAT IIIb is intended for operations with a DH higher lower than 50 ft or no DH at all, and a RVR within 50 and 175 m.
 - CAT IIIc is intended for operations with no DH and no RVR limitations.

There are some variations and complementary systems to improve the efficacy of the readings, but considering the purpose of this Thesis only the ILS LOC was studied, due to its band of frequencies being the only one close to FM broadcasting systems, i.e., [87.5, 108] MHz, [ANAC13].

2.2.2 LOC System

The LOC ground system is typically composed of an antenna array of either Log-Periodic Dipoles Arrays (LPDA) or dipoles with a reflection screen [THAL05a]. The transmitted signals are polarised horizontally, and an ILS LOC system can be single or dual frequency. When operating in single frequency, the array only transmits a course signal, but in dual frequency it also transmits a clearance one [THAL04]. The single frequency operation is typically used in landing runways without significant reflecting obstacles.

Those two signals transmit the same information but have different purposes. The course signals' radiation pattern corresponds to lobes with a longer range that radiate up to 10° deviation of the extended runway centreline with a coverage range up to 25 NM. On the other hand, clearance signals are used for a shorter but broader range, covering azimuth angles within 10° and 35° from the extended runway centreline, reaching up to 17 NM. The coverage range of these signals may be reduced, depending on the topographical features of the terrain, down to 18 and 10 NM, respectively [ITUR10]. Focusing on the vertical propagation, an ILS LOC must cover the region situated between 2° and 7° vertically for ground distances lower than 4.7 NM. For regions farther away, it must cover every region between the altitudes of 305 and 1 900 m.

Figure 2.4 illustrates the range of an ILS LOC system both vertically and horizontally. For an ILS LOC to be considered functional, a minimum signal level of -86 dBm must be guaranteed in every point

inside the covered region [ICAO96].

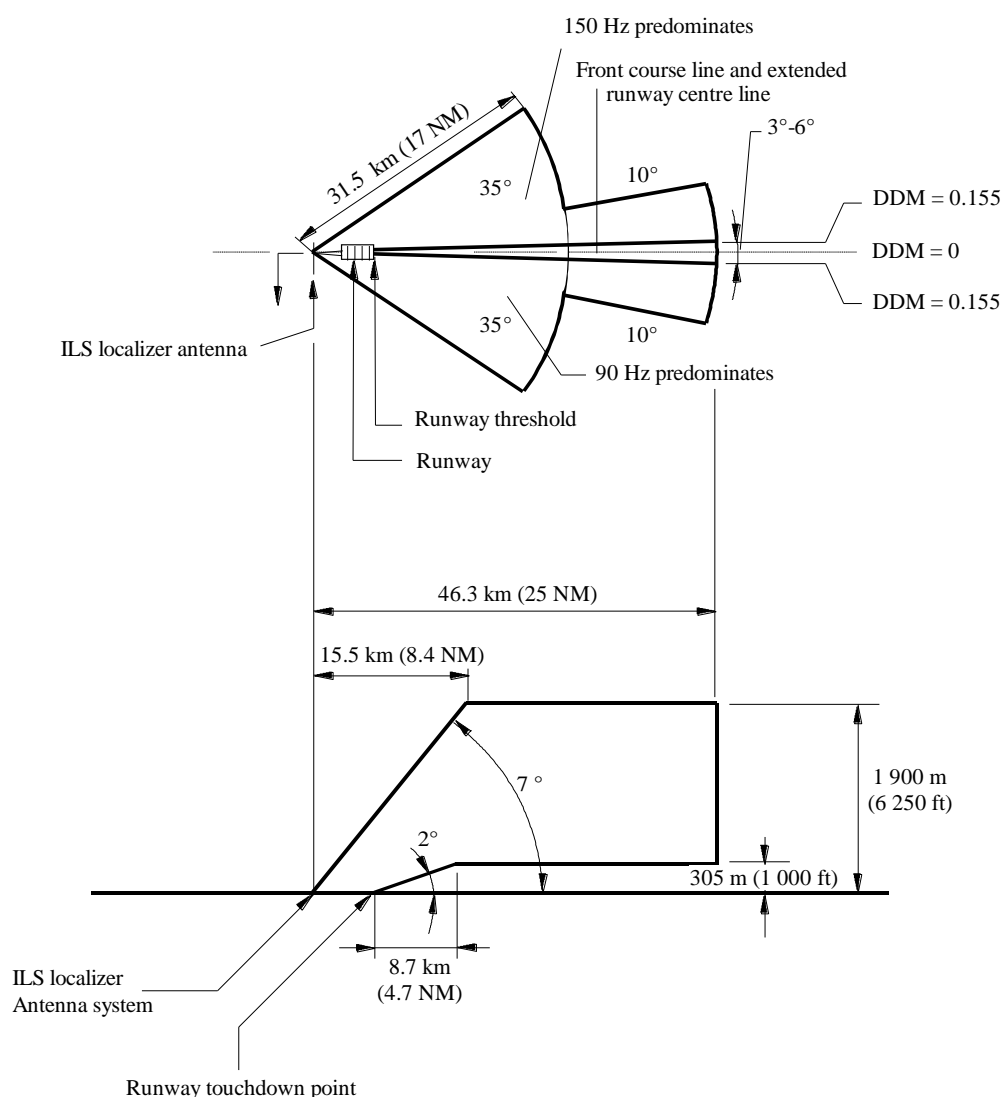


Figure 2.4 - Coverage of an ILS LOC system (extracted from [ITUR10]).

An antenna array of a dual frequency LOC system transmits the course and the clearance signals, and it is normally defined by its total number of elements. In some arrays, it is defined by the number of elements transmitting the course and clearance signals, i.e., a 14/10 Localiser Array corresponds to all 14 elements radiating course signals and the centre 10 transmitting clearance signals. The maximum output power of these signals rounds 25 W [THAL04].

The course signal is transmitted in the ILS LOC carrier frequency, and the clearance signal is transmitted with an offset of ± 4 kHz [NAV14b] and [THAL05b].

The array transmits two different RF signals: a Carrier-plus-sideband (CSB) and a Sideband Only (SBO). The CSB signals are radiated by pairs of antennas having equal amplitude and in-phase, resulting on a waveform with a peak on the runway's centreline and decreasing as the angle of deviation increases. The SBO signals are transmitted with equal amplitude but each pair is 180° out of phase from each other. This generates a signal composed of only sidebands with a suppressed carrier.

The DDM results from the comparison of the SBO and CSB signal strengths, and it increases as the value of SBO signal decreases relatively to CSB signal. Thus the extended runway centreline (0° deviation) the point in which the SBO signal, and by association the DDM, are null. Figure 2.5 shows the radiation patterns of the two signals for the course and clearance signals, where one can see the evolution of DDM as the absolute azimuth angle increases. The radiation patterns depend on the characteristics of the array, i.e., the number of pairs of antennas present in the array, their spacing and the current distribution among these elements.

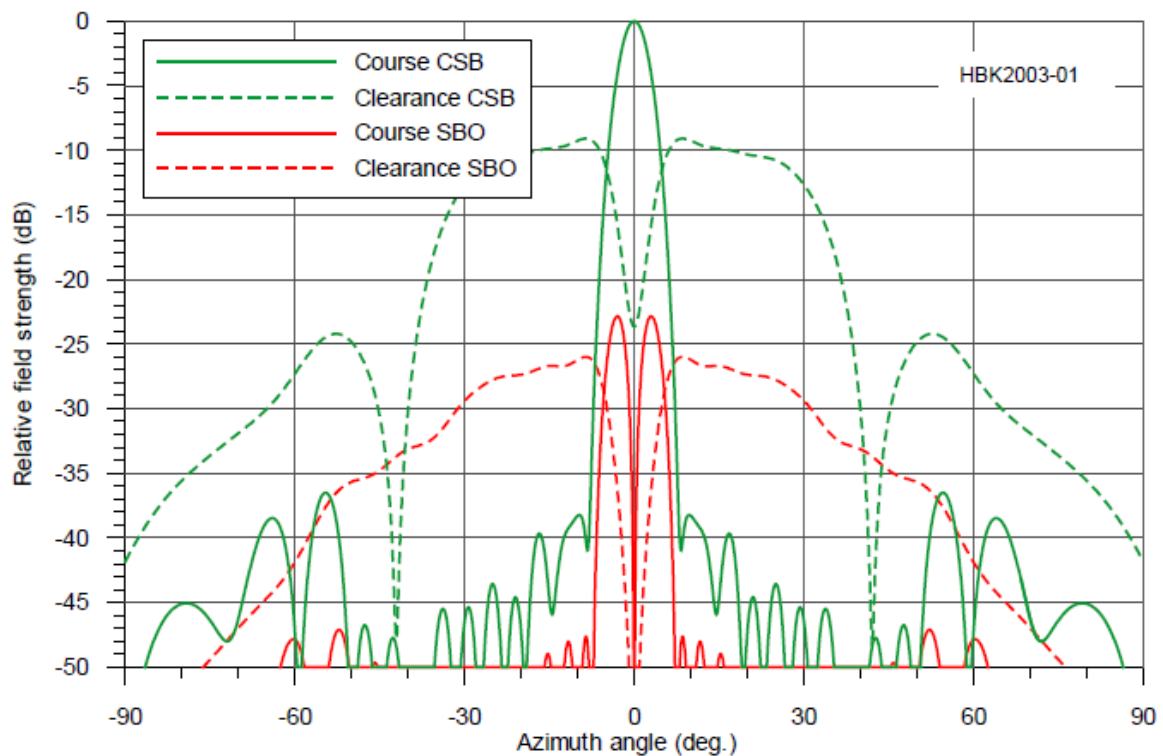


Figure 2.5 - CSB and SBO field strength using a two-frequency 16-element LPDA (extracted from [Indr13]).

2.3 FM Broadcasting

This section presents an overview of a FM broadcasting system and its radio interface according to Portuguese standards.

2.3.1 System Overview

FM audio broadcasting systems provide channels to users through transmissions in the VHF band. The system is composed of a broadcasting antenna in the transmitter end that can cover up to several kilometres. FM broadcasting is provided virtually everywhere. To that end, there are stations scattered throughout every region of the territory. Each one of these stations has an output power that defines a

maximum coverage range, depending also on the environment and interference sources. The coverage range of a station corresponds to the region where the signal can be protected against interference for over 99% of the time [ITU84].

The frequency allocations for each broadcast station vary from region to region as to optimise the band and avoid interference. The installation of the stations is carefully studied in order to provide an optimal coverage for the least cost and also to avoid co-channel interference.

In some countries, such as Brazil and USA, FM broadcasting stations are divided in various classes and each class is defined by its reference facilities and protected contours [FCC14a]. A service contour corresponds to the circular-shaped form inside which a certain electric field can be guaranteed. In Portugal, FM radio stations are categorised as national, local or regional, which is directly related to their transmission power.

Broadcasting antennas are typically located at a high altitude, since it typically implies a larger coverage range. The height of a communication tower is typically around 20 m, although it can be over 100 m, such as the Centro Emissor de Monsanto which is one of the most distinctive communication towers in Portugal with around 120 m.

Depending on the transmitting power and its location, a broadcast station is able to cover up tens of kilometres. The Effective Radiated Power (ERP) of a commercial FM broadcasting station can go over 100 kW, depending on the scenario and the desirable coverage range. In Lisbon, the typical maximum ERP rounds 100 kW [ANAC14].

In 1984, the worldwide standards for FM broadcasting were defined in an international agreement made by ITU [ITU84]. These standards define, amongst others, the frequency spectrum characteristics and the installation procedures regarding co-channel and even air navigation radionavigation interference. In Portugal, the RF allocation of FM broadcasting throughout the country is controlled by ANACOM.

2.3.2 Radio Interface

Since the radio interface of FM broadcasting services may vary from country to country, the standards presented are those taken in Portugal.

Broadcasting stations transmit RF signals in any polarisation, even though nowadays they are adopting circular polarisation, since it presents a better solution in terms of shadowing and out-of-phase reflection destructive interference and, additionally, it covers both linear polarisations (with a 3 dB loss).

There is a big variety of antennas used by FM broadcasting stations depending on the scenario. Some of the antennas used are presented in [OnDy07], such as:

- Ring stub and twisted ring.
- Shunt and series fed slanted dipole.
- Multi-arm short helix.

- Panel with crossed dipoles.

The RF signals are transmitted in the VHF band within [87.5, 108.0] MHz. The spacing between carriers is not standard, and it can go up to 200 kHz [ANAC13]. The maximum allowed frequency deviation in FM broadcasting corresponds to ± 75 kHz according to ITU Radiocommunication Sector (ITU-R) standards [ITUR01]. The type of transmission that is typically used is a stereophonic one, using a pilot tone system.

The stereo coder adds the left and right audio signals, composing a mono signal that occupies up to 15 kHz of deviation. To compose a stereo audio signal, the pilot tone system also transmits a subcarrier that permits the receiver to split the left and right audio signals. This subcarrier is a double-sideband suppressed-carrier (DSB-SC), which ideally means that the information is transmitted only in its sidebands and none in the carrier frequency (suppressed carrier). This subcarrier carries information corresponding to the difference between the right and left audio signals. The subcarrier's central frequency is at 38 kHz deviation, thus occupying the sidebands from 23 to 53 kHz. To allow the demodulation of the left and right signals, the stereo coder also transmits a pilot tone at 19 kHz (half of the frequency of the DSB-SC), allowing the receiver to access the subcarrier [ITUR01].

It is possible to reproduce a stereo signal using only 53 kHz of spectrum, although nowadays additional information besides the stereo audio is transmitted. Radio Data System (RDS) can carry a big variety of information, such as broadcast station information, time or even an alternative frequency for the same station in case of weak signal at the receiver. The RDS subcarrier is at 57 kHz, which corresponds to twice the frequency of the pilot tone, allowing the decoder to easily access this subcarrier. Besides RDS, FM broadcasting stations also transmit a Subsidiary Communications Authority (SCA) signal, which is not part of the regular FM audio broadcast, and cannot be received by common FM receivers [FCC14b]. The SCA signal is used for purposes that are not related to the audio broadcasting, but rather for, e.g., paging, traffic control signal switching or even bus dispatching; there can be multiple SCA signals. Figure 2.6 presents the spectrum of an FM broadcast signal using a pilot tone system.

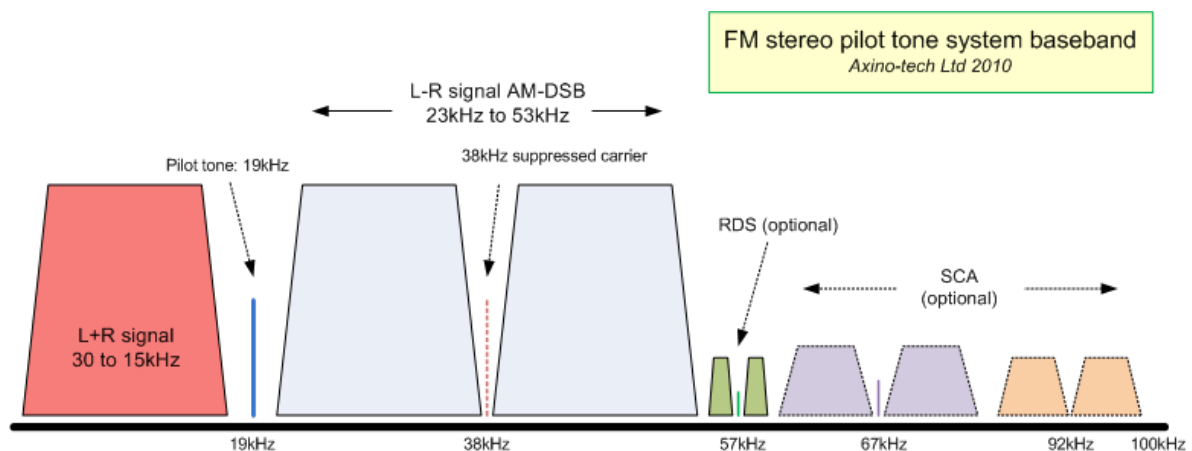


Figure 2.6 - FM stereo pilot tone system baseband (extracted from [AxTe14]).

2.4 Interference

In this section, one addresses the interference that FM broadcasting may cause on both ILS LOC and VOR, being based on ICAO and ITU-R recommendations, [ICAO08] and [ITUR10].

2.4.1 Problem Assessment

A high density of FM broadcasting channels is expected in any urban area, and aircraft navigation routes are not an exception. Thus, radionavigation systems are susceptible to interference originated from FM broadcasting stations that are transmitting in a neighbouring frequency band. FM broadcasting signals could be regarded as noise when considering the overview of ILS LOC and VOR, but since both aeronautical systems use very specific frequencies to provide critical guidance to aircrafts, it makes them prone to interference. In the case of ILS LOC, it corresponds to frequency shifts of 90 and 150 Hz, and for VOR to 30 and 9 960 Hz [ITUR10]. The impact of interference on an aeronautical receiver is non-negligible. It can cause a VOR receiver to present a bearing to a different ground station that is using an adjacent co-channel, or make an ILS LOC deviation signal erratic and generate sound in its voice channel [ICAO02].

Presently, there are two official models for ILS and VOR receivers developed by ICAO, which are used to calculate the impact of the interference caused by FM Broadcasting: one was agreed at a meeting of Task Group 12/1 in Montreal in 1992 (Montreal receivers), and the other was published in Annex 10 in 1996, presenting better interference immunity criteria [ICAO96]. Annex 10 also presents various regulations and standards that the aeronautical receivers must fulfil.

ICAO defines the FM Broadcasting interference in aeronautical radionavigation systems by dividing its effects in two categories [ICAO08]:

- Type A interference corresponds to the interference caused by FM broadcast emissions into the aeronautical frequency band.
- Type B interference is generated in the aeronautical receiver due to side effects of emissions outside of the aeronautical band.

2.4.2 Interference Mechanisms

In what follows, one assesses each of the categories defined by ICAO and verifies which interference mechanisms are involved. Both Type A and Type B interferences are subdivided into subcategories.

Type A1 interference is caused by a spurious transmission of an FM broadcasting transmitter or by the intermodulation of various transmitters generating an interfering component in the aeronautical band.

Spurious emissions are located outside the reference carrier frequency band, including effects such as harmonic and parasitic emissions. They correspond to emissions that do not carry any information relevant to the transmission, and can be reduced without causing any effect on transmission.

Intermodulation Distortion (IMD) is an effect that occurs due to the interaction of harmonics of two or

more signals with different frequencies. These harmonics are generated due to the non-linearity of the components pertaining in the signal modulation process, e.g., amplifiers and oscillators. The sum of the harmonics will generate various IMD products outside the carriers' bands, and the frequencies of these products correspond to the ratio of the carriers frequencies.

Figure 2.7 presents the frequency of the IMD products of two signals and an approximate scale of their amplitudes. The most relevant for the interference with neighbouring frequency bands are the 3rd order products due to being the products with frequency closer to the carriers and also for having significant amplitudes.

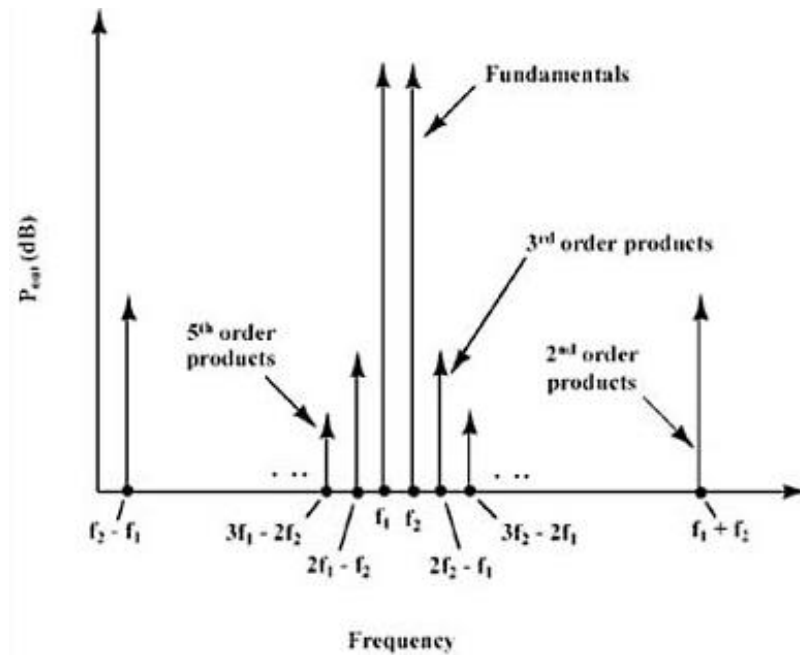


Figure 2.7 - IMD products of two signals and their frequency relations with the carriers (extracted from [RFGN14]).

There are also interfering non-negligible components of FM broadcasting signals in the aeronautical band that cannot be reduced without damaging the information being transmitted, due to their proximity to the carrier band, contrary to spurious emissions. This type of interference is named by ICAO as Type A2 one, and these components correspond to the out-of-band emissions that spill into the aeronautical band. According to [ITUR14], out-of-band emissions correspond to those with a deviation lower than 250% of the wanted bandwidth of the signal, and spurious emissions for a separation higher than 250%.

Unlike Type A interference, Type B one is generated specifically in the aeronautical receiver, being also divided into two categories. Type B1 occurs when the intermodulation of two or more FM broadcast signals is generated in the receiver due to being forced into non-linearity by the presence of FM broadcasting signals outside the aeronautical band [ITUR10].

Since the aeronautical receiver has to be driven into regions of non-linearity, at least one of the signals needs to have enough strength to do so. Besides the power of the signal, for this interference to take place, there must exist a ratio in between the frequencies of the FM broadcast channels that will

create an IMD product in the RF channel in use by the aeronautical receiver. Only 3rd order IMD products are considered, hence the cases analysed correspond to the intermodulation of two or three signals.

Along with Type B1 interference, if the signal strength of the FM broadcast signal(s) at the input of the receiver is too high, it can also cause saturation of the front end, resulting in the desensitisation of the receiver. This phenomenon is called Type B2 interference, and occurs when the power of the input signal nears the maximum input power of the receiver, making it incapable of discerning the oscillations of the wanted signal.

2.5 State of the Art

ILS started its appearance in commercial aircrafts in the 1940s and VOR in the 1960s, and since then lots of studies have been developed about interfering sources. The research on the impact of FM broadcasting signals on these systems has been progressing over the years. In this section, some of the studies that allowed the understanding and analysis of this interference effect are presented.

These studies peaked in the 1970s and early 1980s, due to the uprising of both the radionavigation systems and FM broadcasting, which led to a change in the frequency spectrum agreement in Europe and in some parts of Asia. In 1979, ITU announced at the World Administrative Radio Conference (WARC) that the frequency band usable by broadcasting stations, which had an upper limit of 100 MHz in half the world until then, was to be increased up to 108 MHz, thus increasing the available band for FM broadcasting and also the risk of interference with the aeronautical radionavigation systems [ITU79].

Essman and Loos in [EsLo78] developed theoretical models that allow a further understanding and prediction of the interference effect that FM broadcasting has on an aeronautical receiver. This study took the various interfering mechanisms into account, such as the spill over into the aeronautical frequency band and the interference occurred during the RF-amplifier stage, which are similar to the categories defined by ITU as Type A and Type B interferences, respectively. For every stage, Essman and Loos developed analytical models for each of these components and then compared the theoretical values obtained from these models with experimental results. Essman and Loos also designed a computer program capable of predicting the interference effects of the FM broadcasting stations by analysing the different parameters of the scenario.

Also in 1978, Sawtelle and Dong in [SaDo78] studied the impact of IMD interference in the radionavigation receiver. To that end, they did flight tests with controlled interference input to determine if it was possible to improve receivers' immunity to this interference. Sawtelle and Dong concluded that by increasing the rejection of FM signals by 10 dB on the aeronautical receiver, it would eliminate most of the FM broadcasting interferences.

In 1981, the Radio Technical Commission for Aeronautics (RTCA) published a report [RTCA81], which

involves the study of the effects of the interference of FM broadcasting on the ILS, VOR and VHF communications used in aeronautics. Besides the study of the interference effect caused by FM broadcasting and the development of models, there were also studies concerning the improvement of the receiver in order to reduce this effect.

Badinelli and Cushman in [BaCu91] tested the implementation of various external filters in order to reduce Type B interference. The authors mentioned that the study only focused on the attenuation of the interference through external passive filters, without considering the cost efficiency or the environmental conditions. Badinelli and Cushman concluded that external passive filters can reduce Type B1 interference, i.e., they can reduce the IMD generated in the receiver by high power FM broadcasting signals.

In response to these studies, ICAO proposed in Montreal in 1992 a model for the receivers (which were called Montreal receivers), and later on in [ICAO96] a revised model for the ILS LOC and VOR receivers. With this document, ICAO presented global standards that must be applied to every aeronautical radionavigation receiver according to various interference immunity criteria, and, as of January 1st 1998, every avionics receiver is in agreement with these standards.

In 1995, ITU-R presented Recommendation SM.1009-1, which presents regulations for airborne receivers and FM broadcasting stations in order to allow compatibility between the two neighbouring frequency bands. This document has been regularly updated, the most recent recommendation being published in 2010 [ITUR10].

Chapter 3

Model Development

This chapter presents the models that were developed for this Thesis, followed by the explanation of the methodology used in the simulator, as well as the assessment of the aforesaid simulator and models.

3.1 Propagation Models

This section contains information regarding the signal propagation models necessary for the analysis of the transmission links. The model depends on the transmitter and on the scenario under evaluation.

Figure 3.1 presents the general scheme of the system under analysis in this Thesis. One needs to assess the ratio between the wanted signals transmitted by the air radionavigation ground stations and the interfering components received in the aircraft. To quantify this relation, the modelling of the RF propagation losses is imperative.

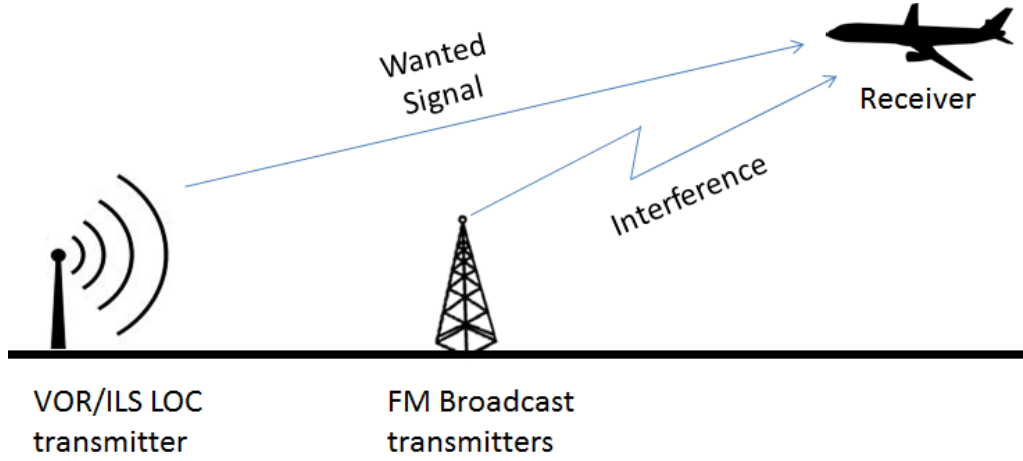


Figure 3.1 - Diagram of the links of the system in study.

The systems have working frequencies in the VHF band, so, factors such as the atmosphere and rain are not taken into account, since that their impact caused is too small to be taken into consideration.

When considering long distance radio communications, the Earth's effective radius considered is obtained through (3.1) due to the impact that the atmosphere has on the radio waves,

$$R_e \text{ [km]} = K R \text{ [km]} \quad (3.1)$$

where:

- R_e : effective Earth's radius.
- K : multiplication factor, typically with the value 4/3.
- R : Earth's radius.

One should also take into account the distance to the radio horizon that can be calculated by (3.2),

$$d_{RH} \text{ [km]} = \sqrt{(R_e \text{ [km]} + h_{t,MSL} \text{ [km]})^2 - R_e^2 \text{ [km]}} \simeq \sqrt{2R_e \text{ [km]} h_{t,MSL} \text{ [km]}} , \text{ for } R_e \gg h_{t,MSL} \quad (3.2)$$

where:

- d_{RH} : distance from the terminal to its radio horizon.
- $h_{t,MSL}$: height above Mean Sea Level (MSL) of the terminal.

In order to obtain the distance between the two terminals, one can use their geographic coordinates in (3.3) to calculate the Earth circumference angle between them, followed by (3.4) to obtain the ground distance [Pint11].

$$\theta_{t-air}[\text{rad}] = \text{acos}[\cos(\phi_{air}) \cos(\phi_t) \cos(\lambda_t - \lambda_{air}) + \sin(\phi_{air}) \sin(\phi_t)] \quad (3.3)$$

$$d_{[\text{km}]} = R_{[\text{km}]} \theta_{t-air}[\text{rad}] \quad (3.4)$$

where:

- θ_{t-air} : Earth circumference angle between the station and the aircraft.
- ϕ_{air} : Latitude of the station position.
- ϕ_s : Latitude of the aircraft position.
- λ_t : Longitude of the station position.
- λ_{air} : Longitude of the aircraft position.
- d : ground distance between terminal and aircraft.

In this Thesis, there are 3 types of transmissions that are analysed. VOR transmitters are considered to be ideally located for the surrounding airspace, hence, line of sight is always considered to be unobstructed, so, for this transmission, a free-space propagation model is applied. In the case of the ILS LOC, since it is located near the threshold of the runway and the runway can be assessed as flat, one assesses both the Flat and Spherical Earth models, depending on the characteristics of the link. Finally, FM broadcasting transmitters are spread throughout the various regions to provide radio coverage to most of the country: it is expected to be a high number of obstacles in the propagation of waves, for which the Knife-Edge and Deygout models are used.

In free-space propagation, path loss is given by [Corr14a]:

$$L_o[\text{dB}] = 32.4 + 20 \log(d_{dr}[\text{km}]) + 20 \log(f_{[\text{MHz}]}) \quad (3.5)$$

where:

- d_{dr} : length of the direct ray.
- f : frequency of the signal.

The Flat Earth propagation model can be considered for short distances, since the effect of the Earth's curvature is negligible. Figure 3.2 depicts the transmission ray in between terminals when applying this model. Equation (3.6) presents a reasonable criterion that should be fulfilled to apply this model; it presents the phase error of using the Flat Earth model instead of the Spherical Earth one [Figa12b]. The length of the direct ray in between terminals is given by (3.7),

$$\Delta\phi_{[\text{rad}]} \simeq \frac{2\pi}{\lambda_{[\text{m}]}} \frac{h_t[\text{m}] h_{air}[\text{m}]}{h_t[\text{m}] + h_{air}[\text{m}]} \frac{d_{[\text{m}]}}{R_e[\text{m}]} \ll 1 \quad (3.6)$$

$$d_{dr[m]} = \sqrt{d_{[m]}^2 + (h_{air[m]} - h_{t[m]})^2} \quad (3.7)$$

where:

- $\Delta\phi$: phase difference between using the Flat and Spherical Earth Models.
- λ : wavelength of the transmitted signal.
- h_t : height of the transmitter.
- h_{air} : height of the aircraft.

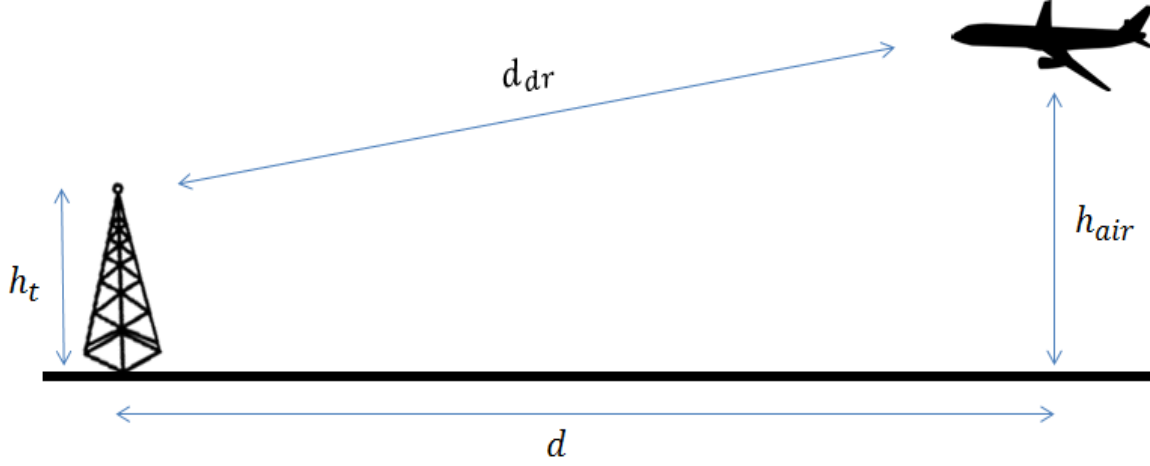


Figure 3.2 - Diagram of the Flat Earth Model.

When considering the Flat Earth model, the received power should be calculated from [Corr14a]:

$$P_{r[\text{dBm}]} = -120 + P_{t[\text{dBm}]} + G_{t[\text{dBi}]} + G_{r[\text{dBi}]} + 20 \log(h_{t[\text{m}]}) + 20 \log(h_{r[\text{m}]}) - 40 \log(d_{dr[\text{km}]}) \quad (3.8)$$

where:

- P_r : power of the signal at the receiver.
- P_t : power of the signal transmitted.
- G_t : gain of the transmitter antenna.
- G_r : gain of the receiver antenna.
- h_r : height of the receiver.

The Spherical Earth model presents a more accurate approach for communications with longer distances [Corr14a]. Figure 3.3 presents the overview of the communication considering a spherical Earth. The objective is to obtain the values of the equivalent effective heights of the terminals (h_{ef}) and transform them into the Flat Earth equivalent.

The following expressions were taken from [Figa12a], which gives the effective heights of both terminals using a reference reflection point. Equation (3.9) is a third order equation from which the location of the reference reflection point can be obtained. Equations (3.10), (3.11) and (3.12) allow the calculation of the effective heights of both terminals.

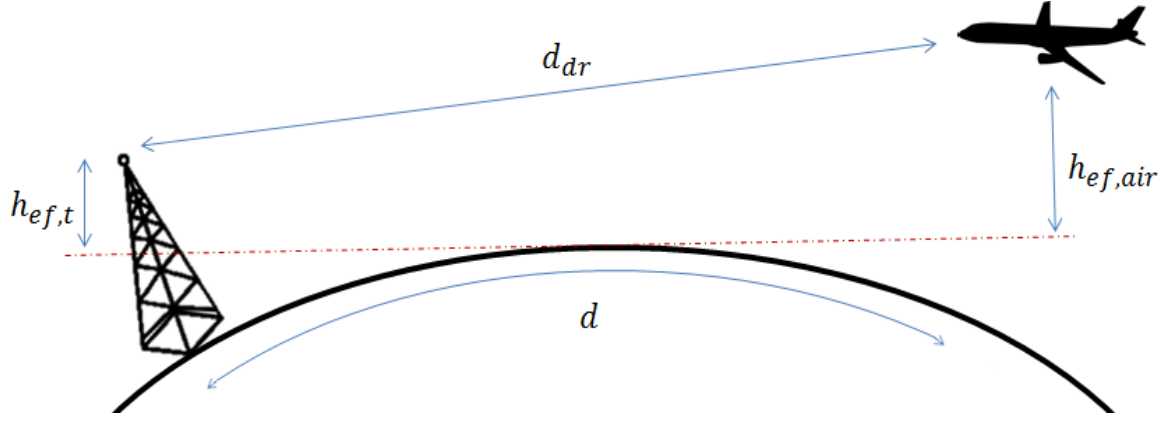


Figure 3.3 - Diagram of the Spherical Earth Model and the Flat Earth equivalent parameters.

$$d_{1[\text{km}]}^3 - \frac{3}{2}d_{[\text{km}]}d_{1[\text{km}]}^2 + \left[\frac{1}{2}d_{[\text{km}]}^2 - R_{e[\text{km}]}(h_{t[\text{km}]} + h_{air[\text{km}]}) \right]d_{1[\text{km}]} + h_{t[\text{km}]}d_{[\text{km}]}R_{e[\text{km}]} = 0 \quad (3.9)$$

$$d_{[\text{km}]} = d_{1[\text{km}]} + d_{2[\text{km}]} \quad (3.10)$$

$$h_{ef,t[\text{km}]} = h_{t[\text{km}]} - \frac{d_{1[\text{km}]}^2}{2R_{[\text{km}]}} \quad (3.11)$$

$$h_{ef,air[\text{km}]} = h_{air[\text{km}]} - \frac{d_{2[\text{km}]}^2}{2R_{[\text{km}]}} \quad (3.12)$$

where:

- d_1 : ground distance between the station and the reflection point.
- d_2 : ground distance between the aircraft and the reflection point.
- $h_{ef,t}$: equivalent effective height of the terminal in the Flat Earth model.
- $h_{ef,air}$: equivalent effective height of the aircraft in the Flat Earth model.

For the power assessment, for the Spherical Earth Model, instead of the physical heights of the stations, one uses the effective height of the terminals, $h_{ef,t}$ and $h_{ef,air}$, in (3.8).

When analysing the line of sight between two points, one should check if there are any obstacles that may cause extra attenuation. The best approach is to verify if the first Fresnel's Ellipsoid is being obstructed, since most of the transmitted energy is concentrated in this region. Equation (3.13) provides the radius of Fresnel's Ellipsoid of order n depending on the distance z to the terminals. The ellipsoid is symmetric, thus, the distance z can be referred to any of the antennas [RoSa14].

$$R_{fe,n[\text{m}]} = \sqrt{n \frac{z_{[\text{m}]}(d_{dr[\text{m}]} - z_{[\text{m}]})}{d_{dr[\text{m}]}} \lambda_{[\text{m}]}} \quad (3.13)$$

where:

- $R_{fe,n}$: radius of the Fresnel Ellipsoid of order n in a point with a distance z to the terminal.

- n : order of the Fresnel Ellipsoid.
- z : distance from the point to the terminal.

When the first Fresnel's Ellipsoid is obstructed, the impact of the obstacle on the link should be quantified. The Knife-Edge model is only applied when the obstacle dimensions are substantially larger than the signal's wavelength [Corr14a]. Since the frequencies in this work are in the VHF band, they comprise a wavelength of roughly 3 m, thus fulfilling the conditions of this model. The impact is quantified by parameter v as in (3.14) [Corr14a]. The higher is the obstruction of the first Fresnel's Ellipsoid, the higher is the value of v and of the attenuation.

$$v = h_{ofe[m]} \sqrt{\frac{2d_{[m]}}{\lambda_{[m]}d_{t[m]}d_{r[m]}}} \quad (3.14)$$

where:

- v : obstacle impediment coefficient.
- h_{ofe} : height from the tip of obstacle to the centre of the ellipsoid (it can have negative values when the obstacle is below the line of sight).
- d_t : distance from the obstacle to the transmitter.
- d_r : distance from the obstacle to the receiver.

The Knife-Edge model path loss generated by the obstacle can be approximated by (3.15). For values of $v \leq -0.8$ the path loss is considered negligible [Corr14a].

$$L_{KE[dB]} = 6.4 + 20 \log(v + \sqrt{v^2 + 1}) \quad (3.15)$$

For the situation where there are multiple obstacles obstructing communication, the Deygout method presents the most reasonable approach, since it is of simple implementation and works very well for most cases. Its disadvantage in relation to other models is that it presents an overestimation of the path loss when the obstacles are too close to each other [Salo13].

First, the v coefficient is calculated for all obstacles, and the one with the highest value of v is labelled as the main obstacle. One obtains the path loss caused by the main obstacle using (3.15) and then the path is divided in two segments with the main obstacle's edge as a new terminal point. Next, the two smaller paths are analysed and the same process is repeated until all obstacles are considered. The total path loss caused by the obstacles ($L_{Deygout}$) corresponds to the sum of all path losses.

3.2 Radiation Patterns

In this section, the radiation patterns of the various antennas are being considered. Both the vertical and horizontal planes must be considered, to obtain the total gain of the antenna depending on the relative position of the aircraft.

3.2.1 Navigation Systems

In order to successfully analyse the different zones of coverage and ranges of propagation, the 3 dimensional radiation patterns of the VOR and ILS LOC systems must be modelled.

The radiation patterns of the VOR array are presented first. VOR ground beacons are modelled as DVOR, which use a circular array of 48 Alford Loop antennas, each of these being defined by an omnidirectional radiation pattern in the horizontal plane. As for the normalised vertical radiation pattern of the VOR array, it is given by [NAV14b]:

$$G_v = \sin\left(\frac{2\pi}{\lambda_{[m]}} h_{t[m]} \sin(\theta)\right) \quad (3.16)$$

where:

- θ : angle between the antenna angle of fire and the receiver in the vertical plane.

Figure 3.4 corresponds to the normalised vertical radiation pattern of a DVOR antenna. For this representation, the characteristics of the VOR located in Lisbon (LIS) were considered, as described in Section 4.1. As one can observe, for angles higher than 60° relative to the ground, VOR coverage is more limited, which represents the beginning of cone of silence located above the VOR.

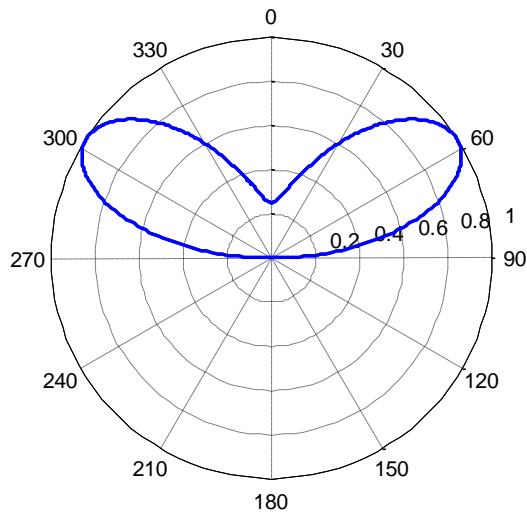


Figure 3.4 - VOR normalised vertical radiation pattern.

Given the horizontal and vertical radiation patterns, the total gain of the antenna is defined by:

$$G_t = G_{max} G_v G_h \quad (3.17)$$

where:

- G_{max} : maximum gain of the antenna.
- G_h : normalised horizontal gain.

For this Thesis, the antenna considered for the ILS LOC is an LPDA one, the modelling being based on the specifications in [Indr13] and [NAV14b].

First of all, it is necessary to characterise the elements composing the antenna system. In [Kibo13], a simple model for the radiation pattern of an LPDA by doing an approximation to a dipole is presented. The horizontal normalised gain of a dipole is given by:

$$G_{h,dip} = \frac{\cos\left(\frac{\pi}{\lambda_{[m]}} l_{dip[m]} \cos(\varphi)\right) - \cos\left(\frac{\pi}{\lambda_{[m]}} l_{dip[m]}\right)}{\sin(\varphi)} \quad (3.18)$$

where:

- l_{dip} : length of the dipole.
- φ : angle between the beam direction and the receiver azimuth in the horizontal plane.

The length corresponds to λ , in order to have a half-power beamwidth similar to the specifications in [Indr13]. Figure 3.5 presents the horizontal radiation pattern of the LPDA, the half-power beamwidth being 48° .

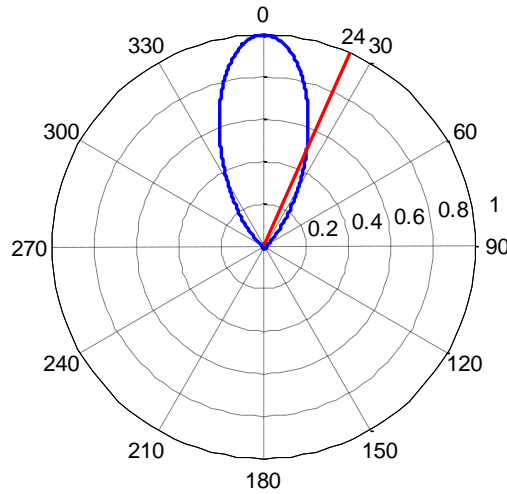


Figure 3.5 - Horizontal radiation pattern of an LPDA.

For the antenna system, one considers the radiation pattern of the course CSB signal, since it corresponds to the signal received by the aircraft at longer distances. The main concern of the modelling is the main lobe of the course signal, since the analysed signal is inside of the section covered by it. The array radiation pattern is given by [More14]:

$$G_{array} = G_{antenna} F_a \quad (3.19)$$

where:

- $G_{antenna}$: gain of the array antenna element.
- F_a : array factor.

F_a depends on the excitation distributed among the various antennas and the distance between elements. The elements of the ILS LOC antenna system are fed differently, depending on the transmitted signal. The normalised antenna factor is given by [More14]:

$$F_a = \sum_{q=1}^{N_{ant}} \left(\frac{a_q}{N_{ant}} e^{j(q-1)\gamma} \right) \quad (3.20)$$

$$\gamma = kd_{dip[m]} \cos(\varphi) + \delta_{[rad]} \quad (3.21)$$

where:

- N_{ant} : number of elements in the array.
- a_q : electrical current ratio between the N^{th} antenna and the reference one.
- γ : phase delay.
- k : wave number.
- d_{dip} : distance between the dipoles.
- δ : electric phase difference between the N^{th} antenna and the reference one.

Most of the LPDA antenna systems used in an ILS LOC are composed of 12 to 24 elements. For the development of this Thesis, all ILS LOCs have the same radiation pattern, independent of the number of elements in the system since their formats are similar and the differences are negligible. As for the ILS LOC horizontal radiation pattern, one considers a 16-element LPDA antenna system [Indr13].

In the scenarios assessment, every point of the aircraft approach is analysed, hence, the selection of the course CSB signal, as it corresponds to the signal that covers the approach following the extended runway centreline. So, for the course CSB signal, one considers the distribution depicted in Table 3.1. One assesses the distance between dipoles constant, equal to 2 m, which is around the lowest distance between the various elements, as observed in Table 3.1.

Table 3.1 - 16-element LPDA antenna system course CSB characteristics (adapted from [Indr13]).

Antenna no.	Distance from centreline [m]	Course CSB	
		a_q	Phase [°]
1	-19.23	0.09	0
2	-16.09	0.18	0
3	-13.13	0.37	0
4	-10.34	0.60	0
5	-7.73	0.80	0
6	-5.30	0.93	0
7	-3.04	1.00	0
8	-0.95	1.00	0
9	0.95	1.00	0
10	3.04	1.00	0
11	5.30	0.93	0
12	7.73	0.80	0
13	10.34	0.60	0
14	13.13	0.37	0
15	16.09	0.18	0
16	19.23	0.09	0

The resulting horizontal radiation pattern is plotted in Figure 3.6; by comparing it with the one in Figure 2.5, one can observe that it is a valid approach to the one presented in Figure 2.5. The half-power beamwidth corresponds to 6° , which is a close approximation of the 5.2° indicated in [Indr13].

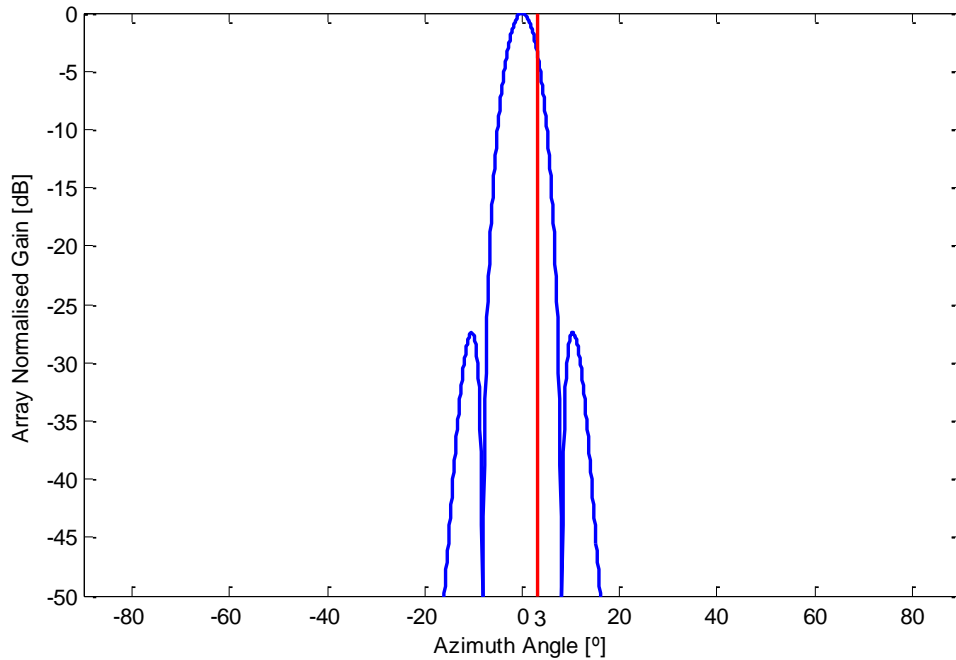


Figure 3.6 - 16-element LPDA antenna system course CSB radiation pattern.

As for the vertical radiation pattern of the ILS array, it is also modelled using (3.16) [NAV14b]. According to the information provided in [ITUR10] regarding vertical ranges, the ILS LOC covers regions located up to a maximum of 7° relative to the ground. Hence, one only addresses the lobe resulting from (3.16) that covers the relevant regions for the study. Figure 3.7 presents an example of the vertical radiation pattern that was modelled for the ILS LOC, considering the transmitting characteristics of the ILS LOC located in Lisbon runway 03, as specified in Section 4.1.

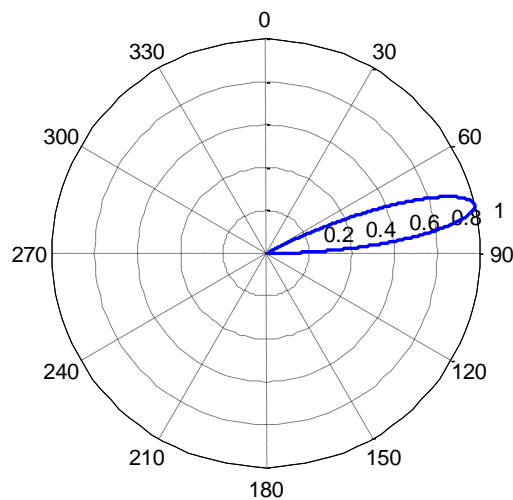


Figure 3.7 - Vertical radiation pattern of the ILS LOC in Lisbon RWY03.

As stated in [Indr13], the gain of each of the LPDA elements composing the ILS LOC is 9.5 dBi (± 0.5 dBi). The maximum gain of each ILS LOC array varies, depending on the installation and number of elements, even though the normalised radiation patterns are considered equal independently of the number of elements. Later on, in Subsection 4.1, one lists the maximum gains for each of the ILS LOCs.

3.2.2 FM Broadcasting

As stated in Section 2.3, there are multiple antennas that are used in FM broadcasting stations. This is due to the variety of possible scenarios in which they are inserted, hence, a global radiation pattern does not exist.

The transmitting power of FM broadcasting stations is defined by their ERP, which corresponds to the power obtained in the direction of the main lobe, including both the losses and gains of the system. ERP also includes the antenna gain, compared to a half wavelength dipole, hence, the gain of an FM station is only given by the vertical and horizontal normalised gains of the antenna.

Most of the broadcasting stations have omnidirectional antennas to cover the surrounding region. There are also installations in which highly directional antennas are positioned pointing to various directions to cover more efficiently the targeted areas by using antennas with higher gains, e.g., a Yagi-Uda antenna or an LPDA.

In this Thesis, three different radiation patterns are assessed to approach the stations considering different directional gains, half-power beamwidth and tilt.

First of all, concerning the type of transmitting stations, one considers a Vertical Dipole Array (VDA) as broadcasting stations' antennas. It presents a realistic approach to a broadcasting antenna and its horizontal omnidirectional characteristics make it a good model to be applied in the simulator. There is no standardised half-power beamwidth, and depending on the installation, it can vary from less than 10° up to 90° , or even more. Since FM stations are defined by their ERP, this implies that their impact on the airspace increases directly with the half-power beamwidth.

Since the array consists of a VDA, the vertical radiation pattern of the array is calculated by (3.18), (3.19) and (3.20). For this Thesis, one considers an array of half-wavelength dipoles. As one increases the number of elements, the half-power beamwidth decreases, thus, three models were developed for scenarios assessment in order to allow for pessimistically, realistically and optimistic evaluation.

One assesses a VDA with 2 dipoles spaced by $\lambda/2$, which presents a pessimist case, since the lower the number of elements a VDA is composed of, the larger the radiation pattern, hence, a higher antennas gain into airspace. By applying the expressions listed above, it is possible to obtain the vertical radiation pattern of the antenna, Figure 3.8, its half-power beamwidth being 54° .

To obtain high transmitting gains, FM stations are composed of arrays with high gains. This implies that they use antenna arrays with a high number of elements, being able to achieve ERP in the order

of 100 kW. So, for a most realistic approach, a VDA with 12 dipoles with $\lambda/2$ spacing is considered, corresponding to the radiation pattern depicted on Figure 3.9. This array presents a vertical half-power beamwidth of 12° .

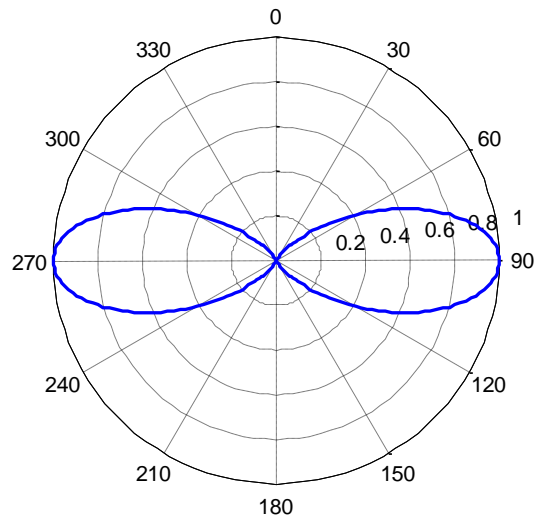


Figure 3.8 - VDA vertical radiation pattern (2 elements).

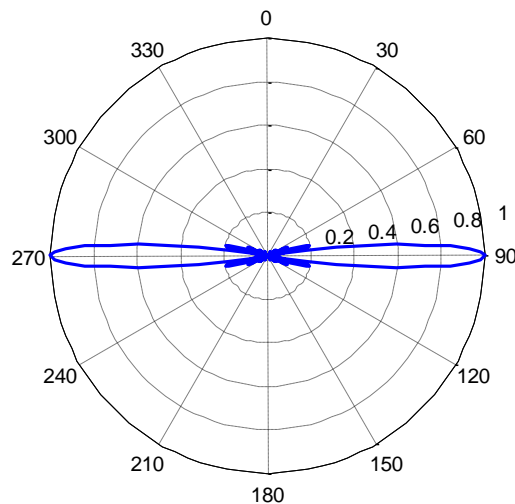


Figure 3.9 - VDA vertical radiation pattern (12 elements).

The last model corresponds also to a 12 elements VDA, but with a down tilt in its radiation pattern. The variation of the maximum gain direction is typically generated by modifying the phase shift of the different array elements. This presents the best approximation to the real antenna systems, since most FM stations tilt down their antennas to cover terminals located at ground level more efficiently. This also implies that the impact of the FM signal on airspace is reduced, compared to the non-tilted case. For modelling purposes, a tilt of -10° relative to the horizontal plane was implemented. The radiation pattern of the tilted 12 element VDA is shown in Figure 3.10.

As for the propagation in the horizontal plane in FM broadcasting antennas, it is normally considered to be omnidirectional, except in cases such as the directional antennas' scenario presented earlier. Hence, one considers an omnidirectional horizontal radiation pattern similar to a VDA.

Both the vertical and horizontal radiation patterns are based on theoretical models. It should be taken

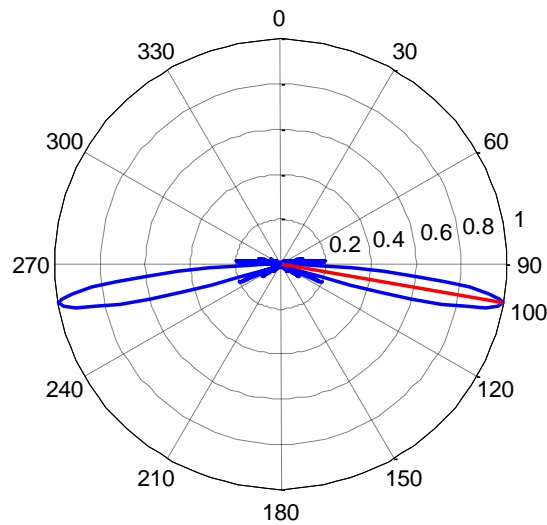


Figure 3.10 - VDA vertical radiation pattern (tilted 12 elements).

into account that, in a real array, there is a minor front-to-back ratio that could affect the lobes in the vertical radiation pattern. One should also denote that the real horizontal propagation also depends on the directivity of the antenna or array, not being ideal as the one presented here.

3.3 Flight Routes

This section covers the modelling of the aircraft's position through the various flight routes and approaches. This section is mostly based on [Pint11], since it contains a thorough approach to the topics required for this work.

First, the route angle travelled by the aircraft should be taken into consideration. The shortest path between two points implies a constant variation of the route angle due to the Earth's spherical form. This curve is called an orthodrome. Since a constant bearing correction is not convenient for manual navigation, flight routes correspond to loxodromes, i.e., paths taken by aircrafts by using a constant angle of travel. However, for long flights, flight routes through loxodromes may present a significant longer path and, subsequently, an increase of costs. With the present technology, auto-pilots realise the constant adjustment of the path bearing to allow flights along orthodromes.

One assesses flight routes as loxodromes, since the evaluated flight routes do not correspond to long enough flights. There are various significant points spread throughout the airspace, and aircrafts use constant route angles between each of those checkpoints. These flight routes are defined by their specific name and also Flight Level (FL) limitations. The FL of a route is characterised by a number, which corresponds to the altitude calculated in the aircraft at a specific calibration, and is expressed in hundreds of feet, e.g., FL300 corresponds to a displayed altitude of 30 000 ft.

When verifying magnetic bearings, one must take into account that there is a variation to the real angle depending on which zone of the Earth the verification of the magnetic bearing is done in. To compensate that deviation, every navigational chart contains its value, being given by [Pint11]:

$$\alpha_{real}[^{\circ}] = \alpha_{mag}[^{\circ}] - \alpha_{var}[^{\circ}] \quad (3.22)$$

where:

- α_{real} : real route angle.
- α_{mag} : magnetic route angle.
- α_{var} : variation angle given in relation to the magnetic West.

The loxodrome between two points can be defined by using their geographical coordinates [Pint11]:

$$\alpha_{real}[\text{rad}] = \text{acot}\left(\frac{\sum\phi_B - \sum\phi_A}{\lambda_B[\text{rad}] - \lambda_A[\text{rad}]}\right)_{[\text{rad}]} \quad (3.23)$$

$$\sum\phi_i = \ln\left(\tan\left(\frac{\pi}{4} + \frac{\phi_i[\text{rad}]}{2}\right)\right) \quad (3.24)$$

$$d_{path}[\text{NM}] = R_{[\text{NM}]} \times |\phi_B[\text{rad}] - \phi_A[\text{rad}]| \times |\sec \alpha_{real}| \quad (3.25)$$

where:

- $\sum\phi_i$: vertical spacing of parallel i .
- d_{path} : length of the path between the two points.

Equation (3.23) gives the value of the loxodrome angle, its length being given by (3.25). Thus, with the variation and the magnetic route angles obtained in a map, it is possible to obtain the real angle by applying (3.22).

Since the expressions use trigonometric functions, the assessment on the existence of two solutions is a must. Also, there is a specific case in (3.25) that occurs when the aircraft is traveling always in the same parallel which would result in $|\phi_B - \phi_A| = 0 \Rightarrow d_{path} = 0$. Since it presents an incorrect value for the distance, for this situation, one should use [Alex04].

$$d_{path}[\text{NM}] = R_{Earth}[\text{NM}] \times \frac{\lambda_B[\text{rad}] - \lambda_A[\text{rad}]}{\sec(\phi)} \quad (3.26)$$

In (3.26), $\sec(\phi)$ corresponds to the stretching factor for a parallel with Latitude ϕ . And as it can be observed, if the aircraft is traveling in the equator, then (3.26) would be equivalent to (3.25) with a α_{real} of 0° or 180° .

The previous expressions allow for the calculation of all flight routes to be considered in this study. The remaining situation that needs to be defined is the approach of the aircraft to the runway. The approach distance and the altitude are given by [Pint11]:

$$d_{path[m]} = \frac{h_{initial[m]} - h_{final[m]}}{\tan \alpha_{desc}} \quad (3.27)$$

$$h_{i[m]} = h_{initial[m]} - d_{i[m]} \tan(\alpha_{desc}) \quad (3.28)$$

where:

- $h_{initial}$: approach initial height above MSL.
- h_{final} : airport runway height above MSL.
- α_{desc} : descent angle.
- h_i : height in a point i of the approach.
- d_i : relative distance in a point i to the end of the approach.

Since the considered scenarios imply the analysis of various points of a flight route, the distances and coordinates have to be defined in each of these points. These values can be obtained by:

$$d_{interval[NM]} = \frac{d_{path[NM]}}{N_{points}-1} \quad (3.29)$$

$$\phi_{i[rad]} = \phi_{initial[rad]} + \frac{d_{interval[NM]}}{R_{Earth[NM]}|\sec(\alpha_{real})|} \times (i - 1) \quad (3.30)$$

$$\lambda_{i[rad]} = \lambda_{initial[rad]} - \frac{\sum \phi_{i[rad]} - \sum \phi_{initial[rad]}}{\cot(\alpha_{real})} \quad (3.31)$$

where:

- $d_{interval}$: distance between fixed intervals.
- N_{points} : number of points to be tested in the path.
- i : current test position, considering $i = 0$ the initial point and $i = N_{points} - 1$ the final point.

3.4 Radio Characterisation

In this section, the power spectrum of the various systems integrated in this Thesis is presented. One presents both radionavigation systems, and characterises FM broadcasting systems.

3.4.1 Radionavigation Systems

For both of navigation systems, the signals transmitted are idealised, i.e., signals are represented only by their transmitting bandwidth. Since there is no interference between channels and this Thesis' objective is to pinpoint the impact of interference of FM broadcasting onto these systems, this approximation has no influence on the results.

The frequency spectrum of an ILS LOC radio channel is depicted on Figure 3.11. One should denote that the course and clearance signals would have to be implemented differently, due to their different

radiation patterns, as stated in Subsection 3.2.1.

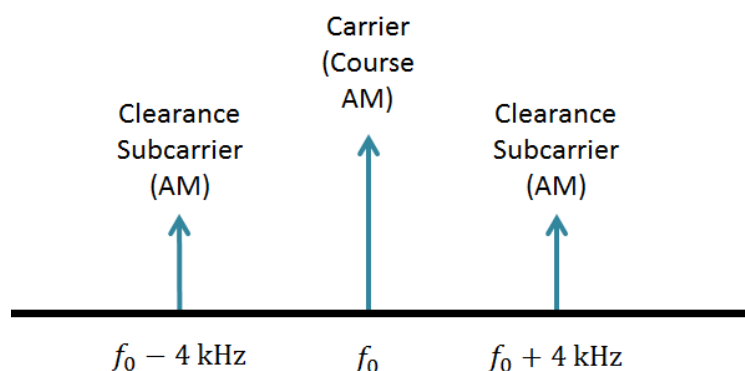


Figure 3.11 - Frequency spectrum of an ILS LOC carrier with frequency f_0 .

For the VOR, the band allocation has been presented on Subsection 2.1.3. For simplification purposes, one considers the transmitted signal by the VOR beacon as a signal with a bandwidth covering all components. The maximum frequency deviation corresponds to $9\,960 + 480$ Hz, which makes a total of $B=20.88$ kHz. Any unwanted signal pertaining in this band must be analysed to assess its impact. Figure 3.12 presents the various elements constituting the VOR signal and the bandwidth of the interfering zone.

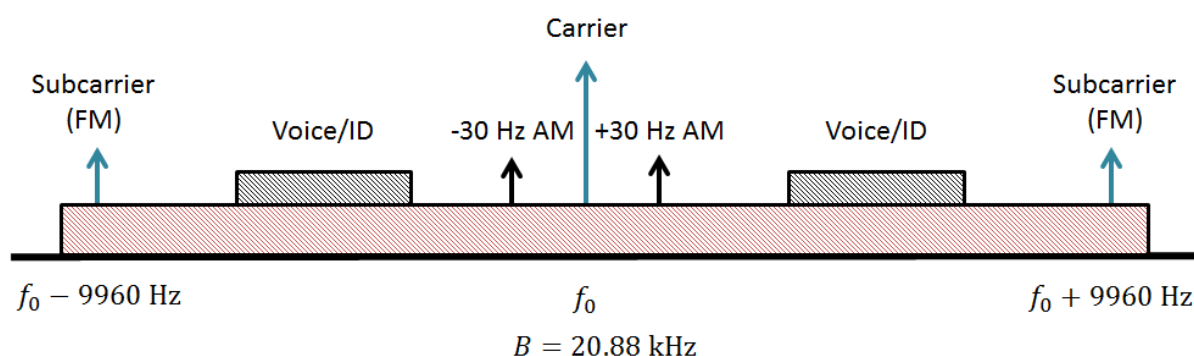


Figure 3.12 - Frequency spectrum of a VOR carrier with frequency f_0 and the total bandwidth.

For the assessment of the power of the navigation systems, one considers the frequency of the carrier in the signal propagation calculations instead of separately calculating each of the elements of both navigation systems. It is true that frequency affects the values of the path and obstacle losses, but since the maximum deviation relative to the carrier in these systems is around 4 kHz in the ILS LOC and 10.44 kHz in the VOR, the impact of this approximation is negligible. Yet, to study the results for each of the elements separately, its frequency and bandwidth should be used instead of the carrier's.

For a complete listing of the aeronautical channels in use by both radionavigation systems, one lists every ILS LOC and VOR channel frequencies in Annex A.

3.4.2 FM Broadcasting

When considering an emission of an FM audio broadcasting, one should evaluate what kind of signal

and which components are being transmitted. As stated in Subsection 2.3.2, a mono signal only needs up to 15 kHz of audio bandwidth, and the 200 kHz allocated bandwidth allows for a ± 75 kHz carrier frequency deviation plus guard bands for reducing interference. For stereo signals, the audio bandwidth is 53 kHz, which entails that, for the same carrier frequency deviation, it is more prone to interfere with adjacent channels.

Unlike navigation systems, FM broadcasting signals have to be fully modelled, including the unwanted emissions. To that end, a linear approximation is done to define the signal. In [ITUR14], out-of-band emission limits for FM broadcasting transmitters, when considering a carrier with 200 kHz bandwidth, are presented. Figure 3.13 depicts the linearised transmission mask of an FM emission, and Table 3.2 presents the break points of the mask depending on the frequency deviation f_Δ relative to the central frequency f_c ($f_\Delta = f - f_c$).

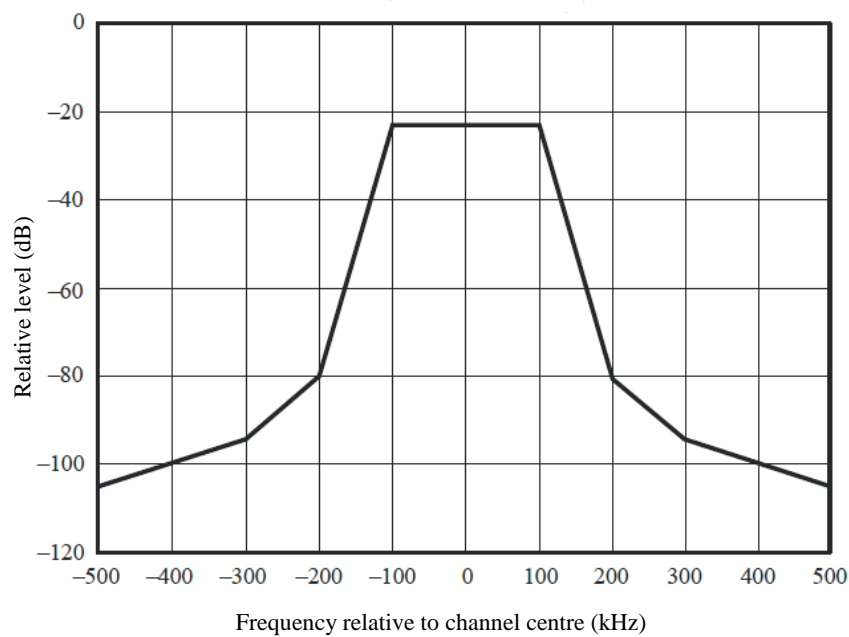


Figure 3.13 - Out-of-band transmission mask for FM broadcasting transmitters (extracted from [ITUR14]).

Table 3.2 - Break points of spectrum limit mask for FM broadcasting (extracted from [ITUR14]).

f_Δ [MHz]	Relative level [dB]
-0.5	-105
-0.3	-94
-0.2	-80
-0.1	-23
0.1	-23
0.2	-80
0.3	-94
0.5	-105

Thus, in the modelling of the FM broadcasting signal, the considered out-of-band emissions are the same as the limits imposed by ITU-R, and using the break points presented in Table 3.2, one can model the power decrease of out-of-band signals depending on the value of f_{Δ} . In Portugal, the allotted bandwidth for FM sound broadcasting is ± 75 kHz, which is transmitted with the rated power of the station. In the deviation interval between 75 and 100 kHz, one can linearise the output power decrease. For values of f_{Δ} higher than 0.5 MHz, the power of the FM broadcast is considered as null.

Using these considerations, one can obtain (3.32) which defines the power decrease of the signal relative to the wanted signal output relative to the value of f_{Δ} .

$$A_{t[\text{dB}]}(f_{\Delta[\text{MHz}]}) = \begin{cases} 0 & , & |f_{\Delta[\text{MHz}]}| \leq 0.075 \\ 920(|f_{\Delta[\text{MHz}]}| - 0.075) & , & 0.075 < |f_{\Delta[\text{MHz}]}| \leq 0.100 \\ 23 + 570(|f_{\Delta[\text{MHz}]}| - 0.100) & , & 0.100 < |f_{\Delta[\text{MHz}]}| \leq 0.200 \\ 80 + 140(|f_{\Delta[\text{MHz}]}| - 0.200) & , & 0.200 < |f_{\Delta[\text{MHz}]}| \leq 0.300 \\ 94 + 110(|f_{\Delta[\text{MHz}]}| - 0.300) & , & 0.300 < |f_{\Delta[\text{MHz}]}| \leq 0.500 \end{cases} \quad (3.32)$$

where:

- A_t : decrease of the power level relative to the maximum output power.

3.5 Interference Assessment

In this section, the establishment of the procedures to analyse the impact of interference on the receiver is done, accompanied by a thorough study of the various interference mechanisms and the presentation of the various criteria proposed by ITU-R and ICAO.

3.5.1 FM Broadcasting Selection

As previously mentioned, the FM broadcasting network located in Portugal pertains hundreds of stations located throughout the whole territory. The existence of such a high number of stations is due to the range limitation of each of these stations, and that is why one must assess and exclude stations according to the coverage area and the area in study in each of the scenario.

To that end, one established an exclusion criterion to reduce the assessed FM stations depending on the scenario. To assess the relevance of an FM broadcasting station, the characteristics of the installation must be considered. The value of d_{max} , above which stations' influence is negligible, is based on the station classification used in the USA. Depending on the ERP and the Height Above Average Terrain (HAAT) of a broadcasting station, the Federal Communications Commission (FCC) provides the distance to the protected service contour that corresponds to a circular-shaped form inside which a certain electric field can be guaranteed.

Table 3.3 presents the various FM stations classes defined by FCC, and their respective protected

service contours. The distance corresponding to the radius of the protected service contours is going to be the d_{max} below which a station is studied in the scenario.

Table 3.3 - FM broadcasting stations classes' characteristics (adapted from [FCC14a]).

FM Broadcast Station Class	Reference Maximum Facilities		Distance to Protected Service Contour [km]
	ERP [kW]	HAAT [m]	
Class A	6	100	28.3
Class B1	25	100	44.7
Class B	50	150	65.1
Class C3	25	100	39.1
Class C2	50	150	52.2
Class C1	100	299	72.3
Class C0	100	450	83.4
Class C	100	600	91.8

This creates a model that excludes stations depending on their properties. The value of HAAT of each station is disregarded, and one only applies the distance to protected service contours for the classes with highest HAAT for each of the reference maximum ERP, i.e., the station with classes A, B1, B and C. So, a FM station is categorised uniquely by its ERP, and it belongs to the classification with the smallest maximum ERP higher than its own. This presents a wider range of inclusion and an easier delimitation of the evaluated FM stations.

Even though these classifications are not done in Portugal, the purpose of this assessment is the realisation of an exclusion model. The fact that it is based on a classification done by the FCC and not integrated in Portugal does not present any restrictions on the integrity of the model.

3.5.2 Power Level

First of all, one analyses the power assessment for a signal considering free-space propagation. Besides the path losses given in (3.5), the attenuation caused by obstacles should also be considered, in case there is an obstruction in the link. The received power results from:

$$P_{r[\text{dBm}]} = P_{t[\text{dBm}]} + G_{t[\text{dBi}]} + G_{r[\text{dBi}]} - (L_{o[\text{dB}]} + L_{ob[\text{dB}]}) \quad (3.33)$$

where:

- L_{ob} : loss due to the obstacles (L_{KE} or $L_{Deygout}$).

This can be applied in scenarios where the terrain is not appropriate for Flat and Spherical Earth propagation models, and the aircraft is located in a high altitude.

Regarding the transmissions of FM broadcasting stations, one must take into account that the power output is not constant throughout the considered band, being given by:

$$P_{t,FM}[\text{dB}] = P_{t,max}[\text{dB}] - A_t[\text{dB}] \quad (3.34)$$

where:

- $P_{t,FM}$: power of the signal transmitted by the FM broadcasting station.
- $P_{t,max}$: maximum transmitted power of the FM broadcasting station.

Having the power of the signals at the input of the receiver, one has to assess the possible IMD products that FM broadcasting generates and that may cause significant interference on the reception of aeronautical signals.

In order to distinguish the resistance of a receiver to IMD, a standardised figure of merit called third-order intercept point (IP3) is used. A receiver with higher IP3 presents better immunity to IMD. IP3 is considered at the front end of the receiver, which means it already considers the non-linearity of all the components inside the instrument, including the amplifier and the band-pass filter. The value of IP3 is highly dependent on the individual characteristics of a receiver and not all of them contain this information concerning IMD. The figure of merit method of calculation was derived from [Agil12]:

$$F_{IP3}[\text{dBm}] = \frac{P_1[\text{dBm}] + P_2[\text{dBm}] + P_3[\text{dBm}] - P_{IMD3}[\text{dBm}]}{2} \quad (3.35)$$

where:

- F_{IP3} : figure of merit regarding the IMD.
- P_1, P_2 and P_3 are the power levels of the signals at the input.
- P_{IMD3} : power level of the generated 3rd order IMD product.

In case of an IMD product generated by two signals instead of three, the power of the signal with higher frequency is taken as $P_1 = P_2 = P_H$ and the lower frequency signal's power as $P_2 = P_L$. It can be noted that as the average power of the input increases 1 dB, the power of the IMD product increases by 3 dB.

It must be noted that IMD products are originated by FM broadcasting signals, and they have a transmitting bandwidth, which implies that the generated IMD product also contains a bandwidth. In [Agil12], it is said that a frequency deviation on the carriers causes an equal deviation on the IMD products without affecting the power levels. This implies that a band surrounding the input signal originates a band with the size at the output. So, the bandwidth considered for the IMD products is equal to the band of the input signal. Although, since there is a cubic power ratio between the input and the generated products, the band of the IMD products is defined by the triple in logarithmic scale of the decrease of transmitted power in relation to the frequency depicted in Subsection 3.4.2

The power of the IMD product in the aeronautical frequency is obtained in:

$$P_{r,IMD3}[\text{dBm}] = P_{IMD3}[\text{dBm}] - 3A_t[\text{dB}] \quad (3.36)$$

According to [NSA11] and [Holm14], a typical receiver has an IP3 of around +30 dBm. In this study, this value is considered for the aeronautical receiver, thus, one can obtain the value of P_{IMD3}

depending on the possible interferers in the input by using (3.36).

Having the power levels at the receiver, the Carrier to Interference Ratio (CIR) can be analysed, corresponding to the ratio between the power of the wanted signal and the interfering ones, given by:

$$(C/I)_{[dB]} = 10 \log \left(\frac{P_{r,C[W]}}{P_{r,I[W]}} \right) \quad (3.37)$$

where:

- $P_{r,C}$: received power of the carrier signal.
- $P_{r,I}$: sum of the received powers of the interfering signal(s) given by:

$$P_{r,I[W]} = \sum_{k=1}^{n_i} (P_{r,I,k[W]}) \quad (3.38)$$

where:

- $P_{r,I,k}$: power of a interfering signal.
- n_i : number of interfering signals.

Interfering signals are only taken if their power is higher than the average noise power of the receiver:

$$P_{r,I,k[dBm]} > P_{N[dBm]} \quad (3.39)$$

where:

- P_N : average noise power of the receiver and it is defined by [Corr14b]:

$$P_{N[dBm]} = -174 + 10 \log(B_{[Hz]}) + F_{N[dB]} \quad (3.40)$$

where:

- B : signal bandwidth.
- F_N : noise figure of the receiver.

Each receiver equipment has a value of $(C/I)_{min}$ that guarantees a proper functioning of the equipment without damaging the link. In worst case scenario, for low values of CIR, the communication can be dropped, hence, the main criterion used to quantify interference is the CIR of the communication in each of the scenarios and different positioning of the receiver.

3.5.3 ITU-R Recommendation

In ITU-R Recommendation SM.1009-1 [ITUR10], various standards are presented regarding Type A and Type B interferences. This recommendation takes into account an interference threshold above which the performance of the aeronautical receiver becomes unacceptably degraded.

For the ILS LOC and considering a wanted signal with DDM of 0.093, this threshold corresponds to one of the following criteria:

- A change in the course deflection current of 7.5 μ A.
- The appearance of the flag.

The flag is an indicator that lights up when the equipment is inoperative or not operating adequately, or the power level or the quality of the signal is below the acceptable threshold. The signal can supply faulty readings before the appearance of the flag, hence the differentiation of both events.

For the VOR, the interference threshold is defined by:

- A change in the course deflection current of 7.5 μ A, which corresponds to a 0.5° deviation of the bearing indication.
- A change in the audio voltage level by 3 dB.
- The appearance of the flag for more than 1 s.

Before assessing the various standards defined by ITU-R, one should analyse the various mechanisms. The IMD products that are generated by multiple signals have a frequency relationship with the original signals. Equation (3.41) shows how the frequencies of the IMD products are obtained, and (3.42) defines the order of the IMD product. The amplitude of the IMD product is lower as its order increases.

$$f_{IMD[Hz]} = k_1 f_{1[Hz]} + k_2 f_{2[Hz]} + \dots + k_n f_{n[Hz]} \quad (3.41)$$

$$N = |k_1| + |k_2| + \dots + |k_n| \quad (3.42)$$

where:

- f_{IMD} : frequency of the IMD product.
- k_1, k_2, \dots, k_n : random integer values for each of the n signals.
- f_1, f_2, \dots, f_n : frequency of each of the n signals.
- N : order of the IMD product generated by the transmitted signals.

In this study, only the 3rd order IMD products are considered, since for n^{th} order products with n even, the frequency of the products is outside the aeronautical band, and for an order higher than 3, the amplitude is low enough to be considered negligible. The following expressions depict the frequency of the IMD products for the two and three signals cases, which can be derived from (3.43) and (3.44), considering $f_1 \geq f_2 \geq f_3$.

$$f_{IMD[Hz]} = 2f_{1[Hz]} - f_{2[Hz]} \quad , \text{ two-signals case} \quad (3.43)$$

$$f_{IMD[Hz]} = f_{1[Hz]} + f_{2[Hz]} - f_{3[Hz]} \quad , \text{ three-signals case} \quad (3.44)$$

Regarding the Type A1 interference, Table 3.4 presents the protection ratios that should be attended for the various differences of frequency between the spurious emission or IMD product and the wanted signal. This type of interference is not accounted for a difference higher than 200 kHz.

Type A2 interference is neglected for a frequency difference between the wanted signal and the broadcasting signal carrier higher than 300 kHz. Table 3.5 shows the protection ratio that an

aeronautical receiver must present to be immune to this kind of interference for various frequency differences.

Table 3.4 - Type A1 interference protection ratios for aeronautical receivers (extracted from [ITUR10]).

Frequency difference between wanted signal and spurious emission [kHz]	Protection ratio [dB]
0	14
50	7
100	-4
150	-19
200	-38

Table 3.5 - Type A2 interference protection ratios for aeronautical receivers (extracted from [ITUR10]).

Frequency difference between wanted signal and broadcasting signal [kHz]	Protection ratio [dB]
150	-14
200	-50
250	-59
300	-68

For the study of Type B1 interference, the considered receiver is according to ICAO Annex 10, since it presents a more accurate approach than the Montreal one. Equation (3.45) shows the correction factor to account for changes in Type B1 interference immunity resulting from changes in wanted power levels [ITUR10].

$$L_{C1[\text{dB}]} = P_{r,A[\text{dBm}]} - P_{r,ref[\text{dBm}]} \quad (3.45)$$

where:

- L_{C1} : correction factor to account for changes in the wanted signal level.
- $P_{r,A}$: wanted aeronautical signal level at the input of the receiver.
- $P_{r,ref}$: reference level of the wanted aeronautical signal at the input of the aeronautical receiver, considering the ICAO Annex 10 receiver:
 - -86 dBm for the ILS LOC.
 - -79 dBm for the VOR.

It is considered that the aeronautical receiver has a good immunity to this type of interference if it fulfils the criterion in (3.46) for the two-signal case and in (3.47) for the three-signal one.

$$2 \left[P_{r,1[\text{dBm}]} - 20 \log \frac{\max(0.4; 108.1 - f_{1[\text{MHz}]})}{0.4} \right] + \quad (3.46)$$

$$P_{r,2[\text{dBm}]} - 20 \log \frac{\max(0.4; 108.1 - f_{2[\text{MHz}]})}{0.4} + K - L_{C1[\text{dB}]} + S_{[\text{dB}]} > 0$$

where:

- $P_{r,1}, P_{r,2}$: FM broadcasting signal levels in the aeronautical receiver corresponding to the signal with f_1 and f_2 .
- f_1, f_2 : FM broadcasting frequencies, with $f_1 > f_2$.
- $K = 78 \text{ dB}$.
- S : 3 dB margin to take account that the equation does not provide comprehensive compatibility assessment expressions.

$$\begin{aligned} &P_{r,1[\text{dBm}]} - 20 \log \frac{\max(0.4; 108.1 - f_{1[\text{MHz}]})}{0.4} + \\ &P_{r,2[\text{dBm}]} - 20 \log \frac{\max(0.4; 108.1 - f_{2[\text{MHz}]})}{0.4} + \\ &P_{r,3[\text{dBm}]} - 20 \log \frac{\max(0.4; 108.1 - f_{3[\text{MHz}]})}{0.4} + K + 6 - L_{C1[\text{dB}]} + S_{[\text{dB}]} > 0 \end{aligned} \quad (3.47)$$

where:

- $P_{r,1}, P_{r,2}, P_{r,3}$: FM broadcasting signal levels in the aeronautical receiver corresponding to the signal with frequencies f_1, f_2 and f_3 , respectively.
- f_1, f_2, f_3 : frequencies of the FM broadcasting signals, with $f_1 \geq f_2 > f_3$.

If there is a deviation between f_{IMD} and the frequency of the aeronautical signal f_A , in order to accurately verify the impact of interference, a correction to the IMD product signal level must be done. Hence, before applying (3.46) or (3.47), FM broadcasting signal levels have to be corrected by using:

$$P_{r,cor[\text{dB}]} = P_{r,s[\text{dB}]} - C_{t[\text{dB}]} \quad (3.48)$$

where:

- $P_{r,cor}$: corrected signal level.
- $P_{r,s}$: real signal level.
- C_t : correction term as defined in Table 3.6.

Table 3.6 - C_t depending on the frequency difference between the wanted signal and IMD products (extracted from [ITUR10]).

Frequency difference between the wanted signal and the IMD product [kHz]	C_t [dB]
0	0
50	2
100	5
150	11

For a frequency difference higher than 150 kHz, Type B1 interference is not considered.

To study the Type B2 interference, both of the Montreal and the ICAO Annex 10 receivers present a good approach. Equations (3.49) and (3.50) represent the maximum acceptable FM broadcast signal levels at the input of the receivers of both studies, respectively. Even though the ICAO Annex 10 receiver was developed more recently, there are some combinations of frequency and wanted signal level at which the Montreal receivers present better immunity criteria to Type B2 interference. Therefore, when considering the maximum allowed value of an input FM broadcast signal, the lowest value should be the one considered.

$$P_{r,max[\text{dBm}]} = -20 + 20 \log \left(\frac{\max(0.4; f_{A[\text{MHz}]} - f_{B[\text{MHz}]})}{0.4} \right) \quad (3.49)$$

where:

- $P_{r,max}$: maximum allowed FM broadcast signal level at the input of the aeronautical receiver.
- f_B : frequency of the FM broadcasting signal.

$$P_{r,max[\text{dBm}]} = \min \left[15; -10 + 20 \log \left(\frac{\max(0.4; 108.1 - f_{B[\text{MHz}]})}{0.4} \right) + L_{C2[\text{dB}]} - S_{[\text{dB}]} \right] \quad (3.50)$$

where:

- L_{C2} : correction factor to account for the changes in the wanted signal level as calculated in (3.51).

$$L_{C2[\text{dB}]} = \max[0; 0.5 (P_{r,A[\text{dBm}]} - P_{r,ref[\text{dBm}]})] \quad (3.51)$$

3.6 Simulator Development

In this section, one presents the simulator developed in Mathworks Matlab r2013a [MatL13] that was used to assess the impact of the interference throughout various scenarios. One briefly presents the general functionality of the simulator, and explains further the implementation of the essential functions.

3.6.1 Methodology and Input Data

First of all, one defines the basic structure of the simulator and how the diverse interference parameters are calculated. The initial focus of this simulator is to rapidly calculate the power of the signals received by the aircraft in multiple points in a certain flight route.

Figure 3.14 presents the general structure of the simulator. It begins by reading various input data and converting it into parameters defining the scenario. Afterwards, the propagation models are applied to the transmitting stations to assess the received power, and in case there is a need to consider the

obstacles between terminals, obstacles losses are calculated and added to the path loss. Finally, to determine the existence of significant interference in the scenario, both the CIR and the ITU-R standards are evaluated, thus producing the final results.

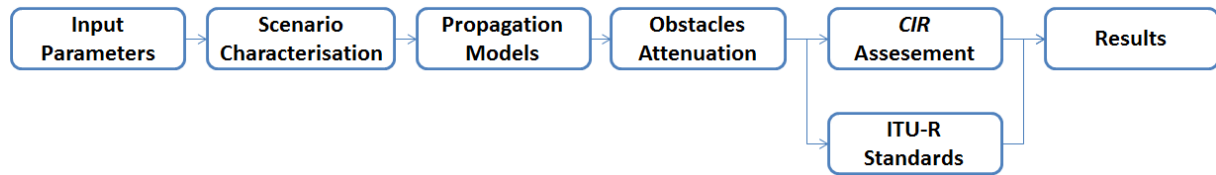


Figure 3.14 - General methodology of the simulator.

Regarding input data, they consist of locations and characteristics of the aeronautical and FM broadcasting transmitters. Among the data, there is also detailed information about the flight route or approach that is going to be considered. This is divided into 5 main Excel files:

- Information regarding the evaluated approach paths, containing coordinates of the touchdown zone, the approach bearing, the total path distance, and the initial height. These data consist of scenarios to be tested with an ILS LOC.
- Definition of the flight routes that are going to be assessed in a VOR scenario, their altitude being considered constant. Along with the height of the receiver, the geographical coordinates of the initial and final points of the path taken by the aircraft are also listed.
- List of all FM broadcasting stations in Portugal and their characteristics, composed of their locations, transmitting frequencies and radiated powers, as well as the height of the station and the terrain. The input data are listed in Annex B.
- Data about the VORs managed by NAV Portugal, i.e., their location, transmitting frequencies and powers, their heights, and the maximum gains of their antennas.
- Input file for the ILS LOCs, with information similar to the VOR input file, as well as the azimuth to which the ILS LOC is directed to, since it is composed of directional antenna arrays.

After deciding which scenario is going to be evaluated, it reads the corresponding required files, e.g., for the VOR link, it only reads the files regarding the flight routes, and the VOR and FM stations characteristics.

Regarding the scenario, it discretises the flight path into various route points, as stated in Section 3.3. To that end, two different functions were implemented to calculate the geographical coordinates and altitude of the receiver at each of these positions. One was implemented for the approach and the other for the flight routes; these two functions were adapted from the simulator developed by Ricardo Santos [Sant13]. Figure 3.15 presents the discretisation of an approach path.

There are various parameters that are fixed for all simulations, such as the receiver characteristics and the value of $(C/I)_{min}$. The essential parameters that are changed depending on the scenario are:

- Terrain profile and heights.
- Position and azimuth of the transmitters.
- P_t : transmitted power from every transmitter.
- G_t : gain of the transmitters' antennas.

- h_t : height of the transmitters.
- f : frequencies of the FM broadcasting and aeronautical signals.
- Path taken by the aircraft.
- h_r : height of the receiver.

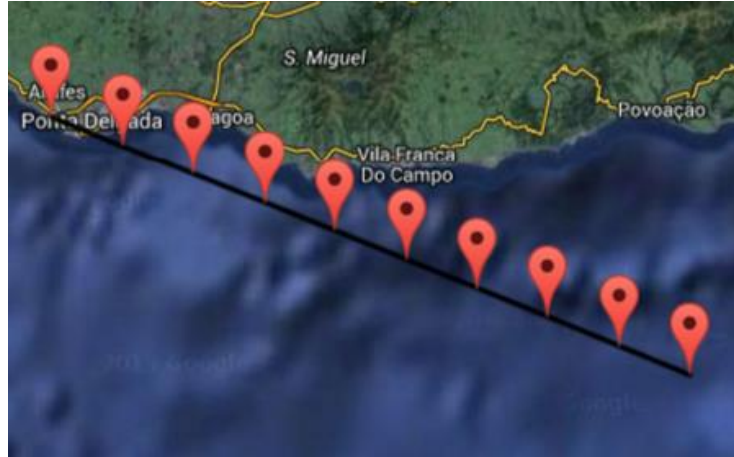


Figure 3.15 - Discretisation of the Ponta Delgada approach path into 10 points.

3.6.2 Transmitters and Receiver

The data link between the aircraft receiver and the radionavigation systems was considered unobstructed since the location of the ground antennas is idealised for aerial communications.

There are over 700 FM broadcasting stations in Portugal [ANAC14], and depending on the considered path, there is only a small percentage of FM stations that is near the receiver and that have significance for the evaluation, thus, being important to implement the FM broadcasting selection criteria. An auxiliary function was developed to check which FM stations are located within a certain range of each of the points of the flight path, calculating how many and which FM stations are within a certain radius of the aircraft position, which depends on the FM broadcasting transmitted power; for stations with higher transmitted power, the radius is higher compared to the low power ones.

Afterwards, the simulator calculates which of these stations may create an IMD product with frequency nearing the aeronautical signal. All of the assessed aeronautical signals have transmitting frequencies far from the lower limit of the aeronautical band (108 MHz), thus Type A interference is not evaluated in the simulator, since it only occurs for two transmitters in neighbouring frequencies. An IMD product is considered for analysis if the frequency spacing Δf is lower than 0.5 MHz from the aeronautical signal's frequency, corresponding to the maximum frequency deviation considered for FM broadcasting signals.

Both of these models were used as exclusion criteria to significantly reduce the number of FM broadcasting stations included in each of the scenarios. Figure 3.16 presents the general structure of the implemented algorithm.

The parameters of the aircraft receiver are considered equal for all scenarios. According to [NAV14b],

an aircraft receiver's $P_{r,min}$ varies between -96 and -113 dBm, and the value of $(C/I)_{min}$ is 20 dB. Besides these values, the receiver is also characterised by $G_r = 2$ dB and $F_N = 6$ dB. One also considers that $P_{r,min} = -113$ dBm for all scenarios, so that the receiver most vulnerable to interference is assessed.

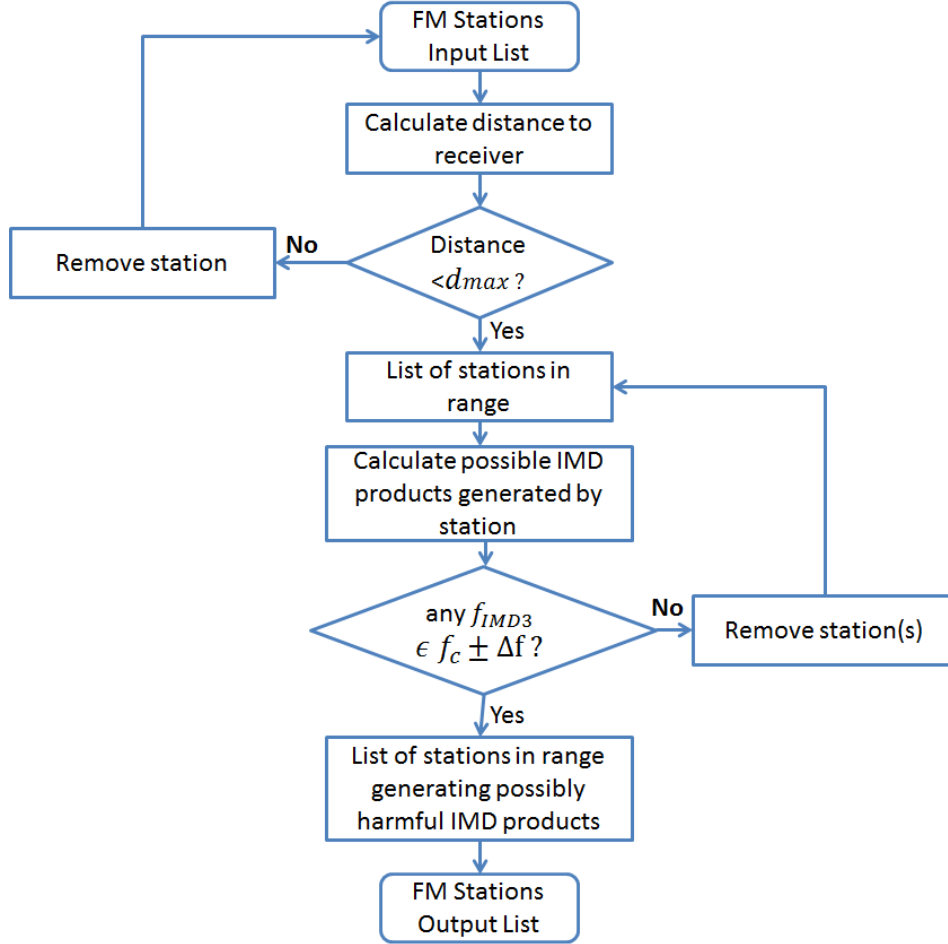


Figure 3.16 - Algorithm for the selection of FM broadcasting stations.

Taking into account the bandwidths considered for the ILS and the VOR in Subsection 3.4.1, one can obtain an estimation of their P_N , being -128.97 and -124.80 dBm, respectively. As the threshold due to noise is lower than the sensitivity of the receiver, the lower limit for the received signals to be perceived is imposed by the sensitivity.

3.6.3 Link Characterisation and Analysis

When considering the link between the transmitter and the receiver in the aircraft, one has to define three different functions for each of the different transmitters, since their propagation models and radiation patterns differ greatly from each other. Before initiating each of these functions, the simulator calculates the angles θ and φ between the two terminals and also the gain of the transmitting antenna according to the radiation patterns stated in Section 3.2.

For the VOR transmission link, one considers that it is positioned ideally and that the aircraft is always

in unobstructed line of sight, hence, the received power is calculated using the free space propagation model. When considering an ILS scenario, the Flat Earth propagation model is used to assess the received power in case the criterion defined in (3.6) is fulfilled, otherwise, the Spherical Earth propagation model is used.

The scenarios are firstly evaluated considering no obstacles between the FM stations and the receiver, hence considering the free space propagation model. This allows the exclusion of every FM station that does not cause interference with an unobstructed line of sight, and thus it is guaranteed that it will not cause damage to the link. In case there are FM stations in the vicinity causing interference in this idealised scenario, a more realistic scenario is assessed, which includes the terrain profiles between these FM stations and the receiver. The approach scenarios are more prone to be affected by the FM stations due to the low altitudes, and thus, the obstacles are more relevant to the assessment.

To that end, the API Javascript of Google Maps v3 [Java14] was used, which obtains the terrain height of various points along a path between two terminals and returns the terrain data in form of a table with the distance and terrain height. The *javascript* file was adapted to include the location of all FM broadcasting stations and the various points of the flight path, in order to easily choose the coordinates of the transmitter and the receiver. Each of the terrain profiles is saved in a corresponding text file (*.txt). For each of the discretised points of each route, there is a folder containing the various terrain profiles between the FM broadcasting stations and the respective path point, the name of the text file being the number ID of the station, as indicated in Annex B.

In case it is necessary, the path loss due to obstacles has to be assessed. An auxiliary function is used, which requires the aforementioned text file as an input, calculating the obstacle losses using the Deygout model; it was also adapted from the simulator that was developed by Ricardo Santos [Sant13]. Afterwards, the free space propagation model is used to calculate the received power, subtracting the losses due to obstacles. One obtains multiple received power levels from this function according to the different VDA models considered for the FM broadcasting stations.

The power level of the relevant IMD products that were listed when doing the exclusion of FM stations is promptly obtained. Taking the number of FM broadcasting stations in evaluation into account, it is safe to assume that there is a high number of generated IMD products, and one must assess which ones are relevant to the study. Every IMD product with calculated power lower than the sensitivity of the receiver is excluded from the following CIR analysis.

Two different functions are created to assess the impact of the interference that FM stations cause on the aeronautical signal: one is based on the receiver's CIR; the other one verifies if the FM broadcasting signals follow the ITU-R Recommendation SM.1009-1 detailed in Subsection 3.5.3. As previously mentioned, Type A interference is not taken into consideration in the ITU-R standards function, since all VOR and ILS channels are spaced more than 1 MHz from the lower limit of the aeronautical band, which is a margin that guarantees the nonexistence of Type A interference. Figure 3.17 depicts the flowchart detailing the result assessment process used in this Thesis.

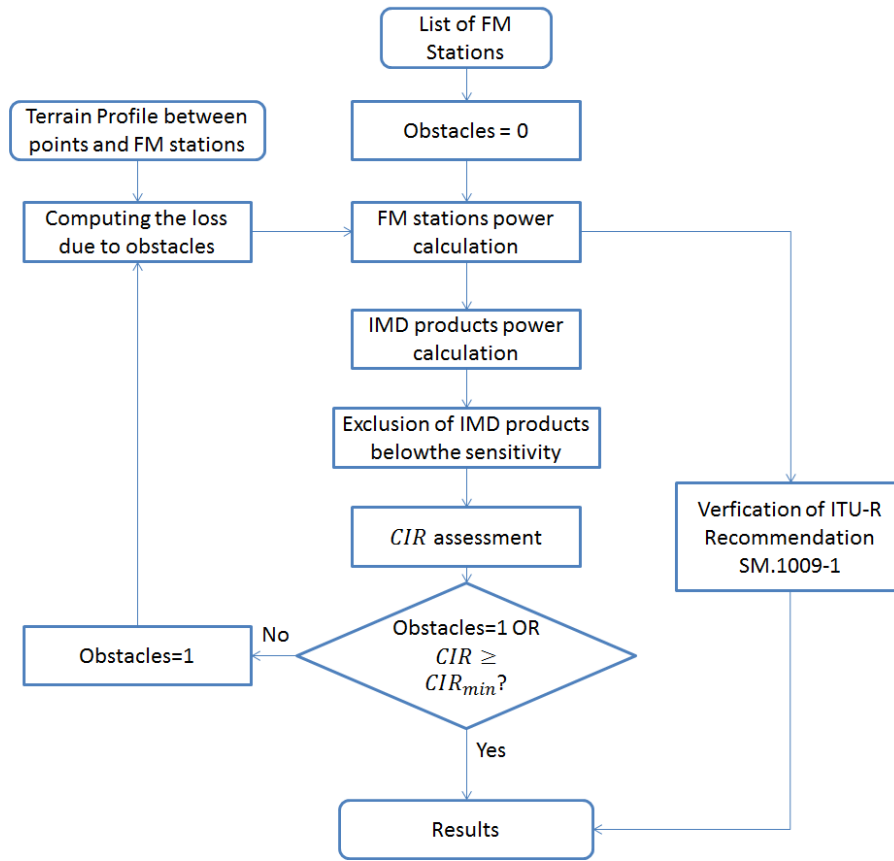


Figure 3.17 - Simulator result assessment flowchart.

3.7 Model Assessment

The main focus of this section is the validation of the models that were implemented in the simulator. Their verification is accompanied by the output of intermediate results obtained from the MATLAB program [MatL13]. One must make sure that the implementation of the models was successful. There are 3 models which implementation must be verified to confirm the accuracy of the simulator, i.e., the radiation pattern of the transmitters, the propagation models, and the power assessment.

The scenarios depend on which aeronautical system is being evaluated; hence, two scenarios were simulated to investigate the implementation of the models. In one, the receiver moved through a constant altitude flight route, to analyse the variation of the VOR and FM broadcasting signals. The other consists of an approach manoeuvre, allowing the verification of the ILS LOC installed in the runway. A single FM station was considered in the VOR scenario, to analyse the variation of its signal in a constant height flight. One has chosen the flight route RN870a, the VOR transmitters located in Lisbon (LIS), and the FM station located in Sintra, which corresponds to the ID 634, Figure 3.18. The approach scenario used to evaluate the ILS LOC is the one installed in Ponta Delgada, and the path depicted previously in Figure 3.15. Both of these scenarios are described in Section 4.2.



Figure 3.18 - Flight route RN870a and relevant transmitters.

The first assessment concerned the radiation patterns and directive gains of each of the modelled transmitters. Figure 3.19 (a) is the vertical angle θ between the transmitter and the receiver at FL45 and Figure 3.19 (b) represents the normalised gain of the FM stations for the 3 different VDA antenna models. Only the vertical angle θ is relevant to the analysis, since the horizontal radiation pattern considered for the VDA antenna systems is omnidirectional.

When the aircraft is in the closest position relative to the FM station, θ hits the highest value, and, according to the aforementioned radiation patterns, the normalised gain decreases as the aircraft approaches the region above the FM station. It can also be confirmed that the lower the number of elements of the VDA, the higher the normalised gain into the airspace. In the normalised gain graphic, both curves regarding the 12 element VDA have a slight increase in the distance between 50 and 58 km, which corresponds to one of the minor lobes depicted in Figure 3.8 and Figure 3.10.

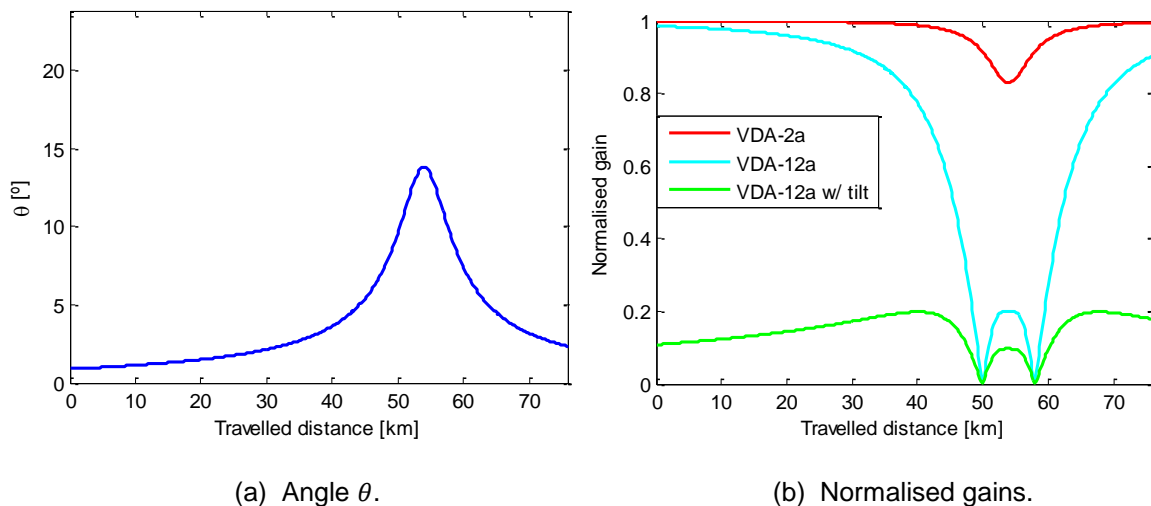


Figure 3.19 - FM station antenna models assessment (FL45).

One should also assess these models for a higher FL. Figure 3.20 presents the assessment of the VDA models when considering a flight route at FL300. At this FL, the link presents a much higher value of θ , Figure 3.20, being observed that the high vertical angle of the transmission causes a big enough variation to distinguish the various lobes defined in the radiation patterns.

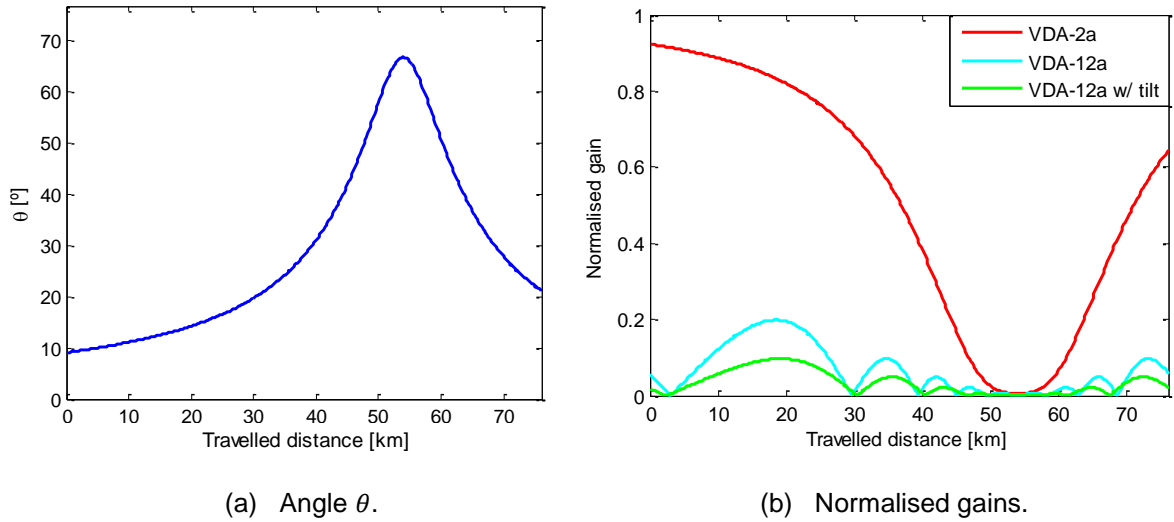


Figure 3.20 - FM station antenna models assessment (FL300).

Regarding the VOR antenna system, Figure 3.21 (a) presents the progression of the angle θ as the aircraft travels through the flight route and Figure 3.21 (b) the normalised gain. Two flight levels were considered, and, taking into account that the aircraft moves in the direction of the VOR ground beacon position, both graphics present curves as expected. As observed in Figure 3.4, the optimum direction of radiation is when the value of θ rounds 35°, and the cone of silence exists for θ higher than 60°. The following graphics present this behaviour, and a steep decrease of the gain can be verified when the receiver approaches the VOR location. The cone of silence corresponds to a larger area for higher altitudes, as simple trigonometry dictates.

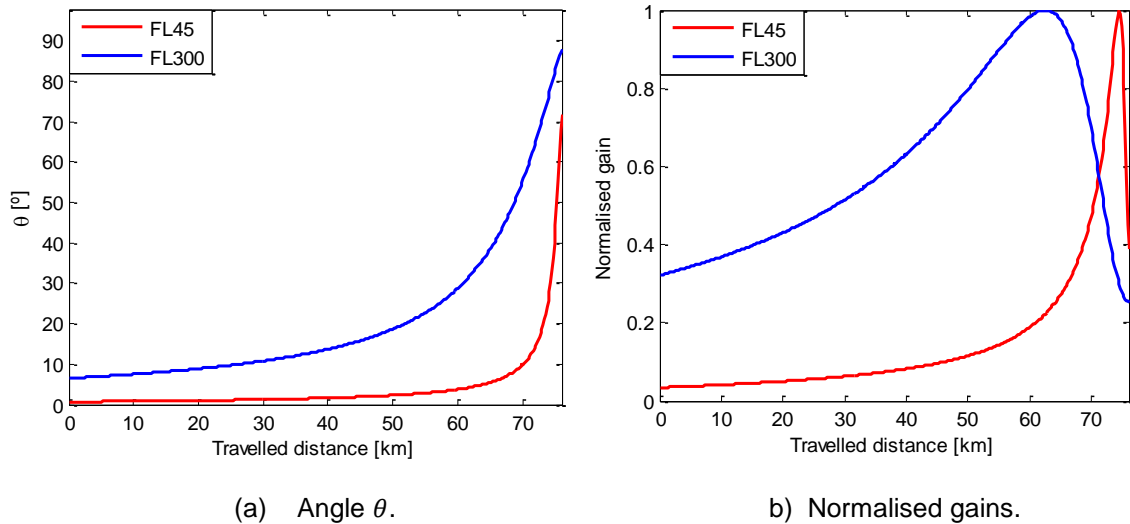


Figure 3.21 - VOR antenna models assessment (FL45 and FL300).

The next step is the verification of the propagation models. The free space propagation model was applied for the propagation of both of these systems, as stated in Subsection 3.6.3. The model implemented to calculate the losses due to obstacles is not included in this verification, since it was developed and tested in [Sant13].

Figure 3.22 contains the curves regarding the received power of the VOR and FM broadcasting signals. In Figure 3.22 (a), the FM signal received power increases as the aircraft closes up on the FM station location, hitting its peak in the nearest position. Even though the gain due to the directivity of the antenna is minimal in this region, the lower distance of propagation is more relevant in the signal strength. The curve depicting the VOR signal power is shown in Figure 3.22 (b). The value of P_r increases as the aircraft approaches the VOR's position, and when considering a higher altitude, one can observe the beginning of the cone of silence. The higher the altitude the larger is the size of this region.

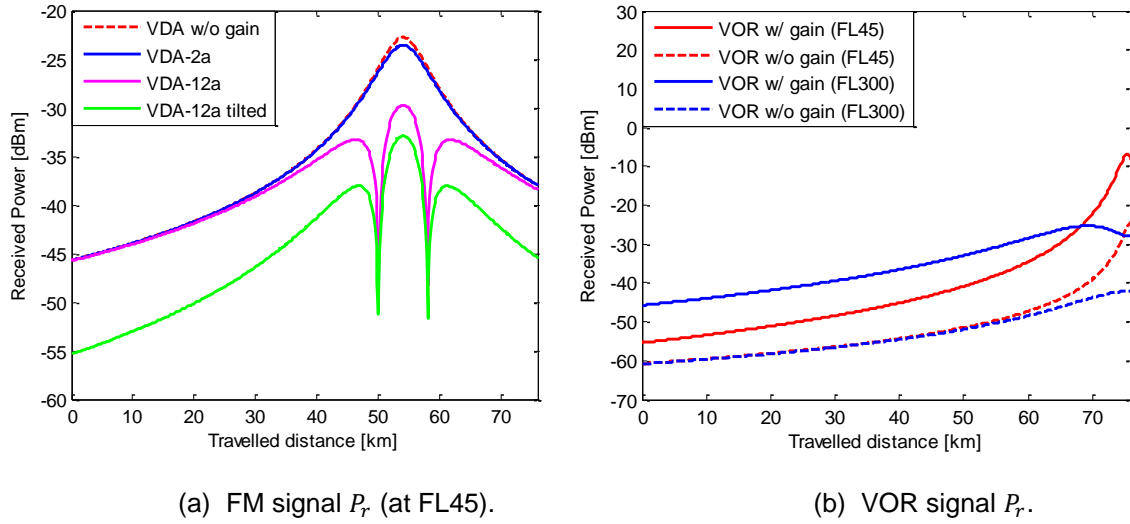


Figure 3.22 - VOR and FM stations signal propagation models assessment.

The following assessment is about the ILS LOC related models. Figure 3.23 presents various intermediate results that allow the confirmation of a proper implemented simulator.

Unlike the antenna models previously presented, the ILS LOC antenna array is not omnidirectional horizontally. Figure 3.23 (a) presents both the angles defining the direction of the direct ray. The evolution of the curves is as expected, although the value of angle φ was modelled to be null, since the approach was considered ideal and centred in the centreline of the runway. This slight deviation is originated by the chosen landing point and by the fact that the approach bearing and the deviation angle are presented in the navigational charts without decimal places, possibly causing a small approximation in the orientation. As it can be observed in Figure 3.23 (b), the deviation from the centreline is negligible, since the horizontal gain is basically omnidirectional. The vertical gain of the ILS LOC is quite low, since the vertical radiation pattern taken for the array has an optimal direction corresponding to $\theta = 13^\circ$.

In Figure 3.23 (c), the propagation model is assessed. The signal power increases as the aircraft closes on the touchdown, with a slight drop of power in the landing point. The low variations on the angles make the gain basically constant and maximised. The flat earth propagation model is used and this drop is explained due to the low height of the aircraft relative to the ground, which generates a minimum caused by destructive interference. The value of $\Delta\phi$ defined in (3.5) varies in

]0.0003, 0.0381[rad, fulfilling the criterion, and thus, only the flat earth propagation model was used in this scenario.

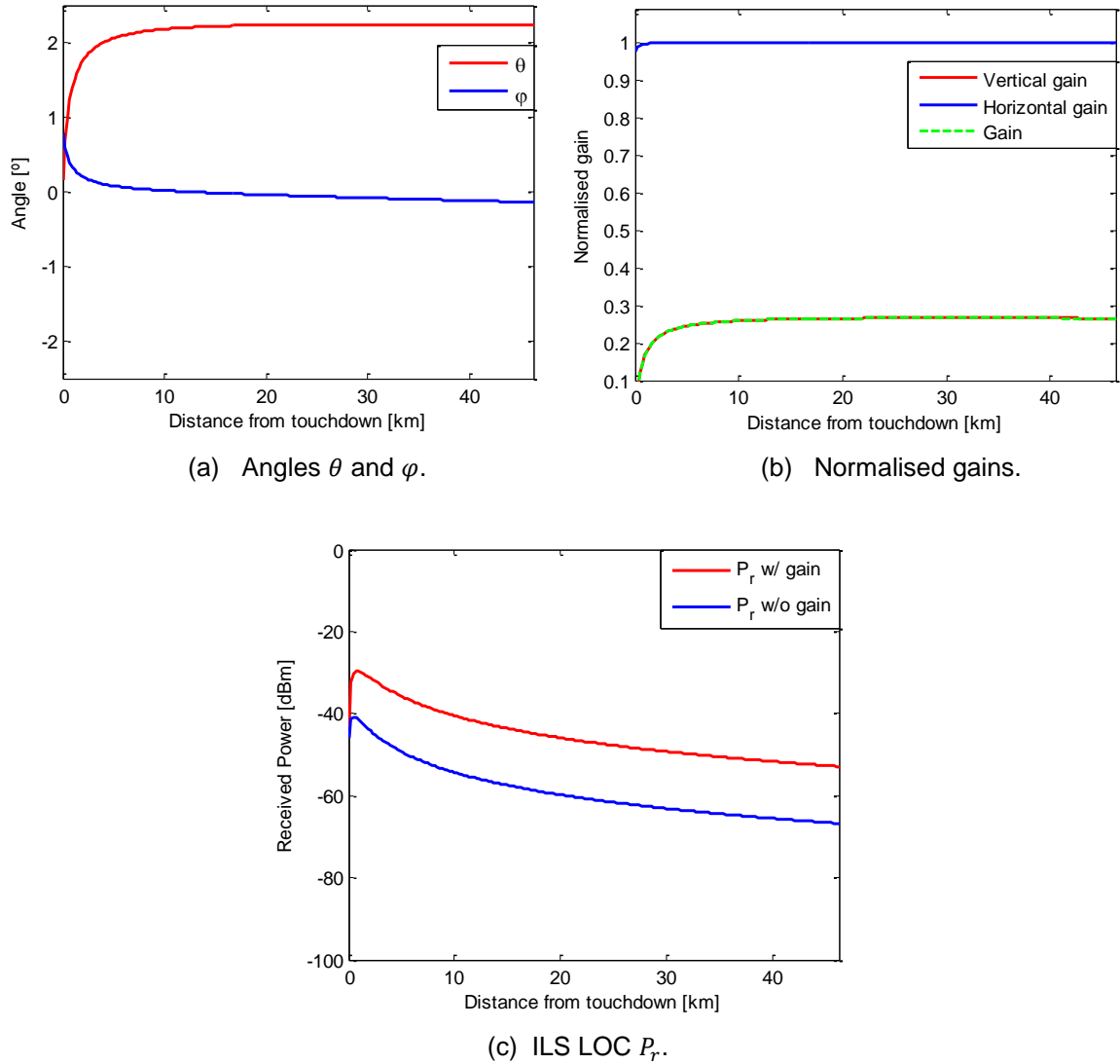


Figure 3.23 - ILS LOC models assessment.

The final model to be checked is the definition of the IMD products' power. This assessment is not scenario dependant, as long there are 2 or 3 FM broadcasting signals to cause IMD. Three FM stations, identified with the IDs 256, 261 and 636, were considered to verify if the 3rd order IMD product is calculated successfully. The first two stations are located in Centro Emissor de Monsanto, and the latter is positioned in Sintra. For this simulation, a 2 element VDA was considered for the FM stations.

Figure 3.24 presents the received power of the signals transmitted by these stations and the generated 3rd order IMD product in the RN870a scenario. The values with received power lower than the receiver sensitivity are displayed even though they are not taken into account on the result assessment. The resulting IMD product presents powers varying in [-162.6, -119.4] dBm. Usually, the power assessment of IMD products is done in dBc, which correspond to the power ratio relative to the

carrier. In this situation, the IMD product presents power ranging in $[-116.9, -91.1]$ dBc, and taking into account the received powers of the FM broadcasting signals, it represents a realistic approach on the IMD assessment.

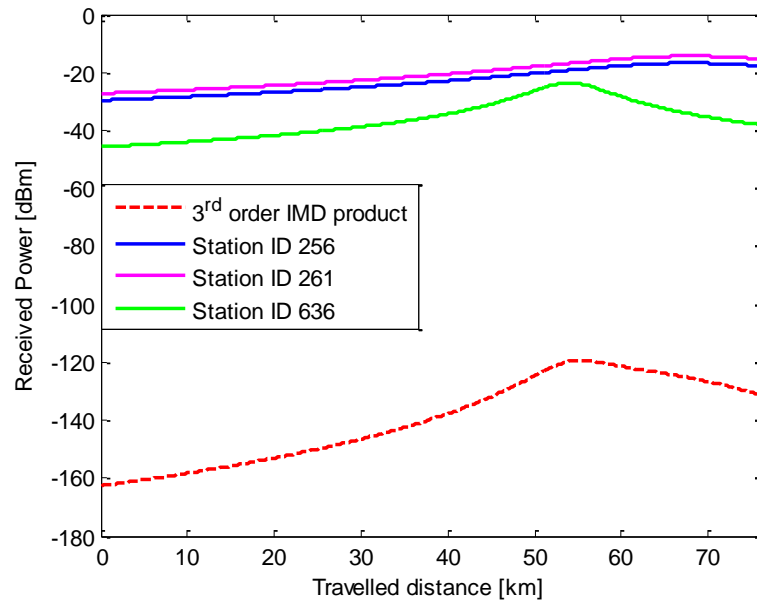


Figure 3.24 - Assessment of the power assessment of an IMD product.

Chapter 4

Data Analysis

This chapter consists of the presentation of the various scenarios to be evaluated and the analysis of the obtained data.

4.1 Transmitters

In this section, one presents the various transmitters that were considered in the studied scenarios. This includes the several installed ILS LOCs and VORs maintained by NAV Portugal, and also the FM broadcasting stations installed in Portugal.

There are VORs spread throughout the territory to provide assistance to all of the country's airspace. Nowadays, most of the aircraft guidance is done throughout routes connecting radio aids, and VORs are presently the most important ground radionavigation aid. Each VOR has a unique frequency that is permanent, which is defined at the moment of installation.

The information regarding the location and frequency of the various VORs is essential to pilots, allowing guidance between ground stations. Table 4.1 presents the VORs' locations and characteristics. It should be noted that Santa Maria's VOR is a CVOR, while the others are DVORs, even though the type of VOR is not relevant when inputting data into the simulator for the assessment of the scenarios.

Table 4.1 - VOR positions and transmitting characteristics (provided by [NAV14b]).

VOR Location	ID	Latitude [°]	Longitude [°]	h_t [m]	Frequency [MHz]	P_t [W]
Santa Maria	VSM	36.96278	-25.15250	1.2	113.700	50
Espichel	ESP	38.42417	-9.18583	1.2	112.500	50
Fátima	FTM	39.66556	-8.49278	1.2	113.500	50
Faro	VFA	37.01361	-7.97500	1.2	112.800	70
Flores	FRS	39.45361	-31.21056	1.2	113.300	50
Funchal	FUN	32.74722	-16.70556	1.2	112.200	50
Horta	VFL	38.51944	-28.62361	1.2	112.700	50
Lisbon	LIS	38.88778	-9.16278	1.2	114.800	70
Nisa	NSA	39.56472	-7.91472	1.2	115.500	50
Ponta Delgada	VMG	37.84611	-25.75806	1.2	114.500	50
Porto Santo	SNT	33.09028	-16.35056	1.2	114.900	50
Porto	PRT	41.27306	-8.68778	1.2	114.100	50
Sagres	SGR	37.08389	-8.94639	1.2	113.900	80
Viseu	VIS	40.72333	-7.88583	1.2	113.100	50

In this Thesis, the geographical coordinates are always represented in degrees. The positive values of Latitude and Longitude correspond to the North and to the Eastern hemispheres, respectively.

In order to properly use the propagation models, one must also consider the height of the terrain upon which the VOR is installed, which is relevant for both distances and the angle of the line of sight, which can affect the gain substantively. To that end, one obtained the elevation of the DME co-located with the VOR presented in the Aeronautical Information Package (AIP) [NAV14c]. The $h_{terrain}$ considered

for the VOR is equal to the elevation of the DME, and the values obtained are shown in Table 4.2.

Table 4.2 - Height of the terrain on VOR locations.

VOR Location	ID	$h_{terrain}$ [m]
Santa Maria	VSM	91.4
Espichel	ESP	182.2
Fátima	FTM	213.4
Faro	VFA	30.5
Flores	FRS	853.4
Funchal	FUN	152.4
Horta	VFL	152.4
Lisbon	LIS	335.3
Nisa	NSA	396.2
Ponta Delgada	VMG	853.4
Porto Santo	SNT	121.9
Porto	PRT	61.0
Sagres	SGR	152.4
Viseu	VIS	640.1

In order to better visualise the distribution of the VOR ground stations throughout the country, the geographical representation is essential. Figure 4.1 presents their location in Portugal mainland, as well in the archipelagos.

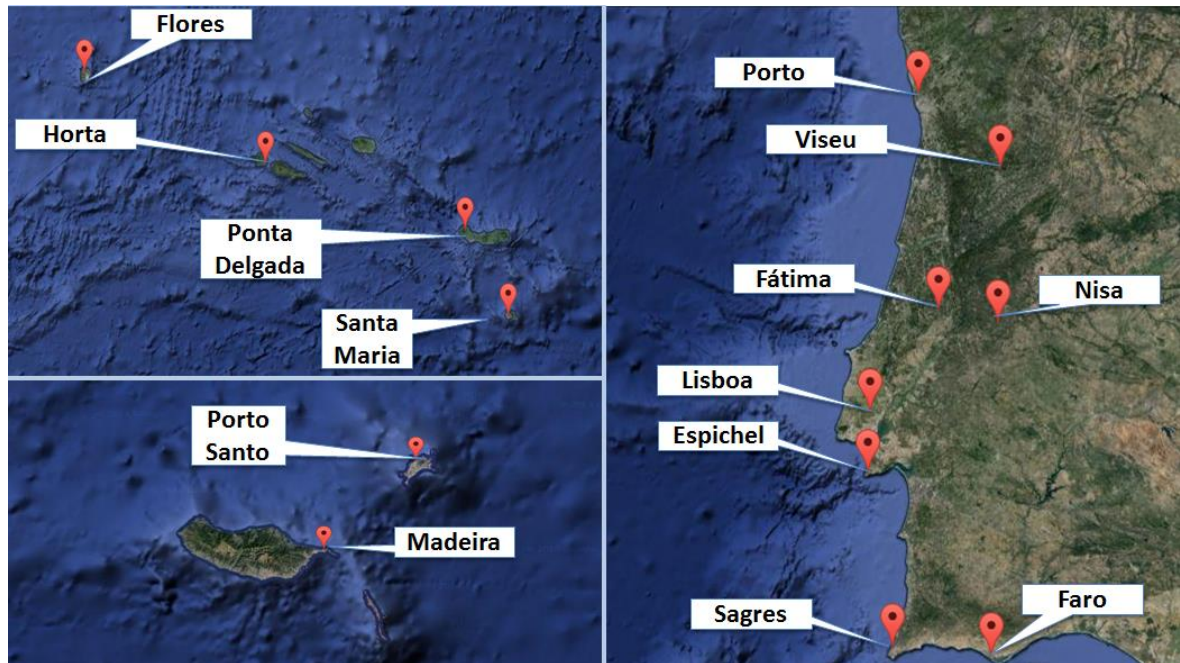


Figure 4.1 - Location of the VOR located in Portugal mainland.

The G_{max} of the VOR antennas depends on the various characteristics of the installation, including the radius of the ring and the height of the antennas. The G_{max} considered for the VOR antennas in this study is 20 dBi [NAV14b].

Landing is one of the most delicate manoeuvres that a pilot has to perform, and NAV Portugal is responsible for providing quality and precise ground support to approaching aircrafts. To that end, there are various ILSs installed throughout the airports in Portugal, NAV Portugal being responsible for 6 of them. Table 4.3 lists the location of the ILS LOCs and their characteristics. The identified runway corresponds to the landing runway in which the ILS LOC is installed, and this number corresponds to the approximate tenth of the bearing of the landing approach in degrees, i.e., for a runway numbered with 30 the landing approach corresponds to a bearing of around 300°, which implies that the azimuth of the ILS LOC is in the opposite direction (120°).

Since the indication of the runway is an approximation of the approach bearing, for the consideration of the ILS LOC azimuth, the exact angle must be assessed. The azimuth of the ILS LOC was obtained by using the approach bearing describe in the navigation charts, which is presented in Subsection 4.2, and the variation angles of the region, allowing for a significant correction of the azimuth.

Table 4.3 - ILS LOC transmitting characteristics and positions (provided by [NAV14b]).

ILS LOC Location and Runway ID	Latitude [°]	Longitude [°]	h_t [m]	Frequency [MHz]	P_t [W]	Azimuth [°]
Lisbon RWY03	38.798889	-9.126389	3	109.100	20	203
Lisbon RWY21	38.762778	-9.145556	3	109.500	20	23
Porto RWY17	41.230000	-8.676389	3	109.900	20	349
S. Maria RWY18	36.955556	-25.167472	3	110.300	20	171
P. Delgada RWY30	37.746667	-25.712500	3	109.500	20	112
Faro RWY28	37.017500	-7.995833	3	109.500	20	100

Besides the information regarding the transmitting equipment, this study must also take the surrounding terrain into account. The approach charts that are used in navigation contain information regarding the elevation of the landing runways, and all the flight routes used in Portugal are presented in the AIP [NAV14c]. Not all runways are of constant height in all their length, so the elevation height corresponds to the altitude of the highest point of the runway. Table 4.4 presents the elevation heights of the runway in which the ILS LOCs are installed. In this Thesis, the runways are modelled with constant height.

Table 4.4 - Approach runways elevation (extracted from [NAV14c]).

Runway ID	$h_{terrain}$ [m]
Lisbon RWY03	100.9
Lisbon RWY21	105.8
Porto RWY17	46.0
S. Maria RWY18	86.3
P. Delgada RWY30	57.0
Faro RWY28	5.5

Figure 4.2 is a geographical representation of the locations of the ILS LOC throughout the country. As

stated before, only the ILS LOC's maintained by NAV Portugal are included in this Thesis.

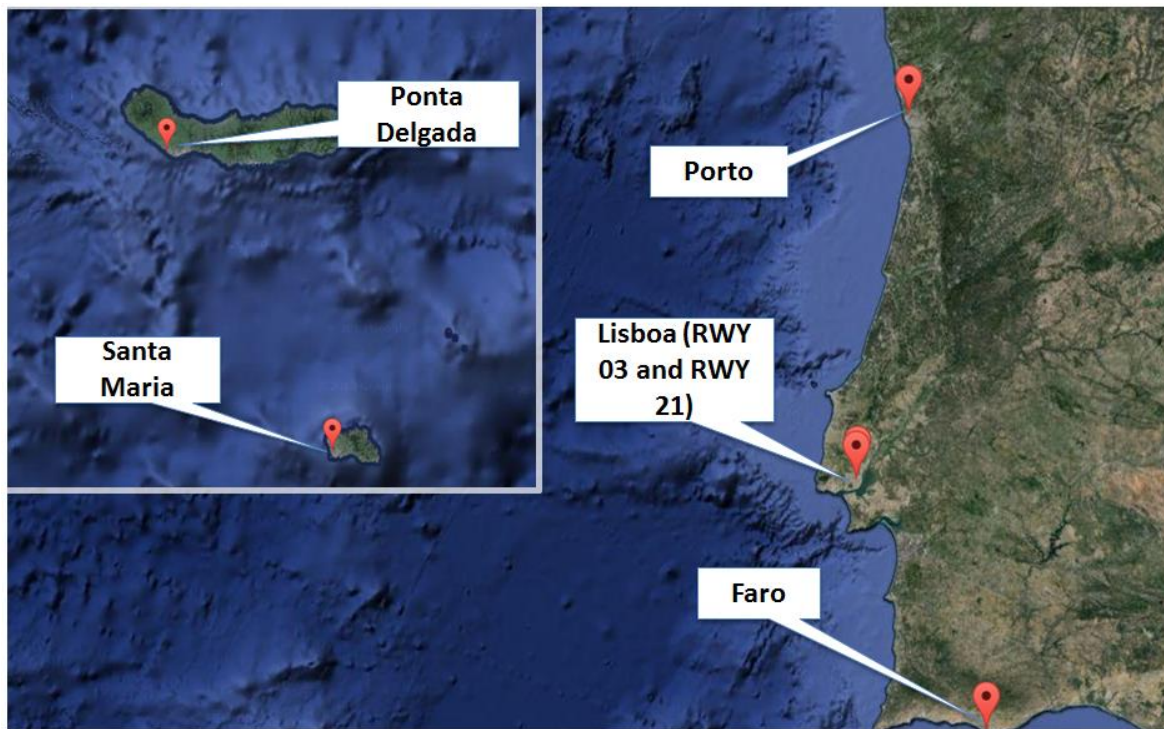


Figure 4.2 - Location of the ILS LOC maintained by NAV Portugal.

As mentioned in Subsection 3.2.1, the maximum gain of each ILS LOC is relative to the number of elements and the characteristics of the installation of the array. Table 4.5 shows the maximum gains of each of the ILS LOC that are going to be considered in each of the scenarios.

Table 4.5 - Maximum gains of the ILS LOC arrays (provided by [NAV14b]).

ILS LOC Location	Number of elements	G_{max} [dBi]
Lisbon RWY03	24	22.24
Lisbon RWY21	24	22.24
Porto RWY17	16	18.25
S. Maria RWY18	12	19.64
P. Delgada RWY30	12	19.64
Faro RWY28	12	19.64

Regarding interfering terminals, there are hundreds of FM sound broadcasting stations in every region of the country, therefore, one must have the detailed characteristics of every single transmitter to properly assess their influence. In Annex B, all the 701 FM broadcasting stations installed in Portugal are listed as of 2014, [ANAC14], being referred by their station ID number in this Thesis.

4.2 Scenarios Definition

This section contains information regarding all the studied scenarios. This includes the VOR or ILS LOC in study, as well the FM stations in the vicinity and the path taken by the aircraft.

4.2.1 Flight Routes

Nowadays, most of the flight routes used in the air navigation are based on the locations and radials transmitted by the ground radio aids. There are multiple routes that pass above each VOR and one must analyse them to verify their transmission reliability. Hence, for the various VOR transmitters, NAV Portugal provided the flight routes that are evaluated in this Thesis [NAV14b]. Each of these segments was discretised into 20 points. Not all of the VOR ground stations were assessed, as the flight routes provided by NAV Portugal corresponded only to the relevant VORs to be studied.

First, the VORs located in Santa Maria FIR were looked at; they are installed throughout Azores and provide critical orientation in the airspace surrounding the archipelago. The input parameters relative to the flight routes inside Santa Maria FIR are listed in Table 4.6.

Table 4.6 - Flight routes considered for evaluation of the VOR located in Santa Maria FIR.

VOR Location	Route ID	Initial Latitude [°]	Initial Longitude [°]	Final Latitude [°]	Final Longitude [°]
Flores	H141	40.54861	-33.38917	39.45361	-31.21056
	H142	39.90583	-33.73389	39.45361	-31.21056
Horta	H131	38.36833	-33.36361	38.51944	-28.62361
	H132	39.45361	-31.21056	38.51944	-28.62361
Santa Maria	H101	38.31972	-28.15806	36.96278	-25.16639
	H105	36.29250	-27.64778	36.96278	-25.16639
	H100	37.47833	-25.51000	36.96278	-25.16639

For the Lisboa FIR, even though its area is much smaller than Santa Maria's, it covers much more airspace above solid ground, which implies a higher number of VORs spread throughout this area and more precise radio aid navigation. Table 4.7 presents the VORs to be studied, and the flight routes for each one of these radio aids. Each of the flight routes is divided into two sections, which correspond to the inbound ('a') and outbound ('b') paths. For the evaluation of the VOR scenarios, one assesses each of the flight routes considering that the aircraft is travelling in two different altitudes, i.e., two FLs. One has chosen to represent the upper airspace, FL 300, and another to take into account the visual flights, FL45, [NAV14c].

4.2.2 Approaches

For the aforementioned ILSs, one considers one approach route for each one, in order to successfully analyse if the FM broadcasting stations significantly damage the transmission links. The approach

routes were chosen taking the range limitations of a typical ILS LOC into account, as well as recommendations provided by NAV Portugal. A constant descent path between touchdown and the farthest coverage distance was considered, both horizontally and vertically, resulting in $\alpha_{desc} = 2.3^\circ$ for all analysed approaches. It does not correspond to the expected 3.0° descent assisted with ILS GS, but the chosen path allows the evaluation of both the limit coverage and a low altitude approach.

Table 4.7 - Flight routes considered for evaluation of the VOR located in Lisboa FIR.

VOR Location	Route ID	Initial Latitude [°]	Initial Longitude [°]	Final Latitude [°]	Final Longitude [°]
Lisbon	RN870 a	38.64262	-9.98194	38.88778	-9.16278
	RN870 b	38.88778	-9.16278	39.17372	-8.39395
	Y207 a	39.66556	-8.49278	38.88778	-9.16278
	Y207 b	38.88778	-9.16278	38.67889	-9.31722
Fátima	A5 a	40.03111	-8.53611	39.66556	-8.49278
	A5 b	39.66556	-8.49278	38.42418	-9.18583
	UP600 a	39.16750	-8.39250	39.66556	-8.49278
	UP600 b	39.66556	-8.49278	40.03111	-8.53611
	UN872 a	40.42972	-8.05639	39.66556	-8.49278
	UN872 b	39.66556	-8.49278	38.42418	-9.18583
Nisa	G52 a	39.16750	-8.39250	39.56472	-7.91454
	G52 b	39.56472	-7.91454	40.32980	-7.09889
	R72 a	38.94556	-7.91417	39.56472	-7.91472
	R72 b	39.56472	-7.91472	40.72333	-7.88583
Sagres	R095 a	37.08511	-8.98898	37.08452	-8.94631
	R095 b	37.08452	-8.94631	37.07641	-8.38466
Porto Santo	UQ11 a	32.33111	-18.13028	33.09028	-16.35056
	UQ11 b	33.09028	-16.35056	33.41861	-15.65833
	R1 a	32.16194	-17.08528	33.09028	-16.35056
	R1 b	33.09028	-16.35056	33.66750	-15.94972
	B18 a	32.44917	-16.22722	33.09028	-16.35056
	B18 b	33.09028	-16.35056	33.55694	-15.78139

Table 4.8 presents the approach scenarios assessed in this Thesis. Approach routes are defined by the coordinates of the touchdown zone, initial height and approach bearing, from which the simulator calculates the various points composing the approach path from the final point backwards. The simulator also takes the variation angle into account as per defined in the approach navigational charts.

The considered initial height corresponds to the first point, being relative to the elevation of the runway track. This is due to the fact that these scenarios are used to analyse the limits of the ILS LOC's coverage range, as defined in Subsection 2.2.2.

The chosen distance corresponds to the maximum horizontal coverage range of the ILS LOC. One considered that the surrounding of the runway does not have obstacles affecting the ILS LOC signal

propagation, hence, that its maximum range is extended to 25 NM (around 46.3 km).

For the assessment of the ILS LOC, the height of the terrain is not relevant, since the positioning of the aircraft was chosen taking the relative position of the ILS LOC and its maximum ranges into account. However, the FM broadcasting signal calculation depends on the altitude of the receiver instead of its height relative to the runway.

Table 4.8 - Approach routes considered for evaluation.

Approach Runway ID	Touchdown Latitude [°]	Touchdown Longitude [°]	Initial height [m]	Bearing [°]	Distance [km]	N_{points}	α_{var} [°]
Lisbon RWY03	38.78627	-9.13320	1 900	27	46.3	100	4
Lisbon RWY21	38.77376	-9.13990	1 900	207	46.3	100	4
Porto RWY17	41.24639	-8.68074	1 900	173	46.3	100	4
S. Maria RWY18	36.96532	-25.16938	1 900	181	46.3	100	10
P. Delgada RWY30	37.74418	-25.70505	1 900	301	46.3	100	9
Faro RWY28	37.01503	-7.97092	1 900	284	46.3	100	4

4.3 Results and Data Assessment

This section contains the results from the simulations of both flight route and approach scenarios. One starts by presenting the overall results, and then performs a thorough analysis of the scenarios that present more sensitive results.

4.3.1 VOR Results

Starting with the VOR results assessment, for each of the scenarios one has calculated the CIR of the link along the path taken by the aircraft. This was done three times for each scenario, varying the radiation patterns of the antenna system used by the FM broadcasting stations. The radiation pattern changes the directional gain and, subsequently, the received power in the aircraft. These three simulations correspond to the three different antenna models defined in Subsection 3.2.1. One assessed the CIR in each of the links for each of the antenna models. Additionally, one also evaluated the scenarios according to the ITU-R Recommendation SM.1009-1.

First, the scenarios analysed at FL45 are presented. Only three of the analysed flight routes have interfering signals above the sensitivity of the receiver; the results from the simulator are presented in Table 4.9.

All remaining scenarios do not present any signs of interfering sources. This means that either there are no FM stations in the vicinity generating IMD products near the aeronautical frequency, or that they generate IMD products with a power below the receiver's $P_{r,min}$, thus, not causing any damage to the wanted signal. The navigation charts of these flight routes are presented in Annex C.

One evaluated the sum of the interfering products as well as the lowest CIR. It can be observed that none of the scenarios goes beyond the established 20 dB $(C/I)_{min}$ threshold, the lowest CIR being 55.4 dB in the UN872a scenario.

Table 4.9 - Results from the scenario assessment at FL45.

Flight Route	VOR Location	VDA Model	Highest $P_{r,I}$ [dBm]	Lowest CIR [dB]
Y207a	Lisbon	2 antennas	-103.2	59.4
		12 antennas (non-tilted)	-106.7	62.8
Y207b	Lisbon	2 antennas	-102.6	68.7
UN872a	Fátima	2 antennas	-107.1	55.4
		12 antennas (non-tilted)	-107.7	56.0

The scenario that shows a higher power derived from interfering sources is Y207b, even though its lowest CIR is the highest among all results. Figure 4.3 depicts the received power of both wanted and interfering signals. There are only signs of interfering sources in the section between 5 and 21 km of the outbound section of flight route Y207. The reason that CIR is higher compared to the remaining scenarios is that the interfering sources affect the initial part of the outgoing route, indicating that the wanted signal in this section is higher; in the other sections, the unwanted sources affect the link in segments farther away from the VOR. The curves depicting the remaining scenarios are presented in Annex D.

Even if considering the minimum guaranteed signal level at the receiver, i.e., -79 dBm for the VOR, the CIR criterion would also be fulfilled in every scenario, since a minimum of $P_{r,I} = -99$ dBm would be needed for CIR to drop below 20 dB.

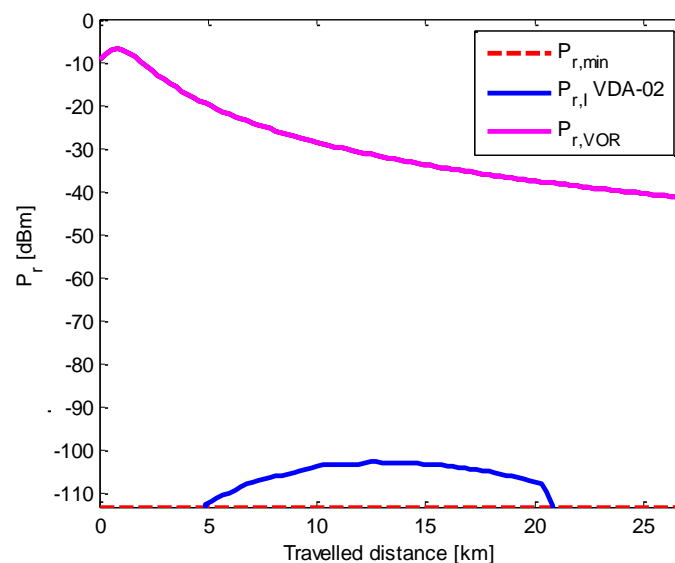


Figure 4.3 - Plot of the received power in flight route Y207b.

As for the ITU-R Recommendation criteria, all scenarios are within the standards, from which one can

conclude that, jointly with the previous results, there is no sign of significant interference in any of the scenarios assessed at FL45.

Besides the assessment considering an altitude corresponding to FL45, FL300 was also simulated. Contrary to the previous assessment, none of the scenarios presented any signs of interfering signals with power above $P_{r,min}$. The results obtained from the ITU-R Recommendation criteria also demonstrated the non-existence of interference in any of the scenarios. Therefore, one can conclude that all scenarios, whether evaluated at FL45 or FL300, fulfil the criteria established for interference assessment.

4.3.2 ILS LOC Results

In this section, the results obtained regarding the ILS LOC scenarios are analysed. First, the results without obstacles are displayed in order to select which approaches are more prone to interference. Afterwards, the results obtained from considering obstacles of those approaches are presented.

In these simulations, every FM broadcasting station was considered to be in an unobstructed line of sight with the aircraft, which leads to unrealistic results. However, they are sufficient to exclude which approaches or segments are irrelevant to the obstacle implementation. This is a fundamental process, since the implementation of terrain profiles into the simulator is time consuming.

One verifies if, for each of the scenarios and FM broadcasting station antenna models, the CIR thresholds are verified, Table 4.10. Only the scenarios regarding the Lisbon approaches are presented, concluding that all the remaining scenarios do not present any signs of interfering sources.

Table 4.10 - Results obtained from the simulator regarding the approach scenarios considering no obstacles in the propagation of FM broadcasting signal.

ILS Location	VDA Model	Highest $P_{r,I}$ [dBm]	Lowest CIR [dB]
Lisbon RWY03	2 antennas	-81.4	43.4
	12 antennas (non-tilted)	-84.6	47.1
Lisbon RWY21	2 antennas	-89.3	35.4
	12 antennas (non-tilted)	-89.6	35.7

This initial assessment indicates that the scenarios corresponding to approaches in Lisbon airport are affected by interfering stations due to the proximity and high density of FM broadcasting stations. However, none of the scenarios are damaged by the FM stations, according to the established CIR criterion.

Figure 4.4 shows the power levels of both wanted and interfering signals of the Lisbon runway 03 scenario. The region up to 17 km from touchdown presents significant levels of interfering signals. Considering a 2 antenna VDA model, IMD products hit a peak of -81.4 dBm, which is sizeable taking into account the power of the received signal. The peak occurs when the aircraft is at around 8 km

from touchdown at an altitude of approximately 440 m. It is expectable that FM stations are near this point of the approach and located at a similar altitude.

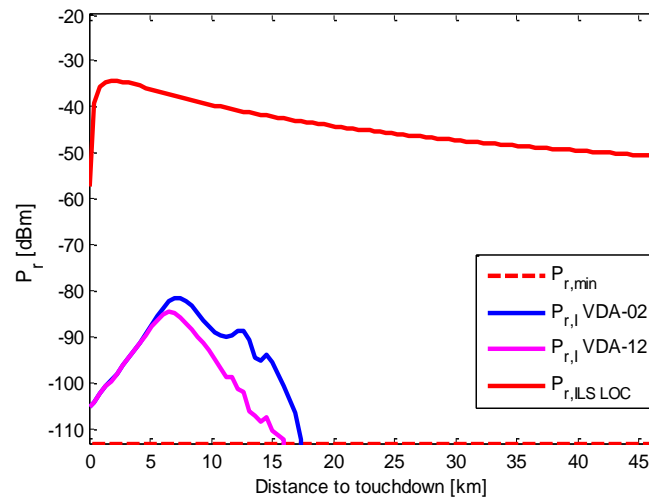


Figure 4.4 - Plot of the received power during the approach to Lisbon runway 03 for the various FM broadcasting antenna models.

Figure 4.5 presents CIR throughout the modelled path for the approach to Lisbon runway 03. The interfering signals start having some impact as the aircraft closes on the ground altitude. As the aircraft descends, it is approaching the horizontal plane of the neighbouring FM broadcasting stations. When a non-tilted FM station is at the same horizontal plane as the aircraft, its gain is optimal, resulting in stronger interfering signals. The existence of a tilt in the antenna renders its impact on the aeronautical signal null, as observed by the non-existence of interfering products of the 12 element tilted VDA.

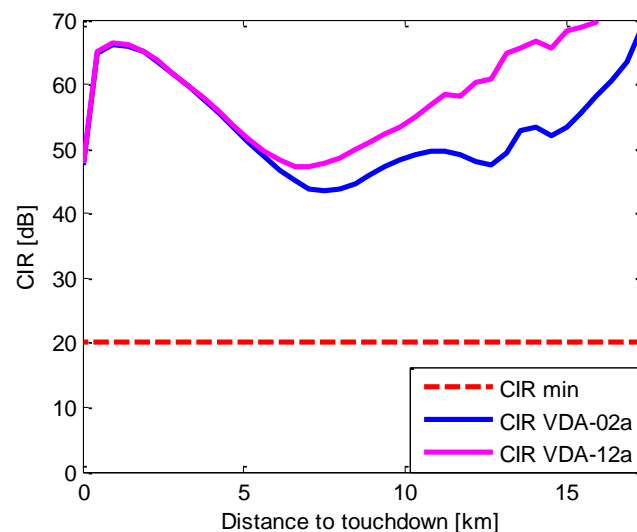


Figure 4.5 - Plot of the CIR of the approach to Lisbon runway 03 for the various FM broadcasting antenna models.

The received power of the wanted signal increases as the aircraft progresses through the approach, however, CIR decreases as the aircraft comes closer to the ground as a consequence of the

increasing FM stations' antenna gain and of the reducing distance between the aircraft and interfering stations.

One should also assess the scenario of the approach on Lisbon runway 21. Figure 4.6 presents the results regarding the received power. Again, only the 2 and 12 element non tilted VDA models generate any IMD products above the receiver's sensitivity. Unlike the previous scenario, $P_{r,I}$ peak value occurs when the aircraft is in the touchdown.

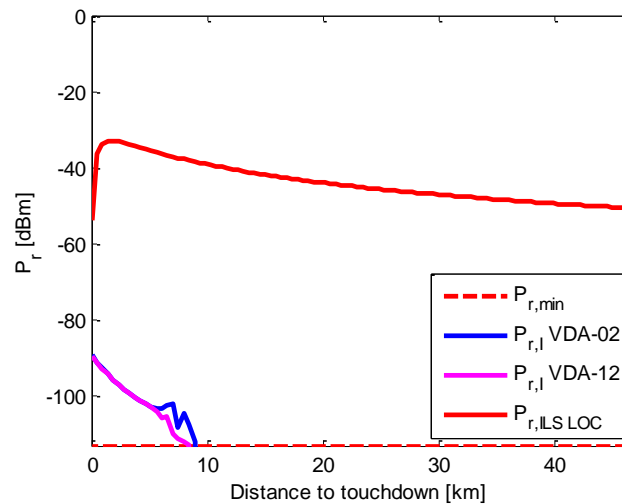


Figure 4.6 - Plot of the received power during the approach to Lisbon runway 21 for the various FM broadcasting antenna models.

Figure 4.7 presents the variation of CIR throughout the final segment of the approach in Lisbon runway 21. The curve depicting the variation of the CIR throughout the path taken by the aircraft is more regular than in the previous scenario and it only presents variations at distances lower than 9 km, when the aircraft is closing on the ground.

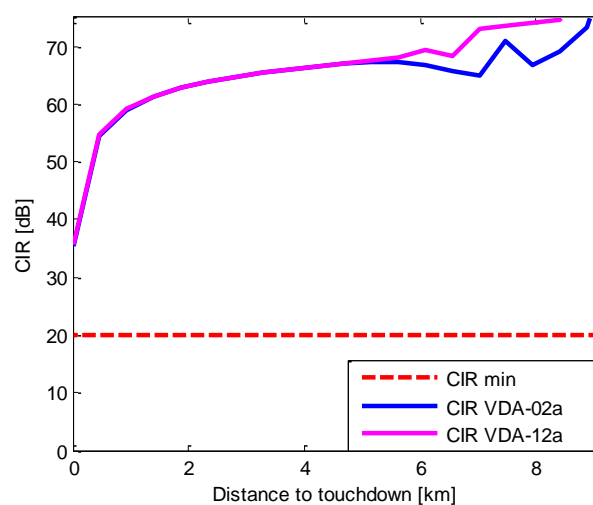


Figure 4.7 - Plot of the CIR of the approach to Lisbon runway 21 for the various FM broadcasting antenna models.

The previous results share a relevant resemblance. The values of CIR decreased as the aircraft

closes on the runway, since both the low altitude and the reduced distance make an ideal situation for the FM broadcasting transmissions. However, these results occur mainly due to the inexistence of obstacles in the simulation. The attenuation due to obstacles is crucial when analysing terminals at lower altitudes.

To further improve the results previously obtained, it was decided that the Lisbon scenarios should undergo a simulation including obstacles. First, one chose which segments of the approaches were crucial to be analysed, since the obstacle implementation requires terrain profiles between each of the FM stations and aircraft positions. The number of points that the aircraft path was discretised into was also significantly reduced, allowing a reduced number of inputs required for the assessment without reducing its accuracy.

As seen previously, the Lisbon runway 03 scenario presents disturbance in the wanted signal in a significant part of the approach, hence, the chosen segment for the assessment with obstacles corresponds to the last 17 km of the approach, discretising it in 16 points. In the Lisbon runway 21 scenario, it was chosen to analyse the last 9 km of the approach, considering a discretisation into 16 points. In Annex E, one lists all the FM broadcasting stations that were evaluated in each of the following scenarios.

In Figure 4.8, the results concerning the variation of the received power and CIR throughout the approach on Lisbon runway 03 are presented. As depicted in Figure 4.8 (a), in the approach on Lisbon runway 03, the interference caused by FM stations still persists, although it was nulled for distances lower than 3 km. At 7 km from the touchdown, the interfering products hit a peak of -81.9 dBm for a 2 antenna model and -88.1 dBm for a 12 antenna model. In Figure 4.8 (b), one can observe the CIR of the link throughout the path. One only presents the segments where interfering signals are not null. For the 2 element VDA, the CIR drops down to 43.5 dBm, which does not present a big variation compared to the no-obstacle assessment. One decided to assess this scenario further in order to better understand the cause of the interfering products.

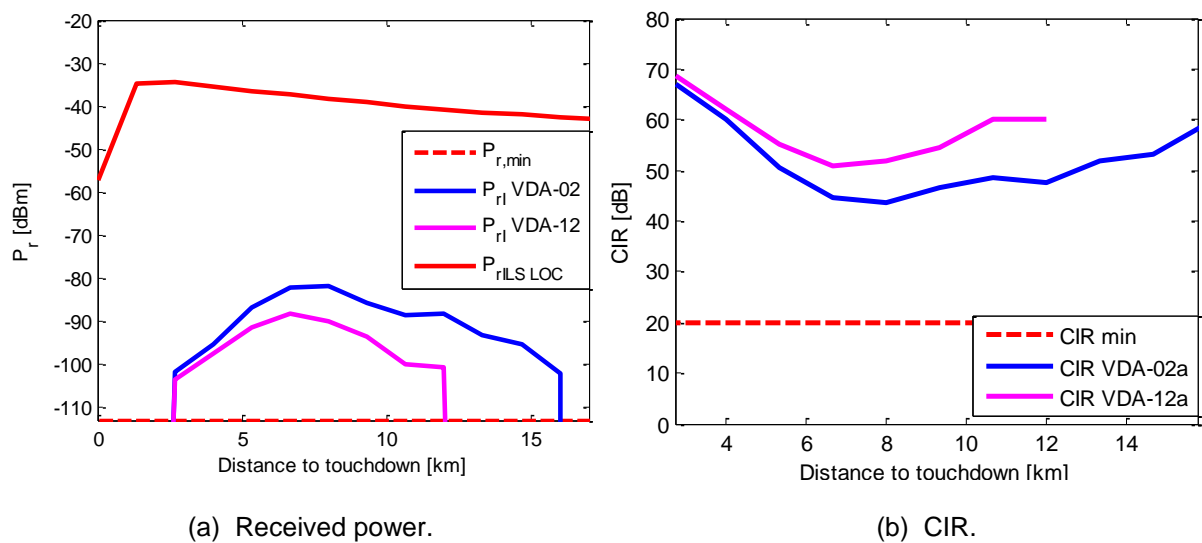


Figure 4.8 - Plot of the obtained results for Lisbon runway 03 scenario for the various FM broadcasting antenna models considering the terrain profiles.

To that end, one studied the geography of all FM stations assessed in this scenario, Figure 4.9; each dot corresponds to a single or a group of stations. To facilitate the visual representation, one distinguishes the transmitters according to their transmitting power. The stations transmitting above 10 kW are marked as red, the ones transmitting in $]1, 10]$ kW are represented in orange, and transmissions equal or lower than 1 kW are marked as yellow.

The group of stations that present a higher risk to the link is represented as a red dot next to the aircraft path. This corresponds to the Centro Emissor de Monsanto, which is composed of numerous transmitters with high transmitting powers (most of the FM stations with ID's between 252 and 264), and due to its proximity to the Lisbon airport, it is the cause of the decrease of the CIR of the transmission link.

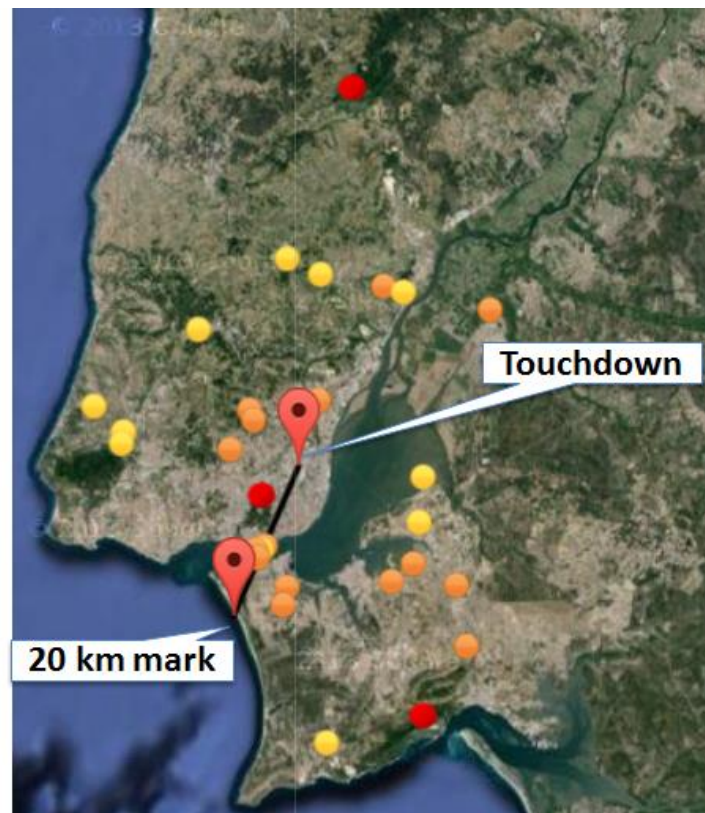


Figure 4.9 - Geographical representation of the FM stations in consideration for the obstacle implementation and simulation in Lisbon runway 03.

Besides the fact that FM stations are ideally located for broadcasting, there are also no obstacles between the transmitters and the runway. In Figure 4.10, the Fresnel's ellipsoid of the link between station 261 and the aircraft located at 7 km from the touchdown is represented. The selection of the analysed point of the approach was based on the fact that, according to simulations, it is in this section of the path that the link presents the lowest value of CIR.

Fresnel's ellipsoid is completely unobstructed, which implies that there is no obstacle attenuation due to the terrain. Hence, all the transmitters located in the vicinity of Centro Emissor de Monsanto are transmitting with an unobstructed line of sight. Since most of those stations are transmitting with more than 10 kW, it is natural to have some effect on the aeronautical receiver.

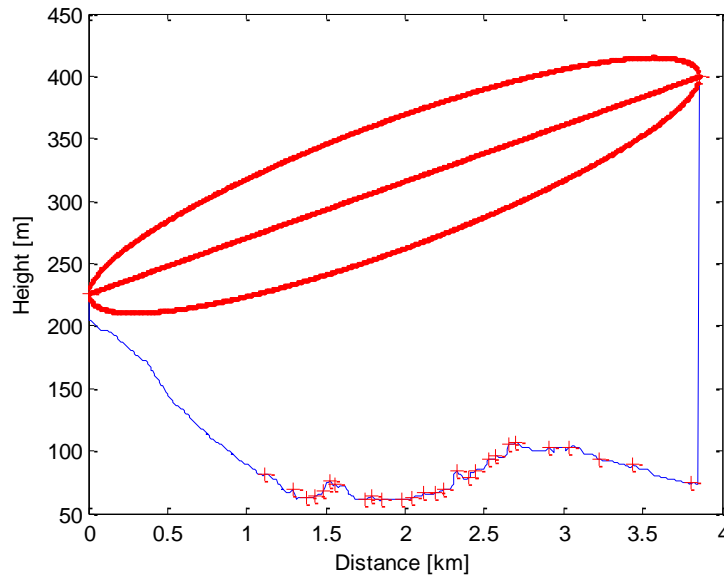


Figure 4.10 - Representation of the terrain profile and Fresnel ellipsoid of the transmission link between FM station 261 and the aircraft at 7 km from the touchdown zone.

The scenario corresponding to the approach to Lisbon runway 21 does not present any interfering signals, i.e., the interfering signals no longer generate IMD products with power levels above $P_{r,min}$. Regarding Type B interference defined in the ITU-R Recommendation SM 1009-1, all scenarios comply with the criteria.

One must take into account that the results obtained from this simulator consider various parameters that are general and not specific to individual stations. One of the main causes that reduces the accuracy of this simulation is the consideration of all FM stations' transmitting arrays as VDA that transmit ideally omnidirectional in the horizontal plane and also that have the optimal direction for $\theta = 0^\circ$. This concept is proven by the results referent to the 12 element VDA with -10° tilt. The existence of a tilt in the antenna eliminates the CIR variations mentioned previously.

Most of the FM stations do not have the optimal directivity in the horizontal plane. FM stations have arrays that are fed to have the radiation pattern pointing down to increase the coverage at low heights. Besides the optimum direction of the arrays, most of the FM stations' arrays are limited by a front-to-back ratio, meaning that the transmission is not done omnidirectionally in the horizontal plane.

To further improve the modelling of these scenarios, one should take the information of each of the transmitters into account. This includes the height at which the antenna is transmitting, the type of antenna or array, the radiation patterns and respective gains.

From the obtained results, one can safely assume that there are no signs of interference in the considered approaches and flight routes. FM broadcasting stations do not interfere directly with their out-of-band or spurious emissions, since the aeronautical frequency is spaced more than 1 MHz from all FM broadcasting signals. The main concern was the products resulting from the 3rd order IMD between groups of FM stations, but as it was analysed by either the CIR criterion or the ITU-R Recommendation SM.1009-1, there is no sign of significant interference, even when considering a

pessimist gain model.

Chapter 5

Conclusions

This chapter summarises the whole study, presenting the main conclusions extracted from the results obtained from the developed model. It also points out various aspects of this Thesis that could be improved in future work.

The main purpose of this Thesis was to evaluate and quantify the interference that modern FM broadcasting stations may cause on both VOR and ILS LOC radionavigation signals. One established various scenarios to be evaluated and through the development of various theoretical models, one successfully fulfilled the initial objectives.

Chapter 2 consists of the presentation of the basic concepts regarding the systems and mechanisms under study. The first section focuses on VOR systems, containing a description of its operation and radio interface. The following section presents the other radionavigation system incorporated in the study, i.e., ILS. It presents an overview of the various components integrated in the system and how they operate, and afterwards, a more detailed approach on the LOC component is presented, noticing that this subsystem is relevant for the study. A general overview on the FM audio broadcasting systems is integrated in the third section, complemented with a more thorough explanation of the radio interface of the technology taking into account Portuguese standardisation. Afterwards, one presents how the main focus of this work should be assessed. Hence, the interference mechanisms that are found to be relevant for this study are presented. The closing section on this chapter contains a brief presentation on the state of the art on this area of study. It references various works related to the study of the impact that FM broadcasting have on both the aeronautical radionavigation systems in study.

In Chapter 3, all the theoretical expressions necessary to fulfil the objective of this work are presented. The models associated with these expressions are thoroughly explained. The initial chapter presents the models relative to the signal propagation, allowing the calculation of the losses caused in the transmitted signal due to the decay throughout a path or obstacles. The following section has information regarding the radiation patterns of the transmitters in study, allowing the evaluation of the propagation of the signal depending on the relative position of the terminals. The movement of the aircraft is also modelled according to the paths under analysis. Taking into account that the paths taken by the aircraft correspond to long distances and that they are defined according to the geographical coordinates, one presents the mathematical expressions used to assess the aircraft positions and its variation depending on the procedure done. Both the approach and flight route are assessed and modelled. The next section defines the radio interface considered for both the aeronautical radionavigation systems and the FM broadcasting as well. Finally, the models developed to analyse and quantify the interference are presented and detailed. This includes the calculation the strength of a signal at the receiver end, the relation between the received signals and the IMD products, and the ratio between the wanted and interfering signals. Besides the direct signal assessment, one also presents the expressions and modelling done in ITU-R Recommendation SM.1009-1. In this section, one was able to establish two different criteria based on the aforementioned models that later on allow the assessment of the existence of interference and its quantification.

Following all theoretical models, one explains the methodology of the implementation of the models into the simulator. The process and approximation done are detailed in this section, including the most critical algorithms applied for the assessment of the focus of this Thesis. The simulator was developed

taking into account a number of input files that could easily define the parameters of the simulation, including the characteristics of all terminals and any values that are relevant to the models.

As a verification of the established theoretical foundations and good implementation of the simulator, one performed some controlled simulations to verify if the results are within the expected parameters and if their implementation was properly done.

Chapter 4 consists of the characterisation of the transmitters included in the evaluation, as well as the scenarios established to realise it. It also includes the results that were obtained from the implementation of the scenarios into the simulator. The definition of the scenarios is divided into two sections. The first one lists all the necessary characteristics of the radionavigation aids considered in the study. This consists of all VORs and ILS LOCs that belong to NAV Portugal. As for the FM audio broadcasting transmitters, their listing is given in an annex, due to the too high number of stations. This section is followed by the establishment of the flight routes and approaches that were assessed to evaluate the VOR and ILS LOC signals.

Chapter 4 includes the results obtained from the simulator divided in two sections. One focuses on the scenarios considered for the assessment of the VOR transmissions, and another one for the ILS LOC scenarios. Each of these sections presents detailed information regarding the interference assessment criteria for each of the evaluated scenarios. The results are accompanied by the observations and conclusions that can be extracted from the various data extracted from the simulator.

In this study, one focused on the assessment of interference caused by the IMD products generated by groups of FM stations. The other possible kind of interference that could have occurred is the spill over FM broadcasting into the aeronautical band, but since the aeronautical channel with lowest frequency corresponds to 109 MHz, there is a margin of 1 MHz to the FM broadcasting band, which excludes any possibility of interference generated by FM broadcasting out-of-band and spurious emissions.

From the results obtained for the scenarios, one was able to individually analyse each of the VORs. For every path, one considered FL45 to evaluate the validity for visual flights, as well as FL300 to verify the behaviour of CIR in the upper airspace. None of the links is damaged by FM broadcasting stations in their vicinity. However, in 3 flight routes, one calculated the existence of IMD products above the sensitivity of the receiver. The scenario that presents the lowest value of CIR due to these products is the flight route UN872a at FL45, in which the results show that CIR drops to a minimum of 55.4 dB.

For each of the groups of stations that are able to generate IMD products near the carrier frequency, the criterion based on the ITU-R Recommendation was also tested. One was able to assess that every group of stations in all scenarios fulfils the criterion, independently of the FL and FM station antenna models assessed.

Regarding the approach scenarios, one was able to successfully analyse all the ILS LOCs maintained by NAV Portugal. One has done initial simulations considering unobstructed line of sight between the

aircraft and all FM broadcasting stations in the vicinity of the aeronautical data link to assess if there were any scenarios that would not fulfil the interference assessment criteria. In this initial simulation, one was able to exclude the possibility of any interference generated by FM broadcasting. None of the scenarios trespass the CIR threshold, and all ITU-R based criteria are fulfilled by all groups of stations.

However, the scenarios corresponding to the approaches to the Lisbon runways presented a significant variation of CIR for the link in the zone nearing the touchdown. One decided to implement the terrain profiles of the FM stations in the vicinity to obtain more trustful data regarding the interference in low altitudes. After the obstacle assessment, only the approach on Lisbon runway 03 presents a decrease on CIR. Through the insertion of obstacles into the simulator, one was able to reduce significantly the interfering signals in the vicinity of the touchdown zone. Still, the peak of the decrease of CIR on the approach on Lisbon runway 03 occurs around 8 km from touchdown, reaching a minimum of 43.5 dB. After further assessment, one was able to verify that the source of the decay of the signal quality are the high power transmitters located in Centro Emissor de Monsanto that are in unobstructed line of sight to the aircraft path, and that jointly with each other or with surrounding stations, generated significant IMD products in the aeronautical frequency.

The models chosen for the development of the simulator successfully fulfil the initial purpose of assessing the impact that FM broadcasting has in radionavigation systems. The application of the models implied the accumulation of various approximations throughout the process. First of all, one considered the antenna systems of every FM broadcasting station equal, when real systems vary greatly between each other. One also simplified the transmission of radionavigation systems' signals. Aeronautical signals are complexly generated, and real systems may present a slight difference from the proposed results. Moreover, ILS LOC transmitted signals are very sensitive to obstacles near the runway, because the reflected signals of this system generate high levels of interference. One of the most relevant approximations that were done was the definition of the receiver. Its parameters were concretised taking into account the typical values expected for such types of receiver, and one must keep in mind that a small variation can impact on the resulting interference.

All obtained results have as a basis the commercial FM broadcasting stations that have been approved by ANACOM. The study proves that there was no interference caused by FM broadcasting stations. One considered FM broadcasting signals as per defined by the limits imposed by ITU, and as long FM stations are transmitting within regulations, the results maintain their validity. However, it must be taken into account that there is the possibility of existing illegal amateur stations. They may generate direct interference by broadcasting outside the assigned band for FM broadcasting or by transmitting outside the expected approved standards regarding out-of-band and spurious emissions.

The results indicate the non-existence of interference throughout all the evaluated scenarios. Both the criteria established to quantify interference proved to be essential to the study. Moreover, the results obtained from the CIR assessment are in agreement with the results obtained from the ITU-R Recommendation.

For future work, one suggests the integration of the models and parameters in this Thesis in order to study and be able to reduce the consequences of the aforementioned approximations. The

improvement of the developed simulator presents a feasible continuation of the Thesis. Additionally, the addition of a wider variety of scenarios is suggested, including a different FM broadcasting network and radionavigation systems. The most interesting data missing in this work are field measurements; this would present a validation of the theoretical models that were implemented, allowing also the reassessment of the approximations done throughout the Thesis.

Annex A

Aeronautical Channel Frequencies

This appendix is composed of tables that list the various possible channel frequencies that can be used by the ILS LOC and the VOR.

A.1 ILS LOC

As stated in Subsection 2.2.1, the ILS LOC channels correspond to $f \in [108.10; 111.95]$ MHz with 50 kHz spacing, and the channels are located only in frequencies with the first decimal place odd. That makes a total of 40 ILS LOC channels, which are listed in Table A.1.

Table A.1 - ILS LOC channel frequencies.

Channel No.	f [MHz]	Channel No.	f [MHz]	Channel No.	f [MHz]
01	108.10	15	109.50	29	110.90
02	108.15	16	109.55	30	110.95
03	108.30	17	109.70	31	111.10
04	108.35	18	109.75	32	111.15
05	108.50	19	109.90	33	111.30
06	108.55	20	109.95	34	111.35
07	108.70	21	110.10	35	111.50
08	108.75	22	110.15	36	111.55
09	108.90	23	110.30	37	111.70
10	108.95	24	110.35	38	111.75
11	109.10	25	110.50	39	111.90
12	109.15	26	110.55	40	111.95
13	109.30	27	110.70		
14	109.35	28	110.75		

A.2 VOR

The frequency band available to the VOR systems is larger than the ILS's. The channels are in the $f \in [108.00; 117.95]$ MHz with a 50 kHz spacing, but for the band shared with ILS only the frequencies with the even tenths are used. They sum up to 160 VOR channels, and they are presented in Table A.2.

Table A.2 - VOR channel frequencies.

Channel No.	f [MHz]	Channel No.	f [MHz]	Channel No.	f [MHz]	Channel No.	f [MHz]
01	108.00	41	112.00	81	114.00	121	116.00
02	108.05	42	112.05	82	114.05	122	116.05
03	108.20	43	112.10	83	114.10	123	116.10
04	108.25	44	112.15	84	114.15	124	116.15
05	108.40	45	112.20	85	114.20	125	116.20
06	108.45	46	112.25	86	114.25	126	116.25
07	108.60	47	112.30	87	114.30	127	116.30
08	108.65	48	112.35	88	114.35	128	116.35
09	108.80	49	112.40	89	114.40	129	116.40
10	108.85	50	112.45	90	114.45	130	116.45
11	109.00	51	112.50	91	114.50	131	116.50
12	109.05	52	112.55	92	114.55	132	116.55
13	109.20	53	112.60	93	114.60	133	116.60
14	109.25	54	112.65	94	114.65	134	116.65
15	109.40	55	112.70	95	114.70	135	116.70
16	109.45	56	112.75	96	114.75	136	116.75
17	109.60	57	112.80	97	114.80	137	116.80
18	109.65	58	112.85	98	114.85	138	116.85
19	109.80	59	112.90	99	114.90	139	116.90
20	109.85	60	112.95	100	114.95	140	116.95
21	110.00	61	113.00	101	115.00	141	117.00
22	110.05	62	113.05	102	115.05	142	117.05
23	110.20	63	113.10	103	115.10	143	117.10
24	110.25	64	113.15	104	115.15	144	117.15
25	110.40	65	113.20	105	115.20	145	117.20
26	110.45	66	113.25	106	115.25	146	117.25
27	110.60	67	113.30	107	115.30	147	117.30
28	110.65	68	113.35	108	115.35	148	117.35
29	110.80	69	113.40	109	115.40	149	117.40
30	110.85	70	113.45	110	115.45	150	117.45
31	111.00	71	113.50	111	115.50	151	117.50
32	111.05	72	113.55	112	115.55	152	117.55
33	111.20	73	113.60	113	115.60	153	117.60
34	111.25	74	113.65	114	115.65	154	117.65
35	111.40	75	113.70	115	115.70	155	117.70
36	111.45	76	113.75	116	115.75	156	117.75
37	111.60	77	113.80	117	115.80	157	117.80
38	111.65	78	113.85	118	115.85	158	117.85
39	111.80	79	113.90	119	115.90	159	117.90
40	111.85	80	113.95	120	115.95	160	117.95

Annex B

FM Broadcasting Stations

This annex contains the tables supplied by ANACOM regarding the characteristics of all FM broadcasting stations in Portugal.

In this annex, it is presented a table containing the necessary information for this work regarding the FM broadcasting stations.

The ID number was added to the original table given by ANACOM to simplify the identification of the stations in the simulator and facilitate the process of looking up stations in the table. The height of the terrain at the location of the FM station was obtained through the API Javascript of Google Maps v3 [Java14]. Table B.1 lists the characteristics of all 701 FM sound broadcasting stations in Portugal.

Table B.1 - Characteristics of the FM sound broadcasting stations in Portugal (adapted from [ANAC14]).

Location ID	f [MHz]	ERP [dBW]	Latitude [°]	Longitude [°]	$h_{terrain}$ [m]	ID no.
A DOS BISPOS	89.1	33.010	38.95917	-9.01833	199	1
ABRANTES	89.7	33.010	39.46667	-8.19167	50	2
ACHADAS DA CRUZ	104.3	30.000	32.82833	-17.20055	932	3
ACHADAS DA CRUZ	105.0	30.000	32.82833	-17.20055	932	4
AEROPORTO DAS LAJES	93.5	21.761	38.76667	-27.08500	84	5
ÁGUEDA	101.8	16.990	40.57694	-8.44500	42	6
AJUDA - RR	94.2	30.000	39.08082	-28.00140	107	7
ALBUFEIRA	94.0	30.000	37.09170	-8.27084	111	8
ALBUFEIRA	101.2	16.990	37.09238	-8.27084	112	9
ALCACER DO SAL	93.9	33.010	38.38778	-8.51583	46	10
ALCÁÇOVAS	104.7	16.990	38.39500	-8.16889	252	11
ALCOCHETE	104.8	30.000	38.75278	-8.96333	6	12
ALCONGOSTA	92.5	26.990	40.10639	-7.50278	1 050	13
ALCOUTIM	88.9	24.771	37.45894	-7.47666	98	14
ALCOUTIM	91.5	24.771	37.45894	-7.47666	98	15
ALCOUTIM	94.4	26.990	37.43250	-7.53833	244	16
ALCOUTIM	101.9	24.771	37.45894	-7.47666	98	17
ALFERCE	91.8	33.010	37.31500	-8.50250	614	18
ALGARVIA	91.8	30.000	37.85015	-25.23094	263	19
ALGARVIA	103.7	30.000	37.85015	-25.23094	263	20
ALHOS VEDROS	96.2	33.010	38.63833	-9.00556	60	21
ALHOS VEDROS	101.1	31.761	38.63833	-9.00556	60	22
ALHOS VEDROS	103.0	33.010	38.63833	-9.00556	60	23
ALIJO	90.2	30.000	41.31528	-7.46250	811	24
ALJUSTREL	92.6	26.990	37.87966	-8.17277	220	25
ALMANSIL	99.7	33.010	37.15944	-8.05889	299	26
ALMEIRIM	96.9	16.990	39.21667	-8.63333	8	27
ALMODOVAR	100.4	16.990	37.37087	-8.08000	574	28
ALTO DAS GAEIRAS	91.0	30.000	39.37528	-9.11222	20	29
ALTO DOS PICOTOS	96.0	30.000	39.74833	-8.98944	104	30
ALTO S. PEDRO	97.5	26.990	38.33306	-7.71611	400	31
ALTO SANTA CATARINA	90.5	33.010	39.68972	-8.32226	415	32

Table B.1 (cont.) - Characteristics of the FM sound broadcasting stations in Portugal (adapted from [ANAC14]).

Location ID	f [MHz]	ERP [dBW]	Latitude [°]	Longitude [°]	$h_{terrain}$ [m]	ID no.
ALVOR	90.1	30.000	37.12444	-8.57917	25	33
ARGANIL	88.5	26.990	40.18604	-8.00161	938	34
ARIEIRO	90.2	16.990	38.42917	-28.44917	50	35
ARÕES	101.0	26.990	40.84667	-8.27833	1 003	36
ARRENTELA	98.7	31.761	38.63083	-9.15111	27	37
ARRIFE	94.5	24.771	38.38899	-28.22629	184	38
ARRIFE	97.5	24.771	38.38899	-28.22629	184	39
ARRUDA DOS VINHOS	97.1	26.990	38.97283	-9.10429	387	40
ASSUNÇÃO	88.6	26.021	41.32694	-8.44667	414	41
AVEIRO	97.4	23.010	40.62704	-8.61654	47	42
AVEIRO	102.5	23.010	40.62704	-8.61654	47	43
AVEIRO	105.6	30.000	40.63639	-8.65083	11	44
AVELEIRA	99.7	30.000	40.25889	-8.34917	527	45
AVESSADA	105.6	30.000	38.91139	-9.27417	421	46
AVOES	97.0	33.010	41.11417	-7.84528	990	47
BALTAR	100.1	33.010	41.20194	-8.38667	444	48
BARBARA GOMES - RR	95.0	40.000	33.07472	-16.36644	222	49
BATALHA	104.8	26.990	39.65000	-8.82694	125	50
BEIRA	107.7	16.990	38.71639	-28.20222	421	51
BEJA	101.4	33.010	38.01222	-7.86250	273	52
BEJA	104.5	33.010	38.01333	-7.85972	280	53
BOAVENTURA	99.2	16.990	32.81250	-16.95167	819	54
BORNES	87.7	26.990	41.43472	-7.00444	1 150	55
BORNES	88.2	26.990	41.43222	-7.00611	1 165	56
BRAGA	88.0	33.010	41.54154	-8.36924	550	57
BRAGA	89.7	30.000	41.53749	-8.36764	4	58
BRAGA	91.3	40.000	41.54154	-8.36924	550	59
BRAGA	92.9	33.010	41.51557	-8.39628	550	60
BRAGA	97.5	30.000	41.51557	-8.39628	550	61
BRAGA	99.2	46.990	41.51405	-8.39559	543	62
BRAGA	101.1	40.000	41.53749	-8.36764	546	63
BRAGA	103.0	40.000	41.54154	-8.36924	550	64
BRAGA	106.0	33.010	41.51557	-8.39628	550	65
BRAGA	106.9	40.000	41.53761	-8.36761	546	66
BRAGANÇA	89.2	30.000	41.71917	-6.85306	1 299	67
BRAGANÇA	90.0	16.990	41.79594	-6.75076	840	68
BRAGANÇA	93.9	40.000	41.71917	-6.85306	1 299	69
BRAGANÇA	96.4	40.000	41.79500	-6.74889	819	70
BRAGANÇA	96.4	40.000	41.79500	-6.74889	819	71
BRAGANÇA	97.3	16.990	41.79583	-6.75028	821	72

Table B.1 (cont.) - Characteristics of the FM sound broadcasting stations in Portugal (adapted from [ANAC14]).

Location ID	f [MHz]	ERP [dBW]	Latitude [°]	Longitude [°]	$h_{terrain}$ [m]	ID no.
BRAGANÇA	97.7	30.000	41.71917	-6.85306	1 299	73
BRAGANÇA	98.2	40.000	41.79601	-6.74733	814	74
BRAGANÇA	99.5	40.000	41.79567	-6.74686	819	75
BRAGANÇA	104.2	40.000	41.79601	-6.74733	814	76
BRAGANÇA	105.7	40.000	41.79567	-6.74686	819	77
BRAGANÇA	107.0	40.000	41.79596	-6.75197	823	78
BRENHA	99.1	33.010	40.19222	-8.83889	175	79
BRUFE	96.4	16.990	41.41889	-8.54528	45	80
BUSTARENGA	95.4	16.990	40.78806	-8.29917	497	81
CABANA MAIOR	100.8	16.990	41.85611	-8.25528	329	82
CABEÇA DE CÃO	100.0	30.000	40.62333	-8.31444	444	83
CABEÇA GORDA - TREMÊS	97.7	33.010	39.33556	-8.74667	150	84
CABEÇO DO CURA - RR	97.3	30.000	32.74477	-16.81457	655	85
CABEÇO GORDO	88.9	40.000	38.57570	-28.71490	1 019	86
CABEÇO GORDO	91.3	26.990	38.57638	-28.71299	1 050	87
CABEÇO GORDO	100.2	26.990	38.57611	-28.71417	1 021	88
CABECO VERDE	94.9	16.990	38.59268	-28.79917	459	89
CABEÇO VERDE	98.1	30.000	38.59261	-28.79916	459	90
CABO GIRÃO	94.8	30.000	32.65969	-17.00484	642	91
CABO GIRÃO	96.7	30.000	32.65969	-17.00484	642	92
CABO GIRÃO	99.4	34.771	32.65969	-17.00484	642	93
CAÇARILHE	105.6	26.990	41.39389	-8.07111	709	94
CALDAS DA RAINHA	103.1	30.000	39.40528	-9.13333	61	95
CALDELAS	104.4	30.000	41.65799	-8.35499	554	96
CALENDÁRIO	94.0	33.010	41.40000	-8.52500	428	97
CALHETA	98.8	26.990	32.74592	-17.11810	1 326	98
CALHETA	102.7	16.990	32.72136	-17.17504	154	99
CAMPO	106.4	33.010	40.71111	-7.90333	623	100
CAMPO MAIOR	95.9	26.990	39.02889	-7.08611	319	101
CANHAS	103.7	26.990	32.68997	-17.10731	226	102
CANIÇO	89.3	26.990	32.65995	-16.83699	445	103
CANIÇO	99.0	26.990	32.65995	-16.83699	445	104
CANIÇO	101.6	26.990	32.65995	-16.83699	445	105
CANTANHEDE	103.0	33.010	40.26944	-8.55694	100	106
CARAMULO	91.2	26.990	40.55333	-8.17917	974	107
CARREGAL DO SAL	101.4	30.000	40.43278	-7.99917	304	108
CARTAXO	102.9	26.990	39.16222	-8.79000	50	109
CARVALHAL	107.0	16.990	39.87167	-8.09833	674	110
CARVELA	93.5	30.000	41.69748	-7.43760	909	111
CASAS DO REGEDOR	92.2	30.000	39.11278	-8.88611	81	112

Table B.1 (cont.) - Characteristics of the FM sound broadcasting stations in Portugal (adapted from [ANAC14]).

Location ID	f [MHz]	ERP [dBW]	Latitude [°]	Longitude [°]	$h_{terrain}$ [m]	ID no.
CASAL DA MADALENA	92.7	16.990	39.79750	-8.22667	379	113
CASCALHO NEGRO	92.2	30.000	37.85365	-25.81427	540	114
CASCALHO NEGRO	93.0	16.990	37.85365	-25.81436	540	115
CASCALHO NEGRO - RR	96.4	30.000	37.85365	-25.81418	537	116
CASTANHEIRA DO VOUGA	99.3	33.010	40.59139	-8.35528	291	117
CASTELEJO	107.0	16.990	40.09806	-7.64944	999	118
CASTELO ABOIM	99.6	30.000	41.77045	-8.37460	756	119
CASTELO BRANCO	89.9	26.990	39.82546	-7.49681	470	120
CASTELO BRANCO	92.0	33.010	39.82489	-7.49711	468	121
CASTELO BRANCO	94.9	26.990	39.82546	-7.49681	470	122
CASTELO BRANCO	97.5	16.990	39.82556	-7.49583	468	123
CASTELO BRANCO	104.3	26.990	39.82546	-7.49681	470	124
CASTELO DE PAIVA	99.5	30.000	40.98500	-8.25472	551	125
CASTELO NOVO	92.7	33.010	41.25833	-8.13333	477	126
CASTRO MARIM	103.3	30.000	37.21667	-7.44167	34	127
CASTRO VERDE	93.0	30.000	37.73194	-8.14472	261	128
CHÃ DE BAIXO	101.7	33.010	39.37861	-8.68194	128	129
CHAMUSCA	104.9	26.990	39.35444	-8.46694	125	130
CHAVÃES	91.5	30.000	41.08944	-7.57472	917	131
COIMBRA	90.0	36.990	40.20889	-8.42139	77	132
COIMBRA	94.9	36.021	40.21724	-8.40593	150	133
COIMBRA	98.4	36.990	40.18389	-8.45361	152	134
COIMBRA	103.4	30.000	40.21724	-8.40593	150	135
COIMBRA	107.9	33.010	40.20139	-8.44361	99	136
CORROIOS	87.6	31.761	38.61222	-9.15667	49	137
CORUCHE	94.7	33.010	38.96611	-8.52833	20	138
COSTAS DE CÃO	105.4	26.021	38.66750	-9.21667	100	139
COVAS DO RIO	93.0	30.000	40.87750	-8.05972	923	140
COVILHÃ	95.6	30.000	40.28444	-7.54083	1 312	141
COVILHÃ	97.0	16.990	40.23389	-7.42111	574	142
CRUZES - RR	91.7	30.000	38.67025	-27.08507	203	143
DEGRACIAS	104.4	30.000	39.99472	-8.53333	550	144
EIRA VEDRA	91.6	30.000	41.65694	-8.13889	715	145
ELVAS	99.8	30.000	38.86139	-7.26722	443	146
ELVAS	102.3	20.000	38.87750	-7.15889	293	147
ELVAS	104.3	16.990	38.88083	-7.16111	293	148
ELVAS	107.1	30.000	38.86139	-7.26722	443	149
ENCUMEADA	89.2	26.990	32.75322	-17.01667	1 031	150
ENCUMEADA	90.8	24.771	32.75010	-17.01344	983	151
ENCUMEADA	93.1	24.771	32.75010	-17.01344	983	152

Table B.1 (cont.) - Characteristics of the FM sound broadcasting stations in Portugal (adapted from [ANAC14]).

Location ID	f [MHz]	ERP [dBW]	Latitude [°]	Longitude [°]	h_{terrain} [m]	ID no.
ENCUMEADA - RR	92.0	30.000	32.75002	-17.01429	998	153
ENTRONCAMENTO	91.1	30.000	39.46958	-8.48173	49	154
ERMIDA	91.3	26.990	39.84611	-7.92861	1 065	155
ERMIDA	98.7	30.000	41.71444	-8.50972	545	156
ESMOLFE	95.6	16.990	40.68556	-7.65861	580	157
ESMORIZ	93.1	30.000	40.95500	-8.62500	37	158
ESPINHAL	93.5	26.990	40.00778	-8.29611	542	159
ESPINHO	88.4	30.000	40.99528	-8.61333	66	160
ESPOSENDE	89.3	26.000	41.54167	-8.75278	160	161
ESPOSENDE	93.2	26.990	41.57937	-8.73511	204	162
ESTARREJA	90.2	30.000	40.75278	-8.56889	22	163
FAFE	103.8	30.000	41.54139	-8.16611	562	164
FAJÃ DA OVELHA	107.1	16.990	32.78079	-17.22474	712	165
FARO	89.6	40.000	37.10165	-7.83061	400	166
FARO	90.9	30.000	37.10042	-7.83495	352	167
FARO	93.4	40.000	37.10177	-7.83157	400	168
FARO	96.1	40.000	37.10176	-7.83072	399	169
FARO	97.6	40.000	37.10177	-7.83157	400	170
FARO	99.1	30.000	37.10177	-7.83157	400	171
FARO	100.7	40.000	37.10177	-7.83157	400	172
FARO	101.6	30.000	37.10167	-7.83139	401	173
FARO	102.7	26.990	37.10131	-7.82988	389	174
FARO	103.8	40.000	37.10165	-7.83061	400	175
FARO	106.1	40.000	37.10176	-7.83072	399	176
FARROCO - RR	97.4	30.000	38.79007	-27.19888	167	177
FAZENDAS DE ALMEIRIM	104.0	30.000	39.15000	-8.57750	149	178
FAZENDAS DE ALMEIRIM	107.8	26.990	39.15000	-8.57750	149	179
FERRAGUDO	100.0	16.990	37.12472	-8.51750	25	180
FERREIRA DO ALENTEJO	104.0	26.990	38.04503	-8.10117	161	181
FERVENÇA	93.1	16.990	41.37139	-8.06167	635	182
FIGUEIRA DA FOZ	92.1	33.010	40.14750	-8.84722	11	183
FIGUEIRÓ DOS VINHOS	97.5	30.000	39.91056	-8.27722	518	184
FOLHADA	93.3	30.000	41.19417	-8.04111	950	185
FONTE BASTARDO	98.4	16.990	38.71139	-27.11306	531	186
FONTELO	92.3	30.000	41.12167	-7.74528	725	187
FORNELO DO MONTE	105.5	33.010	40.64028	-8.10472	809	188
FUNCHAL	88.8	30.000	32.70878	-16.91062	1 476	189
FUNCHAL	89.8	30.000	32.67208	-16.90472	459	190
FUNCHAL	92.0	33.010	32.68427	-16.94678	681	191
FUNCHAL	95.0	6.990	32.64750	-16.91111	27	192

Table B.1 (cont.) - Characteristics of the FM sound broadcasting stations in Portugal (adapted from [ANAC14]).

Location ID	f [MHz]	ERP [dBW]	Latitude [°]	Longitude [°]	$h_{terrain}$ [m]	ID no.
FUNCHAL	100.0	33.010	32.70879	-16.91002	1 473	193
FUNCHAL	102.4	30.000	32.67208	-16.90472	459	194
FUNCHAL	104.6	30.000	32.67208	-16.90472	459	195
FURNAS	93.6	30.000	37.76139	-25.31852	293	196
GAFANHA DA NAZARÉ	105.0	30.000	40.62528	-8.70917	5	197
GAULA	91.3	30.000	32.67716	-16.81969	431	198
GAULA	96.1	26.990	32.68806	-16.82000	490	199
GAULA	98.5	30.000	32.67716	-16.81969	431	200
GAULA	106.3	34.771	32.67716	-16.81969	431	201
GOLEGÃ	88.4	30.000	39.44306	-8.47306	30	202
GOSENDE	88.1	16.990	41.01000	-7.90778	1 029	203
GRANDOLA	91.3	26.021	38.17176	-8.64784	320	204
GRANDOLA	96.8	40.000	38.17250	-8.64806	320	205
GRANDOLA	107.5	40.000	38.17250	-8.64804	320	206
GRÂNDOLA	90.6	40.000	38.16936	-8.64488	307	207
GRÂNDOLA	99.2	40.000	38.16936	-8.64488	307	208
GRÂNDOLA	103.6	40.000	38.16936	-8.64488	307	209
GRANJA DO ULMEIRO	95.7	16.990	40.15917	-8.61528	46	210
GUARDA	88.4	40.000	40.53670	-7.28058	997	211
GUARDA	90.2	40.000	40.53394	-7.27634	1 025	212
GUARDA	90.9	33.010	40.52278	-7.28417	1 050	213
GUARDA	94.7	40.000	40.53670	-7.28058	997	214
GUARDA	96.1	40.000	40.52264	-7.28536	1 039	215
GUARDA	100.6	40.000	40.52297	-7.28377	1 050	216
GUARDA	104.0	40.000	40.53394	-7.27634	1 025	217
GUARDA	105.8	33.010	40.53500	-7.27389	1 026	218
GUARDA	106.6	40.000	40.52278	-7.28524	1 039	219
GUIMARAES	95.8	33.010	41.41972	-8.26722	541	220
GUIMARÃES	98.0	33.010	41.42917	-8.26861	545	221
HORTA	93.8	26.990	38.54832	-28.61805	144	222
HORTA	101.4	26.990	38.54832	-28.61805	144	223
HORTA	102.2	16.990	38.54634	-28.62020	68	224
INFIAS	87.6	26.990	40.62917	-7.54056	651	225
JARDIA	90.9	31.761	38.63333	-8.91667	50	226
LAGARES	94.5	26.990	41.33028	-7.64361	874	227
LAGOA DO PILAR - RR	91.3	30.000	37.89808	-25.78026	304	228
LAGOS	94.6	30.000	37.09056	-8.74306	95	229
LAJES DAS FLORES	97.0	26.990	39.38865	-31.17828	252	230
LAJES DAS FLORES	100.4	30.000	39.42886	-31.25809	321	231
LAJES DAS FLORES	102.6	23.010	39.38865	-31.17828	252	232

Table B.1 (cont.) - Characteristics of the FM sound broadcasting stations in Portugal (adapted from [ANAC14]).

Location ID	f [MHz]	ERP [dBW]	Latitude [°]	Longitude [°]	h_{terrain} [m]	ID no.
LAJES DAS FLORES	103.7	30.000	39.42886	-31.25809	321	233
LAJES DO PICO	88.5	16.990	38.38995	-28.22466	217	234
LAJES DO PICO	93.5	30.000	38.38953	-28.25049	19	235
LAJES DO PICO	96.5	30.000	38.38953	-28.25049	19	236
LAJES DO PICO	98.6	30.000	38.38953	-28.25023	19	237
LAJES DO PICO	104.7	26.990	38.38824	-28.24991	45	238
LAMAS DE OLO	96.3	30.000	41.36417	-7.76056	1 233	239
LAMAS DE OLO	97.4	30.000	41.36417	-7.76056	1 233	240
LAMEGO	88.7	40.000	41.11329	-7.84535	983	241
LAMEGO	94.0	33.010	41.10778	-7.83139	878	242
LAMEGO	98.6	40.792	41.11390	-7.84579	985	243
LAMEGO	106.2	40.792	41.11390	-7.84579	985	244
LAMEGO	107.9	16.990	41.09722	-7.80667	484	245
LAUNDOS	89.0	33.010	41.43333	-8.71528	151	246
LAUNDOS	96.1	33.010	41.43333	-8.69861	84	247
LEIRIA	89.0	30.000	39.68167	-8.75583	410	248
LEIRIA	93.0	33.010	39.68167	-8.75583	410	249
LEIRIA	94.0	33.010	39.68167	-8.75583	410	250
LEIRIA	101.3	33.010	39.68167	-8.75583	410	251
LISBON	89.5	36.990	38.73250	-9.18806	203	252
LISBON	90.4	36.990	38.73861	-9.19000	220	253
LISBON	91.6	36.990	38.73861	-9.19000	220	254
LISBON	92.4	36.990	38.73256	-9.18883	210	255
LISBON	93.2	46.990	38.73256	-9.18883	210	256
LISBON	94.4	50.000	38.73347	-9.18769	206	257
LISBON	95.7	50.000	38.73347	-9.18769	206	258
LISBON	96.6	36.990	38.73861	-9.19000	220	259
LISBON	97.4	46.435	38.73861	-9.19000	220	260
LISBON	100.3	50.000	38.73347	-9.18769	206	261
LISBON	101.5	36.990	38.73347	-9.18769	206	262
LISBON	103.4	46.990	38.73256	-9.18883	210	263
LISBON	104.3	46.990	38.73861	-9.19000	220	264
LOIVO-VILA NOVA CERVEIRA	93.6	26.990	41.92194	-8.71194	614	265
LOMBA DO FOGO - RR	89.7	30.000	38.48915	-28.41621	1 010	266
LOMBA DOS ESPALHAFATOS	95.9	16.990	38.60600	-28.63321	294	267
LOULÉ	95.8	30.000	37.15801	-8.11085	310	268
LOULÉ	103.1	33.010	37.16083	-8.06056	300	269
LOUREDO	89.2	33.010	41.25389	-8.13250	465	270
LOURINHÃ	99.0	30.000	39.21083	-9.29306	150	271
LOUSÃ	87.9	50.000	40.08952	-8.17885	1 184	272

Table B.1 (cont.) - Characteristics of the FM sound broadcasting stations in Portugal (adapted from [ANAC14]).

Location ID	f [MHz]	ERP [dBW]	Latitude [°]	Longitude [°]	$h_{terrain}$ [m]	ID no.
LOUSÃ	89.3	50.000	40.08952	-8.17885	1 184	273
LOUSÃ	90.8	46.435	40.09019	-8.17885	1 170	274
LOUSÃ	91.7	47.482	40.09173	-8.17835	1 174	275
LOUSÃ	102.2	50.000	40.08952	-8.17885	1 184	276
LOUSÃ	106.0	46.990	40.09173	-8.17835	1 174	277
LOUSÃ	107.4	46.990	40.09019	-8.17944	1 170	278
LUSO	92.6	30.000	40.36987	-8.36201	548	279
LUSTOSA	97.2	30.000	41.35556	-8.31250	306	280
MAÇAPEZ	92.0	20.000	32.77081	-17.23832	294	281
MAÇAPEZ	95.7	20.000	32.77081	-17.23832	293	282
MACELA	87.6	30.000	38.71059	-28.20334	464	283
MACELA	93.2	30.000	38.71059	-28.20334	464	284
MANGUALDE	107.1	33.010	40.61444	-7.73472	599	285
MANTEIGAS	91.6	26.990	40.41810	-7.54400	1 319	286
MANTEIGAS	100.3	26.990	40.41810	-7.54400	1 319	287
MANTEIGAS	104.4	26.990	40.40722	-7.56833	1 502	288
MANTEIGAS	104.8	26.990	40.41810	-7.54400	1 319	289
MARÃO	95.2	40.000	41.24845	-7.88678	1 420	290
MARÃO	99.8	40.000	41.24845	-7.88678	1 420	291
MARÃO	101.5	40.000	41.24845	-7.88678	1 420	292
MARÃO	107.6	40.000	41.24811	-7.88681	1 410	293
MARGARIDE	92.2	30.000	41.37333	-8.19333	446	294
MARVILA SANTAREM	105.5	16.990	39.23056	-8.68528	30	295
MATOSINHOS	91.0	31.761	41.18087	-8.69312	7	296
MATRIZ OUT PINHEIROS	93.8	30.000	38.81417	-7.46556	455	297
MEÃ	89.9	30.000	40.75583	-7.71167	687	298
MEDA	96.6	26.990	40.99306	-7.26500	784	299
MELGAÇO	88.5	26.990	42.11508	-8.25043	1 179	300
MÉRTOLA	90.9	26.021	37.64182	-7.66116	59	301
MÉRTOLA	92.2	26.021	37.64182	-7.66116	59	302
MÉRTOLA	95.2	26.990	37.70165	-7.76567	319	303
MÉRTOLA	100.1	26.021	37.64182	-7.66116	59	304
MEZIO	92.5	16.990	40.98056	-7.86972	1 006	305
MINHÉU	88.0	40.000	41.54949	-7.68849	1 180	306
MINHÉU	88.9	40.000	41.54942	-7.68855	1 181	307
MINHÉU	89.8	40.000	41.54994	-7.68849	1 190	308
MINHÉU	94.9	40.000	41.54949	-7.68849	1 180	309
MINHÉU	95.5	30.000	41.55056	-7.68694	1 130	310
MINHÉU	102.6	40.000	41.54994	-7.68849	1 190	311
MINHÉU	104.7	40.000	41.54949	-7.68849	1 180	312

Table B.1 (cont.) - Characteristics of the FM sound broadcasting stations in Portugal (adapted from [ANAC14]).

Location ID	f [MHz]	ERP [dBW]	Latitude [°]	Longitude [°]	$h_{terrain}$ [m]	ID no.
MINHÉU	106.7	40.000	41.54949	-7.68849	1 180	313
MIRANDA DO DOURO	90.3	16.990	41.49778	-6.27806	650	314
MIRANDA DO DOURO	95.7	16.990	41.49778	-6.27806	650	315
MIRANDA DO DOURO	98.9	16.990	41.49778	-6.27806	650	316
MIRANDA DO DOURO	100.1	26.989	41.55222	-6.35222	811	317
MIRANDELA	105.5	16.990	41.48500	-7.17611	253	318
MOIMENTA DA BEIRA	90.5	30.000	41.02806	-7.57250	908	319
MOINHO OUTEIRO	96.2	30.000	40.05778	-8.44667	175	320
MOITA	95.3	31.761	38.65861	-8.97528	28	321
MOLEDO	88.0	26.990	41.83678	-8.86514	145	322
MOLEDO	92.3	26.990	41.83678	-8.86514	145	323
MOLEDO	102.9	26.990	41.83678	-8.86514	145	324
MONCHIQUE	88.1	40.000	37.31555	-8.58947	875	325
MONCHIQUE	88.9	43.979	37.31830	-8.58968	848	326
MONCHIQUE	91.5	43.979	37.31841	-8.58968	847	327
MONCHIQUE	97.1	26.990	37.31577	-8.58952	875	328
MONCHIQUE	98.6	40.792	37.31528	-8.58913	875	329
MONCHIQUE	101.9	43.979	37.31830	-8.58968	848	330
MONCHIQUE	104.9	40.792	37.31528	-8.58913	875	331
MONCHIQUE	107.1	40.000	37.31555	-8.58947	875	332
MONSANTO	98.7	30.000	40.03806	-7.11306	720	333
MONTARGIL	93.6	34.771	39.07694	-8.18694	230	334
MONTARGIL	99.6	34.771	39.07694	-8.18694	230	335
MONTARGIL	105.0	34.771	39.07694	-8.18694	230	336
MONTE	106.8	26.021	32.69302	-16.90303	1 110	337
MONTE COTAO	96.4	30.000	41.95313	-8.49258	815	338
MONTE DA CAPARICA	95.0	31.761	38.66472	-9.19389	50	339
MONTE DA CAPARICA	97.8	33.010	38.67611	-9.18278	120	340
MONTE DA CAPARICA	102.6	31.761	38.67611	-9.18278	120	341
MONTE DA VIRGEM	90.0	36.990	41.10889	-8.58667	220	342
MONTE DA VIRGEM	92.5	50.000	41.10833	-8.58611	211	343
MONTE DA VIRGEM	93.7	46.990	41.11180	-8.59687	185	344
MONTE DA VIRGEM	94.8	36.990	41.10694	-8.59111	216	345
MONTE DA VIRGEM	95.5	33.010	41.10833	-8.58611	211	346
MONTE DA VIRGEM	96.7	50.000	41.10833	-8.58611	211	347
MONTE DA VIRGEM	98.9	36.990	41.10694	-8.59111	216	348
MONTE DA VIRGEM	100.4	50.000	41.10833	-8.58611	211	349
MONTE DA VIRGEM	101.3	33.010	41.10833	-8.58611	211	350
MONTE DA VIRGEM	102.7	33.010	41.10694	-8.59111	216	351
MONTE DA VIRGEM	104.1	46.990	41.11180	-8.59687	185	352

Table B.1 (cont.) - Characteristics of the FM sound broadcasting stations in Portugal (adapted from [ANAC14]).

Location ID	f [MHz]	ERP [dBW]	Latitude [°]	Longitude [°]	$h_{terrain}$ [m]	ID no.
MONTE DA VIRGEM	107.2	26.990	41.10889	-8.58667	220	353
MONTE DAS CRUZES	97.4	30.000	39.45089	-31.13565	179	354
MONTE DAS CRUZES	99.8	30.000	39.45089	-31.13565	179	355
MONTE DE CAPARICA	88.9	24.771	38.67356	-9.18853	113	356
MONTE DE CAPARICA	98.1	34.771	38.67306	-9.19444	100	357
MONTE DE CAPARICA	99.4	30.000	38.67356	-9.18853	113	358
MONTE DE CAPARICA	100.0	24.771	38.67356	-9.18853	113	359
MONTE DE CAPARICA	100.8	33.010	38.67306	-9.19444	100	360
MONTE DO FACHO	97.5	26.990	41.79333	-7.82500	1 228	361
MONTE SANTA LUZIA	90.8	33.010	41.70472	-8.83028	62	362
MONTE STA JUSTA	90.6	33.010	41.17861	-8.49611	355	363
MONTE STA JUSTA	105.8	31.761	41.17861	-8.49611	355	364
MONTEMOR	101.9	33.010	38.82444	-9.20333	318	365
MONTEMOR-O-NOVO	101.3	33.010	38.66726	-8.20952	293	366
MONTEMOR-O-VELHO	101.7	30.000	40.18333	-8.68333	54	367
MONTIJO	106.2	30.000	38.70306	-8.96694	5	368
MORRO ALTO	91.9	30.000	39.46339	-31.22003	895	369
MORRO ALTO	93.5	30.000	39.46339	-31.22003	895	370
MORRO ALTO - RR	96.2	30.000	39.46339	-31.22022	900	371
MOSTEIRO	95.1	20.000	37.87106	-25.84161	197	372
MOSTEIRO	105.2	20.000	37.87106	-25.84161	197	373
MOSTEIRO	107.0	20.000	37.87106	-25.84161	197	374
MOURA	92.8	26.990	38.13889	-7.44778	187	375
MOURÃO	96.2	26.990	38.38474	-7.34679	220	376
MTE PENOITA	94.6	30.000	40.69132	-8.12426	861	377
MURO	88.3	40.000	41.80647	-8.20386	1 325	378
MURO	90.4	43.010	41.81390	-8.19604	1 343	379
MURO	94.6	40.000	41.80647	-8.20386	1 325	380
MURO	102.0	40.000	41.80647	-8.20386	1 325	381
MURO	103.4	40.000	41.81390	-8.19604	1 343	382
MURO	106.5	40.000	41.80647	-8.20416	1 328	383
MURTOSA	98.1	26.990	40.74750	-8.64306	2	384
NAZARE	100.6	30.000	39.60556	-9.07083	96	385
NELAS	96.8	30.000	40.54222	-7.84444	432	386
NORDESTE	104.6	20.000	37.83422	-25.14660	170	387
NORDESTE	106.0	26.990	37.82882	-25.14728	172	388
OLIVEIRA	91.9	33.010	41.57889	-8.56000	303	389
OLIVEIRA	102.4	26.990	41.57500	-8.55694	152	390
OLIVEIRA DO HOSPITAL	100.2	26.990	40.33056	-7.86389	523	391
OLIVEIRA SANTA MARIA	105.0	33.010	41.41750	-8.40361	322	392

Table B.1 (cont.) - Characteristics of the FM sound broadcasting stations in Portugal (adapted from [ANAC14]).

Location ID	f [MHz]	ERP [dBW]	Latitude [°]	Longitude [°]	h_{terrain} [m]	ID no.
OLIVEIRINHA	94.4	33.010	40.60833	-8.59167	50	393
OLIVEIRINHA	96.5	33.010	40.61639	-8.60556	50	394
ORGENS	102.8	33.010	40.66889	-7.91806	480	395
OURIQUE	94.2	26.990	37.65417	-8.22611	236	396
OVAR	98.7	30.000	40.86028	-8.63278	16	397
PAÇÔ	87.6	26.021	41.75583	-8.83750	427	398
PACOS DE FERREIRA	101.8	30.000	41.27528	-8.37444	308	399
PALMELA	102.2	33.010	38.56667	-8.90111	214	400
PAREDES	103.6	26.990	41.20000	-8.41667	235	401
Paredes de Coura	88.0	20.000	41.90786	-8.56464	448	402
Paredes de Coura	92.3	20.000	41.90786	-8.56464	448	403
Paredes de Coura	102.9	20.000	41.90786	-8.56464	448	404
PAUL DA SERRA	93.3	30.000	32.74698	-17.11104	1 403	405
PAUL DA SERRA	101.9	30.000	32.74698	-17.11104	1 403	406
PAUL DA SERRA - RR	97.1	30.000	32.75207	-17.12994	1 294	407
PAUL DO MAR	104.3	16.990	32.75014	-17.21211	558	408
PEDRA MOLE - RR	107.3	30.000	32.67658	-17.04915	390	409
PEDRAS DO AMBROSIO	96.0	33.010	39.16504	-7.99098	249	410
PENA	102.5	20.000	40.69042	-8.12367	860	411
PENAFIEL	91.8	33.010	41.20833	-8.26250	330	412
Penafiel - RFM	102.3	30.000	41.21422	-8.26558	382	413
Penafiel - RR	90.2	30.000	41.21422	-8.26558	382	414
PENAMACOR	87.7	30.000	40.16917	-7.17500	578	415
PENEDO BRANCO	95.0	30.000	41.82242	-8.53999	712	416
PENHA LONGA	88.5	16.990	41.10500	-8.13917	567	417
PERNES	96.1	16.990	39.38639	-8.66139	72	418
PICO ALTO	96.7	40.000	36.98320	-25.09061	559	419
PICO ALTO - RR	90.6	30.000	36.98320	-25.09061	559	420
PICO ALTO VPT	103.2	33.010	36.98320	-25.09061	559	421
PICO ARCO S. JORGE	105.5	16.990	32.81272	-16.94966	807	422
PICO BARTOLOMEU	89.9	26.990	37.77833	-25.16880	854	423
PICO BARTOLOMEU	92.7	30.000	37.77833	-25.16880	854	424
PICO BARTOLOMEU - RR	88.7	30.000	37.77819	-25.16862	854	425
PICO DA BARROSA	88.5	34.771	37.76151	-25.49288	924	426
PICO DA BARROSA	97.9	46.990	37.76041	-25.49163	930	427
PICO DA BARROSA	99.4	34.771	37.76028	-25.49139	930	428
PICO DA BARROSA	101.7	46.990	37.76041	-25.49163	930	429
PICO DA BARROSA	102.4	26.990	37.76166	-25.49324	925	430
PICO DA BARROSA	105.0	26.990	37.76188	-25.49333	930	431
PICO DA BARROSA	105.5	33.010	37.75944	-25.49194	916	432

Table B.1 (cont.) - Characteristics of the FM sound broadcasting stations in Portugal (adapted from [ANAC14]).

Location ID	f [MHz]	ERP [dBW]	Latitude [°]	Longitude [°]	h_{terrain} [m]	ID no.
PICO DA BARROSA	107.2	30.000	37.76144	-25.49298	926	433
PICO DA BARROSA - RR	95.2	46.990	37.76056	-25.49145	930	434
PICO DA CRUZ	98.4	26.990	32.68222	-17.00028	774	435
PICO DA CRUZ	101.0	33.010	32.68430	-17.00446	939	436
PICO DA PENA	104.5	20.000	40.68861	-8.12194	850	437
PICO DA PENA	106.8	20.000	40.68861	-8.12194	850	438
PICO DA PENA	107.9	20.000	40.68861	-8.12194	850	439
PICO DA URZE - RR	92.7	30.000	38.45324	-28.34996	869	440
PICO DAS ÉGUAS	89.5	40.000	37.81903	-25.75148	812	441
PICO DO AREEIRO	92.5	26.990	32.73632	-16.92597	1 792	442
PICO DO AREEIRO	94.1	46.435	32.72075	-16.91582	1 584	443
PICO DO AREEIRO	95.5	46.435	32.72075	-16.91582	1 584	444
PICO DO CASTELO - RR	90.5	30.000	33.07781	-16.33375	250	445
PICO DO FACHO	90.8	20.000	32.72435	-16.75927	276	446
PICO DO FACHO	93.1	20.000	32.72435	-16.75927	276	447
PICO DO FACHO - RR	99.0	30.000	32.72442	-16.75945	271	448
PICO DO GALO - RR	97.9	30.000	32.65992	-17.00442	638	449
PICO DO GERALDO	103.7	30.000	38.40181	-28.23521	460	450
PICO DO GERALDO	107.5	30.000	38.40181	-28.23521	460	451
PICO DO GERALDO - RR	91.6	30.000	38.40174	-28.23503	456	452
PICO DO JARDIM	97.0	30.000	39.08463	-28.01921	110	453
PICO DO SILVA - RR	88.0	46.435	32.69021	-16.87422	1 099	454
PICO MARTIM SIMÃO	89.6	17.000	38.79306	-27.29111	106	455
PICO S JORGE - RR	96.3	30.000	32.81323	-16.94985	798	456
PIEIDADE	105.3	16.990	38.41386	-28.06498	207	457
PINELA	91.5	26.989	41.64517	-6.79120	908	458
PINHEL	99.1	30.000	40.75667	-7.01528	658	459
PIÓDÃO	97.3	16.990	40.26139	-7.83250	937	460
POMBAL	87.6	30.000	39.92056	-8.54056	550	461
PONTA DELGADA	94.1	30.000	37.74584	-25.67062	38	462
PONTA DELGADA	100.8	36.990	37.74584	-25.67062	38	463
PONTA DELGADA	106.3	16.990	37.73968	-25.66747	12	464
PONTA DO PARGO	90.2	30.000	32.81152	-17.25344	390	465
PONTA DO PARGO	94.6	30.000	32.81152	-17.25344	390	466
PONTE DE SOR	105.6	16.990	39.23361	-8.00750	166	467
PORCHES	99.4	30.000	37.13806	-8.40000	58	468
PORTALEGRE	92.9	40.000	39.30869	-7.41281	540	469
PORTALEGRE	95.3	40.000	39.31308	-7.35972	1 010	470
PORTALEGRE	97.9	40.000	39.30869	-7.41281	540	471
PORTALEGRE	98.9	40.000	39.30977	-7.41251	545	472

Table B.1 (cont.) - Characteristics of the FM sound broadcasting stations in Portugal (adapted from [ANAC14]).

Location ID	f [MHz]	ERP [dBW]	Latitude [°]	Longitude [°]	h_{terrain} [m]	ID no.
PORTALEGRE	101.1	40.000	39.31308	-7.35972	1 010	473
PORTALEGRE	102.8	40.000	39.30869	-7.41281	540	474
PORTALEGRE	106.7	40.000	39.30972	-7.41250	545	475
PORTIMÃO	106.5	26.021	37.15333	-8.54361	25	476
PORTO MONIZ	102.9	26.990	32.86085	-17.17699	411	477
PORTO SANTO	91.6	26.990	33.08427	-16.32321	471	478
PORTO SANTO	96.5	40.000	33.06369	-16.37175	172	479
PORTO SANTO	100.5	40.000	33.06369	-16.37175	172	480
PORTO SANTO	103.3	40.000	33.06369	-16.37175	172	481
PÓVOA DE MONTEMURO	89.0	30.000	40.93889	-7.99139	907	482
POVOAÇÃO	91.0	26.990	37.76385	-25.31946	930	483
POVOAÇÃO	97.2	26.990	37.74846	-25.24762	77	484
POVOAÇÃO	102.8	30.000	37.74846	-25.24762	77	485
PRAIA DA VITÓRIA	92.4	16.990	38.73400	-27.05605	21	486
PRAINHA DO PICO	90.0	16.990	38.48794	-28.25028	313	487
REFOJOS DE BASTO	100.6	30.000	41.48917	-8.02472	750	488
REGUENGO DO FETAL	95.1	33.010	39.67197	-8.75839	410	489
REGUENGO DO FETAL	98.7	33.010	39.66764	-8.75121	408	490
REGUENGO DO FETAL	104.2	33.010	39.66764	-8.75121	408	491
REGUENGO DO FETAL	106.4	33.010	39.66764	-8.75121	408	492
REGUENGO DO FETAL	107.7	34.771	39.67197	-8.75839	410	493
REGUENGOS DE MONSARAZ	99.0	26.990	38.43759	-7.54949	249	494
RESENDE	104.9	26.990	41.01000	-7.92778	975	495
RIB. DE NIZA	100.5	33.010	39.30972	-7.41278	540	496
RIBEIRA BRAVA	103.1	30.000	32.68324	-17.06082	385	497
RIBEIRA BRAVA	105.6	30.000	32.68324	-17.06082	385	498
RIO MAIOR	99.5	16.990	39.37167	-8.95639	298	499
ROCAS DO VOUGA	95.2	26.990	40.78259	-8.35719	799	500
ROCAS DO VOUGA	106.7	26.990	40.78259	-8.35719	799	501
ROSAIS	90.8	16.990	38.71776	-28.24754	450	502
S PEDRO	89.6	30.000	40.49194	-7.58750	746	503
S. CRISTOVAO	104.5	16.990	39.28833	-7.41778	540	504
S. GENS	107.8	30.000	41.31806	-8.59444	174	505
S. JOAO DE VER	92.0	30.000	40.95250	-8.51750	304	506
S. JOAO DE VER	104.7	30.000	40.93889	-8.55833	121	507
SABUGAL	96.8	26.990	40.31167	-7.14333	916	508
SALGUEIRO	94.8	30.000	39.31250	-9.12500	190	509
SALVATERRA DE MAGOS	102.5	30.000	39.03333	-8.73333	20	510
SAMORA CORREIA	91.4	33.010	38.93472	-8.86833	10	511
SAMORINHA	98.1	30.000	41.25722	-7.30833	870	512

Table B.1 (cont.) - Characteristics of the FM sound broadcasting stations in Portugal (adapted from [ANAC14]).

Location ID	f [MHz]	ERP [dBW]	Latitude [°]	Longitude [°]	h_{terrain} [m]	ID no.
SANFINS	100.8	16.990	41.01389	-7.72806	800	513
SANTA BARBARA	106.6	30.000	38.73018	-27.31993	1 030	514
SANTA BÁRBARA	90.5	50.000	38.72972	-27.32028	1 005	515
SANTA BÁRBARA	98.9	50.000	38.72972	-27.32028	1 005	516
SANTA BÁRBARA	101.1	26.021	38.72997	-27.32002	1 030	517
SANTA BÁRBARA - RR	88.0	50.000	38.72990	-27.31926	1 030	518
SANTA CRUZ DA GRACIOSA	92.2	16.990	39.02347	-27.99837	70	519
SANTA CRUZ DAS FLORES	104.5	26.990	39.45791	-31.12821	180	520
SANTA LUZIA	101.7	16.990	41.70833	-8.83333	196	521
SANTARÉM	98.8	26.021	39.23417	-8.67639	99	522
SANTIAGO DO CACÉM	102.7	33.010	37.99028	-8.69056	249	523
SANTO AMARO	107.1	26.990	38.67760	-28.17924	435	524
SANTO ANTÓNIO DA NEVE	97.8	26.990	40.07778	-8.15972	1 163	525
SANTO DA SERRA	89.6	30.000	32.74111	-16.81056	571	526
SANTO ESTEVÃO	100.6	16.990	39.04944	-9.01917	149	527
SANTO QUINTINO	106.4	30.000	38.98861	-9.15278	389	528
SÃO BARNABÉ	90.4	27.000	37.37083	-8.08000	574	529
SÃO BENTO DE CASTRIS	94.1	33.010	38.58190	-7.93738	361	530
SÃO BENTO DE CASTRIS	103.2	33.010	38.58134	-7.93799	361	531
SÃO BENTO DE CASTRIS	105.4	33.010	38.58085	-7.93799	361	532
SÃO DOMINGOS	87.9	23.010	41.12068	-7.74657	720	533
SÃO DOMINGOS	89.3	23.010	41.12068	-7.74657	720	534
SÃO DOMINGOS	103.7	23.010	41.12068	-7.74657	720	535
SÃO JOÃO DA PESQUEIRA	99.4	26.990	41.16472	-7.43722	739	536
SÃO JOÃO DA TALHA	92.8	33.010	38.83556	-9.10806	128	537
SÃO MAMEDE PL	93.5	30.000	41.62794	-8.24656	706	538
SÃO MATEUS	103.4	20.000	38.42398	-28.44600	35	539
SÃO MIGUEL O ANJO	94.3	31.761	41.25833	-8.53361	204	540
SÃO MIGUEL O ANJO	100.8	31.761	41.25833	-8.53361	204	541
SÃO ROQUE DO PICO	106.1	26.990	38.48837	-28.25036	320	542
SENHORA DA HORA	89.5	31.761	41.18889	-8.65556	84	543
SERPA	88.5	33.010	37.92977	-7.59341	271	544
SERRA	98.0	33.010	39.60972	-8.31361	304	545
SERRA ALVAIAZERE	92.3	30.000	39.83056	-8.41111	597	546
SERRA BRANCA	107.9	26.990	39.03739	-28.03092	353	547
SERRA CASTANHEIRA	93.1	30.000	41.39278	-6.60722	970	548
SERRA D'AIRES	99.3	33.010	39.53333	-8.63333	651	549
SERRA DA ACHADA SANTANA	103.9	30.000	38.46167	-9.09583	200	550
SERRA DA AMEIXEIRA	105.5	30.000	39.89309	-8.40671	441	551
SERRA DA AMOREIRA	92.0	33.010	38.81333	-9.19722	263	552

Table B.1 (cont.) - Characteristics of the FM sound broadcasting stations in Portugal (adapted from [ANAC14]).

Location ID	f [MHz]	ERP [dBW]	Latitude [°]	Longitude [°]	h_{terrain} [m]	ID no.
SERRA DA ARRÁBIDA	89.9	40.792	38.49275	-8.96209	348	553
SERRA DA ARRÁBIDA	105.8	40.000	38.49275	-8.96209	348	554
SERRA DA ESPERANÇA	102.5	30.000	40.34167	-7.35833	705	555
SERRA DA FREITA	103.2	26.990	40.88395	-8.26602	1 074	556
SERRA DA GARDUNHA	93.9	40.000	40.10306	-7.48639	1 030	557
SERRA DA GARDUNHA	96.4	40.000	40.10306	-7.48639	1 030	558
SERRA DA GARDUNHA	98.2	40.000	40.10306	-7.48639	1 030	559
SERRA DA GARDUNHA	99.5	40.000	40.10276	-7.48808	1 024	560
SERRA DA GARDUNHA	100.0	26.989	40.10278	-7.48806	1 030	561
SERRA DA GARDUNHA	101.3	40.000	40.10306	-7.48639	1 030	562
SERRA DA GARDUNHA	103.4	40.000	40.10276	-7.48808	1 024	563
SERRA DA GARDUNHA	105.1	40.000	40.08029	-7.52552	1 220	564
SERRA DA MAROFA	93.4	43.010	40.86377	-6.99240	961	565
SERRA DA MAROFA	94.2	42.041	40.86466	-6.99120	970	566
SERRA DA MAROFA	97.2	43.010	40.86377	-6.99240	961	567
SERRA DA MAROFA	103.0	40.000	40.86466	-6.99120	970	568
SERRA DA MAROFA	104.6	40.000	40.86377	-6.99240	961	569
SERRA DA MAROFA	105.4	40.000	40.86399	-6.99210	968	570
SERRA DA MELRIÇA	103.2	26.990	39.69417	-8.13028	578	571
SERRA DA MIRA	93.7	31.761	38.78222	-9.23167	240	572
SERRA DA MIRA	107.2	31.761	38.77972	-9.24194	239	573
SERRA DE AIRE	103.7	33.010	39.53611	-8.63500	655	574
SERRA DE ARGÁ	97.0	30.000	41.80278	-8.69194	797	575
SERRA DE ARGÁ	106.2	30.000	41.82750	-8.74528	714	576
SERRA DE BORNES	89.6	40.000	41.43364	-7.00642	1 185	577
SERRA DE BORNES	91.1	40.000	41.43341	-7.00553	1 177	578
SERRA DE BORNES	91.9	40.000	41.43297	-7.00673	1 170	579
SERRA DE BORNES	92.8	40.000	41.43341	-7.00553	1 177	580
SERRA DE BORNES	101.1	40.000	41.43364	-7.00642	1 185	581
SERRA DE BORNES	102.1	40.000	41.43341	-7.00553	1 177	582
SERRA DE BORNES	103.2	40.000	41.43387	-7.00672	1 188	583
SERRA DE EL REI	102.0	30.000	39.33028	-9.26667	126	584
SERRA DE MONTEJUNTO	88.7	46.021	39.17383	-9.05964	660	585
SERRA DE MONTEJUNTO	90.2	40.000	39.17385	-9.05490	660	586
SERRA DE MONTEJUNTO	93.5	26.990	39.17345	-9.06001	651	587
SERRA DE MONTEJUNTO	94.2	26.990	39.17371	-9.05510	660	588
SERRA DE MONTEJUNTO	96.4	40.000	39.17371	-9.05596	660	589
SERRA DE MONTEJUNTO	98.3	46.021	39.17383	-9.05964	660	590
SERRA DE MONTEJUNTO	99.8	40.000	39.17371	-9.05596	660	591
SERRA DE MONTEJUNTO	105.2	46.021	39.17383	-9.05964	660	592

Table B.1 (cont.) - Characteristics of the FM sound broadcasting stations in Portugal (adapted from [ANAC14]).

Location ID	f [MHz]	ERP [dBW]	Latitude [°]	Longitude [°]	$h_{terrain}$ [m]	ID no.
SERRA DE MONTEJUNTO	106.8	40.000	39.17385	-9.05490	660	593
SERRA DE OSSA	88.4	33.010	38.73921	-7.58331	626	594
SERRA DE OSSA	94.5	33.010	38.73876	-7.58303	626	595
SERRA DE OSSA	95.0	26.990	38.73921	-7.58331	626	596
SERRA DE OSSA	97.2	26.990	38.73967	-7.58472	626	597
SERRA DE OSSA	102.1	26.990	38.73921	-7.58331	626	598
SERRA DE SANTA BÁRBARA	104.4	30.000	38.73011	-27.31974	1 030	599
SERRA DO ALVÃO	104.3	30.000	41.36417	-7.76306	1 233	600
SERRA DO ARESTAL	95.9	30.000	40.77694	-8.35694	790	601
SERRA DO BUÇACO	100.8	30.000	40.37222	-8.36444	550	602
SERRA DO CUME	89.2	30.000	38.71045	-27.11281	541	603
SERRA DO CUME	94.7	16.990	38.70972	-27.11111	541	604
SERRA DO CUME	99.7	30.000	38.71045	-27.11281	541	605
SERRA DO MENDRO	87.7	43.010	38.24654	-7.78323	400	606
SERRA DO MENDRO	91.1	43.010	38.24654	-7.78323	400	607
SERRA DO MENDRO	92.0	46.990	38.24654	-7.78352	400	608
SERRA DO MENDRO	96.5	46.990	38.24589	-7.78435	400	609
SERRA DO MENDRO	100.9	46.990	38.24589	-7.78435	400	610
SERRA DO MENDRO	102.4	46.990	38.24654	-7.78323	400	611
SERRA DO MENDRO	106.4	46.990	38.24654	-7.78352	400	612
SERRA DO PEREIRO	89.7	30.000	40.86389	-8.42389	487	613
SERRA DO PEREIRO	97.1	26.990	40.86389	-8.42389	487	614
SERRA DO REBOREDO	95.9	26.990	41.16513	-7.03218	835	615
SERRA DOS CANDEEIROS	92.6	30.000	39.43250	-8.92028	477	616
SERRA DOS CANDEEIROS	100.1	26.990	39.57250	-8.84778	481	617
SERRA DOS CANDEEIROS	104.6	30.000	39.43250	-8.92028	477	618
SERRA LEIRANCO	103.9	26.990	41.73164	-7.64727	1 136	619
SERRA SICO	97.0	30.000	39.91944	-8.54167	539	620
SERRA STA CATARINA	102.7	30.000	39.69333	-8.32250	420	621
SERRA VACARIA	88.1	30.000	40.89833	-8.39167	568	622
SERRO VENTOSO	95.5	30.000	39.55083	-8.86583	590	623
SETE CIDADES	98.4	16.990	37.83940	-25.79532	539	624
SETÚBAL	88.6	33.010	38.52250	-8.91944	122	625
SETÚBAL	98.9	33.010	38.52250	-8.91944	122	626
SETÚBAL	100.6	33.010	38.52639	-8.90556	130	627
SINES	95.9	26.021	37.95330	-8.83674	94	628
SINTRA	88.0	30.000	38.80056	-9.38083	202	629
SINTRA	91.2	30.000	38.78806	-9.38333	428	630
SINTRA	96.0	23.010	38.82795	-9.42199	177	631
SINTRA	96.9	23.010	38.82795	-9.42199	177	632

Table B.1 (cont.) - Characteristics of the FM sound broadcasting stations in Portugal (adapted from [ANAC14]).

Location ID	f [MHz]	ERP [dBW]	Latitude [°]	Longitude [°]	h_{terrain} [m]	ID no.
SINTRA	103.8	23.010	38.82795	-9.42199	177	633
SINTRA	105.0	24.771	38.78639	-9.38528	428	634
SINTRA	106.6	24.771	38.78639	-9.38528	428	635
SINTRA	107.7	30.000	38.78694	-9.38722	430	636
SOALHEIRO	105.2	30.000	41.46085	-7.29291	922	637
SOBREDA	106.0	16.990	41.50639	-6.81556	704	638
STA CRUZ DAS FLORES - RR	94.7	30.000	39.45183	-31.13581	179	639
TAROUQUELA	87.8	30.000	41.06194	-8.17806	663	640
TAVIRA	94.8	33.010	37.24444	-7.73806	425	641
TAVIRA	96.9	33.010	37.24028	-7.73861	420	642
TAVIRA	98.4	16.990	37.13000	-7.64861	25	643
TAVIRA	106.8	16.990	37.12444	-7.64361	18	644
TERÇA - RR	91.5	30.000	32.82889	-17.19774	951	645
TERMAS DE MONFORTINHO	107.8	16.990	39.99722	-6.88889	291	646
TOPO	100.5	26.990	38.54597	-27.84422	442	647
TORRE	93.7	16.990	37.11944	-8.36111	38	648
TORRE	100.8	30.000	40.07972	-7.52667	1 204	649
TORRE E CERCAS	92.4	16.989	37.19167	-8.38417	100	650
TORRES VEDRAS	93.8	30.000	39.08833	-9.25417	61	651
TORRES VEDRAS	97.8	30.000	39.06250	-9.26639	199	652
TRAMAGAL	96.7	33.010	39.43694	-8.26139	125	653
TRANCOSO	92.1	30.000	40.77361	-7.42250	950	654
TRÓIA	99.7	20.000	38.49250	-8.90417	0	655
TRÓIA	106.7	20.000	38.49250	-8.90417	0	656
TRÓIA	107.9	20.000	38.49250	-8.90417	0	657
TURQUEL	88.1	30.000	39.47111	-8.90528	449	658
VACARIA	106.3	30.000	40.89833	-8.39167	568	659
VAGOS	88.8	30.000	40.56667	-8.66667	25	660
VALENÇA	100.0	40.000	42.02231	-8.59379	547	661
VALENÇA	89.6	40.000	42.02164	-8.59348	546	662
VALENÇA	91.7	26.990	42.02000	-8.59194	544	663
VALENÇA	92.8	26.990	42.02000	-8.59194	544	664
VALENÇA	95.4	40.000	42.02231	-8.59379	547	665
VALENÇA	98.2	40.000	42.02164	-8.59348	546	666
VALENÇA	99.0	40.000	42.02141	-8.59348	546	667
VALENÇA	104.0	40.000	42.02164	-8.59348	546	668
VALENÇA	105.7	40.000	42.02231	-8.59349	546	669
VALHELHAS	100.8	30.000	39.51806	-8.51111	150	670
VALONGO	97.7	46.435	41.17203	-8.49401	349	671
VALONGO	105.3	46.990	41.17452	-8.49632	350	672

Table B.1 (cont.) - Characteristics of the FM sound broadcasting stations in Portugal (adapted from [ANAC14]).

Location ID	f [MHz]	ERP [dBW]	Latitude [°]	Longitude [°]	$h_{terrain}$ [m]	ID no.
VALONGO	106.2	30.000	41.17556	-8.49583	350	673
VALPAÇOS	100.2	26.990	41.56306	-7.51833	1 131	674
VELAS	91.9	16.990	38.65530	-28.15258	97	675
VENDAS NOVAS	100.1	30.000	38.67222	-8.46250	143	676
VIANA DO ALENTEJO	95.5	26.990	38.32219	-8.00489	358	677
VILA BOIM	91.5	26.990	38.87222	-7.26083	450	678
VILA BOIM	93.2	39.031	38.87528	-7.26333	450	679
VILA BOIM	101.6	39.031	38.87528	-7.26333	450	680
VILA BOIM	103.8	39.031	38.87528	-7.26333	450	681
VILA DA CALHETA	105.4	20.000	32.72332	-17.18217	144	682
VILA DA CALHETA	107.5	20.000	32.72332	-17.18217	144	683
VILA DE FRADES	90.0	30.000	38.20638	-7.83822	307	684
VILA DO CONDE MOSTEIRO	104.6	33.010	41.35389	-8.74000	20	685
VILA DO CONDE STA EUFÉMIA	98.4	33.010	41.31139	-8.63167	223	686
VILA FRANCA DE XIRA	88.2	33.010	38.95194	-8.98833	15	687
VILA NOVA	94.5	26.990	40.03889	-8.31139	262	688
VILA NOVA DE GAIA	92.8	33.010	41.10794	-8.59012	221	689
VILA NOVA DE PAIVA	98.0	26.990	40.85778	-7.72333	809	690
VILA NOVA DE POIARES	100.5	30.000	40.20972	-8.31972	363	691
VILA REAL DE SANTO ANTÓNIO	90.5	30.000	37.18333	-7.41667	4	692
VILA VIÇOSA	90.6	30.000	38.77000	-7.42944	426	693
VILAR DE PEREGRINOS	100.5	30.000	41.77472	-7.01139	825	694
VILAR FORMOSO	106.9	26.990	40.60222	-6.83056	788	695
VEISEU	88.2	26.990	40.64602	-7.92151	475	696
VEISEU	97.5	26.990	40.64602	-7.92151	475	697
VEISEU	99.4	30.000	40.65611	-7.90667	473	698
VEISEU	101.8	30.000	40.64602	-7.92151	475	699
VEISEU	103.6	30.000	40.65611	-7.90667	473	700
VEISEU	104.8	16.990	40.65667	-7.90528	470	701

Annex C

Fight Route Charts

This appendix is composed of the navigational charts depicting the flight routes that present signs of interfering signals.

All the navigational charts regarding the flight routes are presented in the Portuguese AIP [NAV14c]. In this appendix, one presents only the navigational charts of the flight routes that were assessed in Subsection 4.3.1. Figure C.1 presents both inbound ('a') and outbound ('b') segments of the flight route Y207. Figure C.2 corresponds to the flight route UN872, being the evaluated segment the path taken from point ABETO to Fátima VOR (UN872 a).

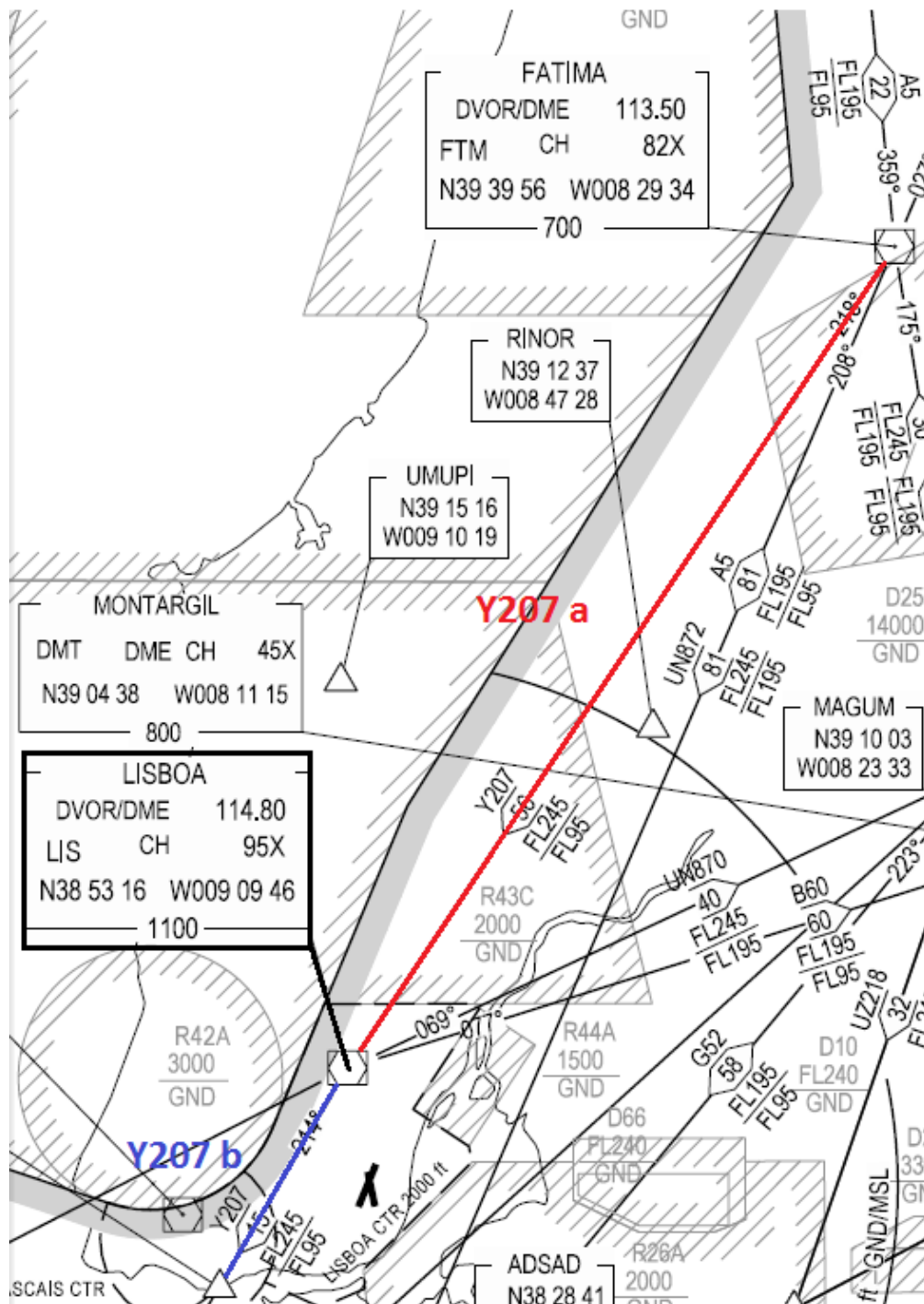


Figure C.1 - Navigational chart presenting both the assessed segments of flight route Y207 (extracted from [NAV14c]).

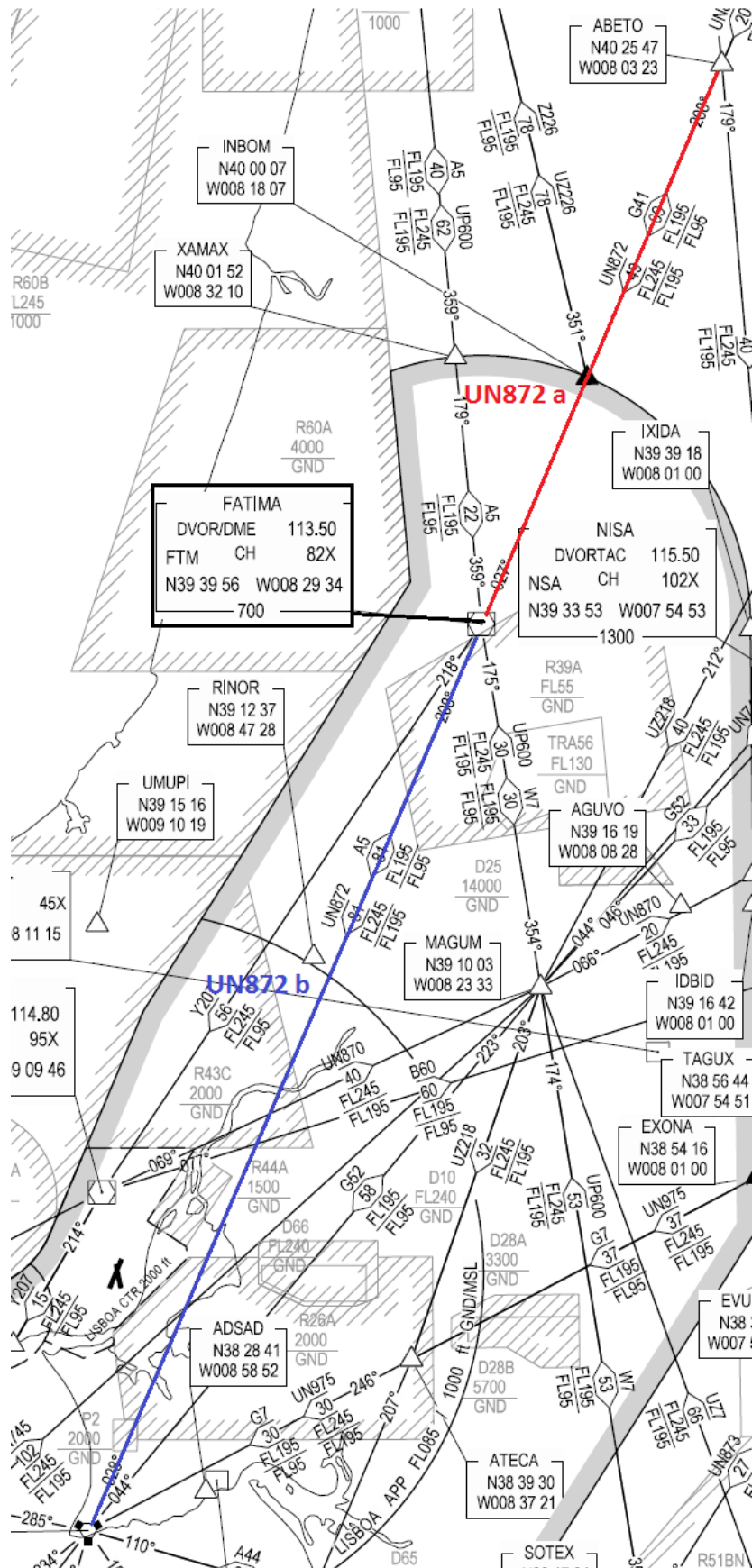


Figure C.2 - Navigational chart presenting both the assessed segments of flight route UN872 (extracted from [NAV14c]).

Annex D

VOR Results

This annex contains the results extracted from the simulator regarding the flight route scenarios assessed for the VOR evaluation.

The following figures present the curves extracted from the simulation in each of the flight route scenarios analysed in Subsection 4.3.1. The CIR curves are presented only for the segment of the path in which the interfering signals are present.

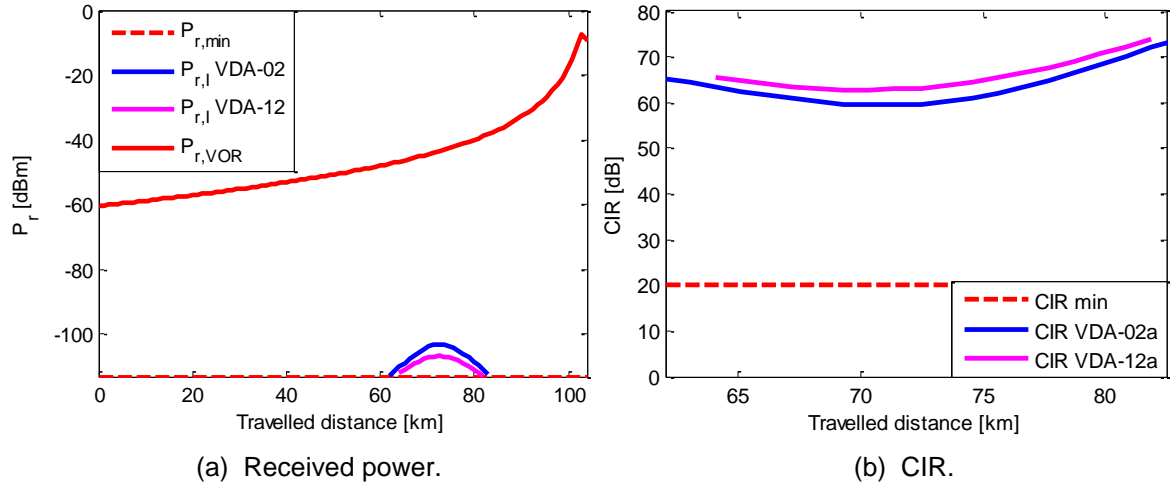


Figure D.1 - Results obtained from the simulation of the Y207a scenario.

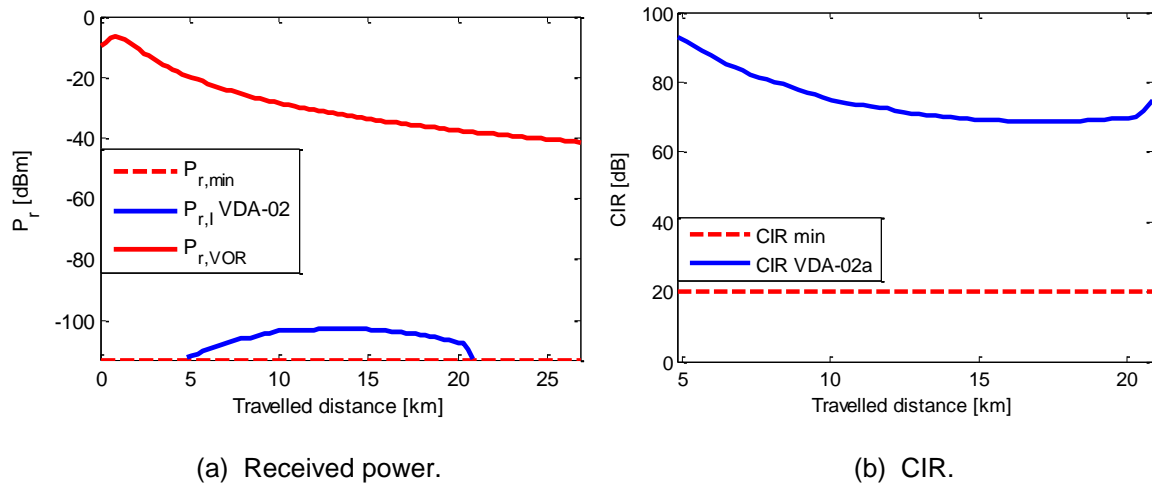


Figure D.2 - Results obtained from the simulation of the Y207b scenario.

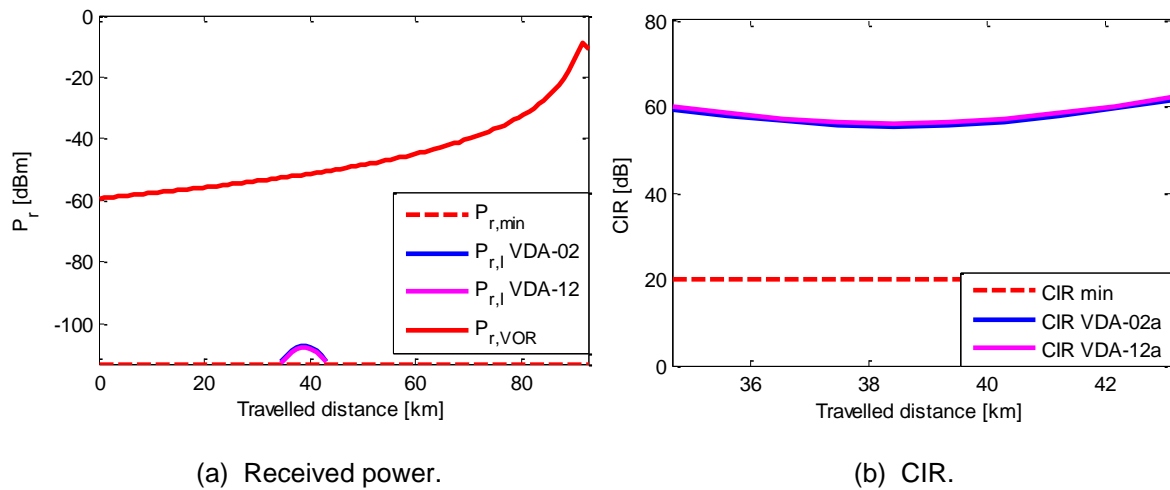


Figure D.3 - Results obtained from the simulation of the UN872a scenario.

Annex E

FM Broadcasting Stations in Evaluation

This appendix is composed of tables that list the FM stations that were considered in the assessment of the most relevant approach scenarios.

In this section one lists the stations that were considered in the evaluation of the Lisbon and Porto scenarios. They are represented by their ID numbers, to simplify the listing. They can be accessed in Annex B.

Table E.1 - List of the FM broadcasting stations considered in Lisbon runway 03 scenario.

FM Broadcasting Stations ID no.											
1	12	21	22	23	37	40	46	137	139	226	252
253	254	255	256	257	258	259	260	261	262	263	264
321	339	340	341	356	357	358	359	360	365	368	400
511	528	537	550	552	553	554	572	573	585	586	589
590	591	592	593	629	630	631	632	633	634	635	636
687											

Table E.2 - List of the FM broadcasting stations considered in Lisbon runway 21 scenario.

FM Broadcasting Stations ID no.											
1	12	21	22	23	37	40	46	137	139	226	252
253	254	255	256	257	258	259	260	261	262	263	264
321	339	340	341	356	357	358	359	360	365	368	511
527	528	537	552	553	554	572	573	585	586	589	590
591	592	593	629	630	631	632	633	634	635	636	652
687											

References

- [Agil12] Agilent Technologies, *IMD Measurement with E5072A ENA Series Network Analyzer*, Jun. 2012 (http://www.keysight.com/upload/cmc_upload/All/ENA_IMD_Measurement_Summary.pdf?&cc=PT&lc=eng).
- [Alex04] Alexander,J., “Loxodromes: A Rhumb Way to Go”, *Mathematics Magazine*, Vol. 77, No 5, Dec. 2004, pp.349-356.
- [ANAC13] ANACOM, *APPENDUM 2013 National Table of Frequency Allocations*, Public Report, ANACOM, Lisbon, Portugal, 2013 (<http://www.anacom.pt/render.jsp?contentId=1173460>).
- [ANAC14] ANACOM, Private Communications, Aug. 2014.
- [AxTe14] *Bandwidth and other technical matters in FM broadcasting*, <http://www.axino-tech.co.nz/documents/Bandwidth%20needed%20for%20FM%20broadcasts.html>, Mar. 2014.
- [Azim14] <http://www.azimut.ru/en/catalogue/navigation/ils>, May 2014.
- [BaCu91] Badinelli,M. and Cushman,A., *Evaluation of external filters in reducing type B1 and B2 FM broadcast interference to VHF communications avionics receivers*, FAA, Atlantic City, NJ, USA, Jul. 1991.
- [Corr14a] Correia,L.M., *Propagation Models*, Lecture Notes of Mobile Communication Systems, IST/UL, Lisbon, Portugal, 2014.
- [Corr14b] Correia,L.M., *Cellular Design*, Lecture Notes of Mobile Communication Systems, IST/UL, Lisbon, Portugal, 2014.
- [EMFA14] <http://www.emfa.pt/www/po/esquadra/link-751-013.006.001-descricao>, Oct. 2014.
- [EsLo78] Essman,J.E. and Loos,T., “Analytical determination of the interference of commercial FM stations with airborne communication and navigation receivers and experimental verifications”, *Vehicular Technology Conference*, Ohio, USA, Mar. 1978.
- [EUCO14] <https://www.eurocontrol.int>, Feb. 2014.
- [FAAG14] http://www.faa.gov/air_traffic/publications/atpubs/aim/aim0101.html, Feb. 2014.
- [FCC14a] <http://www.fcc.gov/encyclopedia/fm-broadcast-station-classes-and-service-contours>, May 2014.
- [FCC14b] <http://www.fcc.gov/encyclopedia/broadcast-radio-subcarriers-or-subsidary-communications-authority-sca>, Mar. 2014.

- [Fern13] Fernandes,J.A., *Assessment of Wind Turbines Generators Influence in Aeronautical Navigation Systems*, M.Sc. Thesis, IST/UL, Lisbon, Portugal, 2013.
- [Figa12a] Figanier,J., “Free Space Propagation”, in Fernandes,C.A. (ed.), *Aspects of Propagation in the Atmosphere* (in Portuguese), AEIST, Lisbon, Portugal, 2012.
- [Figa12b] Figanier,J., “Reflection on terrain”, in Fernandes,C.A. (ed.), *Aspects of Propagation in the Atmosphere* (in Portuguese), AEIST, Lisbon, Portugal, 2012.
- [Holm14] Harmonics, IMD and IP3, <http://www.aholme.co.uk/FracN/IMD.htm>, Aug. 2014.
- [ICAO96] ICAO, *Annex 10 - Aeronautical Telecommunications*, Vol. 1, No. 5, Montreal, Canada, Jul. 1996.
- [ICAO02] ICAO, *Manual on Testing of Radio Navigation Aids – Testing of Ground-Based Radio Navigation Systems*, Doc 8071, Vol. 1, Amendment No.1, Montreal, Canada, Oct. 2002.
- [ICAO08] ICAO, *Assessment of Potential Interference from FM Broadcasting Stations into Aeronautical VDL Mode 4 Systems in the Band 112-117.975 MHz*, ACP 19th Meeting of Working Group F, Reference ACP-WGF-19 WP06, Montreal, Canada, Sep. 2008.
- [ICAO13] ICAO, *Annex 14 Aerodromes - Aerodrome Design and Operations*, Vol. 1, No. 6, Montreal, Canada, Jul. 2013.
- [ICAO14] <http://www.icao.int/>, Feb. 2014.
- [Indr13] Indra Navia AS, *NORMARC 7216A 16-Element Two-frequency Localizer Antenna System – Instruction Manual*, Ref. 24797/Rev1.5/24-Jul-13, Oslo, Norway, 24 Jul. 2013.
- [ILSy14] <http://instrument.landingssystem.com/ils-ground-equipment/>, Feb. 2014.
- [ITU79] ITU, *Report of Ad Hoc Group 5C*, World Administrative Radio Conference, Doc. No DT/122-E, Geneva, Switzerland, 31 Oct. 1979.
- [ITU84] ITU, *Final acts of the Regional Administrative Conference for the Planning of VHF Sound Broadcasting*, Public Report, ITU, Geneva, Switzerland, 1984.
- [ITUR01] ITU-R, *Transmission Standards for FM sound broadcasting at VHF*, Recommendation ITU-R BS450-3, Geneva, Switzerland, 2001 (http://www.itu.int/dms_pubrec/itu-r/rec/bs/R-REC-BS.450-3-200111-!#!PDF-E.pdf).
- [ITUR10] ITU-R, *Compatibility between the sound-broadcasting service in the band of about 87-108 MHz and the aeronautical services in the band 108-137 MHz*, Recommendation ITU-R SM.1009-1, Geneva, Switzerland, 2010 (http://www.itu.int/dms_pubrec/itu-r/rec/sm/R-REC-SM.1009-1-199510-!#!PDF-E.pdf).
- [ITUR14] ITU-R, *Unwanted emissions in the out-of-band domain*, Recommendation ITU-R SM.1541-5, Geneva, Switzerland, 2014 (http://www.itu.int/dms_pubrec/itu-r/rec/sm/R-REC-SM.1541-5-201308-!#!PDF-E.pdf).
- [Java14] <https://developers.google.com/maps/documentation/javascript>, Aug. 2014.

- [Kibo13] Kibona,L., "Gain and Directivity Analysis of the Log Periodic Antenna", *International Journal of Scientific Engineering and Research (IJSER)*, Vol. 1, No. 3, Nov. 2013, pp. 14-18.
- [MatL13] Matlab R2013a Documentation, Documentation, The Mathworks, Natick, MA, USA, 2011 (<http://www.mathworks.com/>).
- [More14] Moreira,A., *Antenna arrays (in Portuguese)*, Lecture Notes of Antennas, IST/UL, Lisbon, Portugal, 2014.
- [NAV12a] NAV Portugal, *DVOR General Information - DVOR/VOR Principle*, Internal Report, NAV Portugal, Lisbon, Portugal, Nov. 2012.
- [NAV12b] NAV Portugal, *VOR*, Internal Report, NAV Portugal, Lisbon, Portugal, Nov. 2012.
- [NAV14a] <http://www.nav.pt/>, Feb. 2014.
- [NAV14b] NAV Portugal, *Private Communications*, 2014.
- [NAV14c] NAV Portugal, *Aeronautical Information Package*, Public Report, Portuguese Aeronautical Information Service – NAV Portugal, Lisbon, Portugal, Oct. 2014 (www.nav.pt/ais/).
- [NSA11] NSA, *Receiver Dynamics*, NSA Doc. no. 3928940, Jan. 2011 (https://www.nsa.gov/public_info/files/cryptologic_quarterly/Receiver_Dynamics.pdf).
- [OnDy07] Onnigian,P.K. and Dye,E., "Radio Transmission - FM Broadcast Antennas", in Williams, E.A., Jones, G.A., Layer, D.H. and Osenkowsky, T.G. (ed), *National Association of Broadcasters - Engineering Handbook*, Elsevier, 10th Edition, USA, 2007.
- [Pint11] Pinto,J.V.P.T., *Assessment and Design of Multilateration Telecommunication Systems installed in NAV Portugal*, M.Sc. Thesis, IST/UL, Lisbon, Portugal, 2011.
- [RFGN14] <http://www.rfglobalnet.com/doc/intermodulation-distortion-imd-measurements-o-0001>, May 2014.
- [RoSa14] Rodrigues,A.J. and Sanguino,J.E., *Hertzian Beams – Formulary (in Portuguese)*, Course Material of Radio Telecommunication Systems, IST/UL, Lisbon, Portugal, 2014.
- [RTCA81] RTCA, *FM Broadcast Interference Related to Airborne ILS, VOR and VHF Communications*, RTCA Doc. no. DO-176, Washington, DC, USA, Nov. 1981.
- [SaDo78] Sawtelle,E.M. and Dong,J.G., *Interference in communications and navigation avionics from commercial FM stations*, Final Report, National Aviation Facilities, Atlantic City, NJ, USA, Jul. 1978.
- [Salo13] Salous,S., *Radio Propagation Measurement and Channel Modelling*, John Wiley & Sons, West Sussex, UK, 2013.
- [Sant13] Santos,R.M., *Assessment of wind turbines generators influence in aeronautical radars*, M.Sc. Thesis, IST/UL, Lisbon, Portugal, 2013.

- [THAL04] Thales Group, *ILS 420 – Short description*, Internal Report, NAV Portugal, Lisbon, Portugal, Jul. 2004.
- [THAL05a] Thales Group, “Theory of Operation”, *Localizer 421 – Technical Manual Part 3*, Ref. No. 83140 55524, Stuttgart, Germany, Apr. 2005.
- [THAL05b] Thales Group, *Localizer 421 – Technical Manual Part 1*, Ref. No. 83140 55525, Stuttgart, Germany, Jun. 2005.
- [ToWy07] Tooley,M. and Wyatt,D., “VHF omnidirectional range”, in Butterworth-Heinemann Ltd, *Aircraft Communications and Navigation Systems: Principles, Operation and Maintenance*, Helsevier, Burlington, USA, 2007.